Investigating The Role of Arsenic Trioxide on The Expression of Survivin Splice Variants and Their Specific MicroRNAs During Cell Cycle Progression and Apoptosis in Breast Cancer MCF-7 Cell Line

By

Laka Kagiso

Dissertation Submitted in fulfilment of the requirements for the degree of Master of Science

In

Biochemistry

In

The
Department of Biochemistry, Microbiology and Biotechnology
School of Molecular and Life Sciences
Faculty of Science and Agriculture

At the

University of Limpopo

Supervisor: Dr. Z. Mbita

2019

i.Table of contents

ii. Declaration

I, Kagiso Laka, hereby, declare that the work submitted in this dissertation to the University of Limpopo for the fulfilment of the Master of Science (Biochemistry). Degree has not previously been submitted by me for a degree at this or any other University and that this is my own work and where use was made of the work of others it has been duly acknowledged.

Signature: _____

Date: _____

iii. Dedication

I dedicate this work to God Almighty for His continuous mercy, my late mother Marshen and to my family (Maureen, Margaret, Tokelo, Faith, Khomotso and Rorisang) for bringing the best out of me and believing in me. Your **Love**, **Prayers** and **Support** are indispensable for the success of this project and my studies.

iv. Acknowledgement

I would like to extend my sincere, forever thankful gratitude and appreciation to the following people:

- The Omnipotent Father, I mean, God Himself, for the sufficient grace, unconditional love, and wisdom without measure imparted upon my life. I thank the Almighty for providing me with strength and vision in this journey and for this life of favour.
- My sincere gratitude goes to my supervisor, Dr Z. Mbita, for his commitment to helping me and encouraging me throughout the study. His skills, wise words and most importantly, his patience and the understanding he had and provided until the end of the project.
- My loving aunts, Maureen and Margaret Laka and my siblings, Tokelo, Faith Khomotso and Rorisang Laka for their everlasting love, support and prayers throughout my studies.
- My sincere gratitude goes to Dr N.C. Hintsho-Mbita from the Department of Chemistry for the help she provided with carbon nanosphere work.
- Department of Biochemistry, Microbiology and Biotechnology staff members and my fellow postgraduate students for their love, support, and provision of a friendly environment that felt like home.
- I am grateful to The National Research Foundation (NRF) of South Africa for financing my studies and funding my research project.
- My dearest friends for the support, love and believing in me throughout. I acknowledge everyone who has contributed directly and indirectly to the success of my study.

v. List of Figures

Figure **Page**

vi. List of Tables

Table **Page**

vii. Presentations and publications

Presentations

- Kagiso Laka and Z Mbita, 2017. Regulation of survivin splice variants during arsenic trioxide-induced cell cycle arrest and apoptosis. Oral presentation during the Faculty of Science and Agriculture research day (20-22 October 2017).
- Kagiso Laka, Lilian Makgoo and Zukile Mbita, 2017. Regulation of survivin splice variants during arsenic trioxide- and curcumin-induced cell cycle arrest and apoptosis in breast cancer cell line MCF-7. Poster presentation during the 1st Ellisras Longitudinal Study International Conference (28-29 November 2017).
- Kagiso Laka and Z Mbita, 2018. The Role of Arsenic Trioxide on the Expression of Survivin Splice Variants during Cell Cycle Progression and Apoptosis in Breast Cancer Cell Line, MCF-7. Poster presentation during the South African Society for Biochemistry and Molecular Biology (SASBMB) Conference (08-11 July 2018).

Publications

- Fly Ash Derived *β*-Cyclodextrin Carbon Nanospheres as Potential Drug Delivery Vehicles. *Advanced Science, Engineering and Medicine* Vol. 10, 9–13, 2018.
- Survivin Splice Variants in Arsenic Trioxide (As2O3)-Induced Deactivation of PI3K and MAPK Cell Signalling Pathways in MCF-7 Cells. *Genes* Vol. 10 (1), 41, 2019.
- Cytotoxic effect of arsenic trioxide-β-cyclodextrin fly ash-derived carbon nanospheres (As_2O_3-β-cyclodextrin CNSs). *Material Research Express*. **In press.**

viii. Abstract

Survivin is the smallest and a well-studied member of the inhibitors of apoptosis proteins (IAPs) family, which is involved in the regulation of cell division, inhibition of both caspase-dependent and -independent apoptosis in cancer cells and promotion of angiogenesis. Survivin is detectable during embryonic and foetal development but is undetectable in normal adult tissues. It is, however, expressed in transformed cell lines as well as in most common types of human cancers. Regulation of survivin remains poorly understood, and the discovery of the regulatory biomolecules, microRNAs (MiRs) present an interesting opportunity to investigate the regulation of this protein and its variants in cancers, especially breast cancer. Additionally, the expression of the survivin splice variants during cell cycle progression and apoptosis is not fully understood.

The aims of this study were to investigate the role of arsenic trioxide on the expression of survivin splice variants and their specific microRNAs during cell cycle progression and apoptosis in human breast cancer MCF-7 cells. The study also aimed at ascertaining the toxicity and efficacy of using coal fly ash-derived *β*-cyclodextrin carbon nanospheres to deliver arsenic trioxide into the MCF-7 cells.

Carbon nanospheres (CNSs) were synthesised using a chemical vapour deposition method while arsenic trioxide was deposited using wet impregnation method to form the arsenic trioxide-*β*-cyclodextrin carbon nanospheres (ATO-*β*-cyclodextrin-CNSs). The formation of the CNSs and the loading of arsenic trioxide to CNSs were confirmed using scanning electron microscopy/energy dispersive X-ray detection (SEM-EDX). The *in vitro* cytotoxicity effect of the *β*-cyclodextrin carbon nanospheres (CNSs), arsenic trioxide and arsenic trioxide-*β*-cyclodextrin CNSs against KMST-6 and MCF-7 cells was analysed using the 3-(4, 5-dimethylthiazol-2-yl)-2, 5 diphenyltetrazolium bromide (MTT) Assay, Muse® Count and Viability Assay and light/fluorescence microscopy. Cellular apoptosis, cell cycle analysis, Multi-Caspase activation, mitochondrial membrane potential, MAPK activation and PI3K activation were analysed using the Muse® Cell Analyser. Polymerase Chain Reaction (PCR) and Immunohistochemistry were used to analyse survivin mRNA variants and protein expression, respectively. The survivin specific MiRs were predicted using both bioinformatics platforms and literature surveys.

In order to understand the applicability of delivering arsenic trioxide for the treatment of breast cancer, skin fibroblast (KMST-6) and MCF-7 cells were exposed to *β*-cyclodextrin CNSs. The novel *β*-cyclodextrin CNSs did not show any cytotoxic effect on the KMST-6 cells but demonstrated such activity against the MCF-7 cells. More so, arsenic trioxide-*β*-cyclodextrin CNSs were found to significantly reduce the viability of the MCF-7 cells and were shown to inhibit their cell growth through the induction of apoptosis.

The MTT Assay results revealed arsenic trioxide inhibited the growth of the MCF-7 cells in a concentration-dependent manner. The Muse® Cell Analyser showed that arsenic trioxide induced G2/M cell cycle arrest and promoted cellular apoptosis without any damage to the mitochondrial membrane of MCF-7 cells. Furthermore, arsenic trioxide also deactivated two survival pathways, Mitogen-Activated Protein Kinase (MAPK) and Phosphoinositide 3-Kinase (PI3K) signalling pathways in MCF-7 cells. The deactivation of the two pathways was shown to be accompanied by the upregulation of survivin 3α during arsenic trioxide-induced G2/M cell cycle arrest and apoptosis. Survivin 2B was found to be upregulated only during arsenic trioxide-induced G2/M cell cycle arrest, but downregulated during arsenic trioxide-induced apoptosis. However, wild-type survivin was highly expressed in untreated MCF-7 cells, but the expression was upregulated during arsenic trioxide-induced G2/M cell cycle arrest and was downregulated during arsenic trioxide-induced apoptosis. Survivin variant ΔEx3 was undetected in both untreated and treated MCF-7 cells. Survivin 2α was upregulated during arsenic trioxide-induced apoptosis whereas, survivin 3B was only detected in the untreated MCF-7 cells. Additionally, survivin proteins were localised in both the nuclei and cytoplasm in MCF-7 cells and highly upregulated during arsenic trioxide-induced G2/M cell cycle arrest, which can be attributed to the upregulation of survivin-2B.

Using TargetScan, MIRD and mirTarbase, a few MiRs were identified and confirmed to target wild-type survivin, survivin 2B and survivin ΔEx3. These include the MiR-542-3p and MiR-335-5p, which are both upregulated during apoptosis and MiR-218-5p, which is upregulated during cell arrest. MiR-218-5p targets survivin 2B, which was upregulated during G2M cell cycle arrest.

The fly ash-derived CNSs can be used to deliver arsenic trioxide for therapeutic purposes, especially against breast cancer. Most importantly, these nanoparticles induced typical apoptotic characteristics in breast cancer MCF-7 cells. Arsenic trioxide can be used as therapeutic target for breast cancer treatment and nanotechnology can be used for its delivery. This study provided the first evidence that novel survivin 2B splice variant may be involved in the regulation of arsenic trioxide-induced G2/M cell cycle arrest only. This splice variant can therefore, be targeted for therapeutic purposes against Luminal A breast cancer cells.

Chapter One: Introduction

1. Introduction

According to the World Health Organisation, cancer remains the leading cause of death, worldwide, accounting for 8.8 million deaths in 2015 (WHO, 2017). Breast cancer is the most frequently diagnosed cancer and the leading cause of cancer death among females worldwide, with an estimated 1.7 million cases and 521,900 deaths. Breast cancer alone accounts for 25% of all cancer cases and 15% of all cancer deaths among females (Torre *et al*., 2015). It is the second cause of cancer deaths globally, following lung cancer (Siegel *et al*., 2015). According to the National Cancer Registry (NCR), more than 100 000 South Africans are dignosed with cancer each year, of which 21% is attributed to breast cancer (Van Vuuren *et al*., 2015). The increase in screening initiatives and the awareness about the disease and advances in the medical field contribute to the rise of breast cancer incidences.

1.1. Breast cancer

Cancer is a group of diseases involving abnormal cell growth with the potential to spread to other parts of the body (Ferreira *et al*., 2014). Cancer arises from numerous gene mutations, especially in genes that regulate cell proliferation, differentiation and programmed cell death (Calon *et al*., 2015). Breast cancer begins in the mammary epithelial tissue of the breast, specifically the milk ducts due to uncontrolled cell proliferation and resistance to apoptosis. It usually spreads to lymph nodes in the armpit nearest to the affected breast due to metastasis. Through the same process, breast cancer can also spread to other parts of the body, including the lungs, bones, and liver. Development of breast cancer is also characterized by deregulation of cell cycle control (Pavlidou *et al*., 2014) in which several pathways are deregulated during carcinogenesis. Most notably, tumour cells can lose cell cycle control and acquire resistance to apoptosis by expressing a number of anti-apoptotic proteins such as the Inhibitors of Apoptosis Protein (IAP) family of proteins that include survivin (Garg *et al*., 2016). These proteins inhibit apoptosis by inhibiting the caspase cascades, which are important in the execution

of apoptosis (Jha *et al.*, 2012). Although, several efforts have been made to reduce the death rates associated with cancer, to date, there has been no ultimate chemotherapeutic drug available to overcome this disease. Studies in search of alternative and better therapeutic strategies for breast cancer treatment has intensified over the years, including the exploration of compounds from natural products and synthetic chemistry. Targeting biomolecules that regulate molecular mechanisms associated with carcinogenesis has become popular and survivin has attracted a lot of research interest across the globe.

1.2. Survivin

Survivin is the smallest member of the inhibitors of apoptosis proteins (IAPs) family, which is involved in the regulation of cell division, inhibition of both caspase-dependent and -independent apoptosis in cancer cells and promotion of angiogenesis (Cheung *et al*., 2010; Coumar *et al*., 2013). Survivin is the best studied member of the family and it is strongly expressed during embryonic and foetal development, yet has not found in normal adult tissues (Mull *et al*., 2014). It is, however, upregulated in transformed cell lines and in some common types of human cancers (Chen *et al*., 2014), where it promotes tumour cell survival by reducing apoptosis as well as favouring endothelial cell proliferation and migration (Lee *et al*., 2016).

1.2.1. Survivin biogenesis

Survivin is encoded by the *BIRC5* gene (NM_001168) and is highly studied compared to its previously identified variants. Alternative splicing of the *BIR5* gene has been reported to produce six survivin splice variants, namely, wild-type survivin, survivin 2B, survivin 2α, survivin 3B, survivin ∆Ex3 and survivin 3α (Khan *et al*., 2014). Survivin variants have been postulated to play different roles during carcinogenesis. It has been documented that survivin wild-type, survivin 3B, survivin 3α and survivin ΔEx3 are anti-apoptotic while survivin 2α is pro-apoptotic and survivin 2B having either anti-apoptotic or pro-apoptotic effects depending on the type of tumour (Moniri *et al*., 2013; Mishra *et al*., 2015). Little information is known about the splice variants, while there is extensive information about the survivin wild-type. For instance, survivin wild type has been reported to be associated

with overexpression of human epidermal growth factor 2 (HER2), vascular endothelial growth factor (VEGF), basic fibroblast growth factor (bFGF), urokinase plasmogen activator (uPA) and phenylalanine ammonia-lyase-1 (PAL-1) [Fernandez *et al*., 2014; Soliman *et al*., 2016]. So far, there is no indication that downregulation of survivin gives rise to a compensatory increase in other members of the IAP family. Many studies found that wild-type survivin is essential for normal cell division and is involved in chromosomal segregation and cytokinesis during embryonic development (Duffy *et al*., 2007; Jha *et al*., 2012; Anthanasoula *et al*., 2014). The problem arises when upregulation of survivin wild-type is detected in normal adult tissues. This makes survivin a suitable anticancer target for the development of new therapeutic strategies. In addition, survivin has been reported as an ideal protein for preventing unwanted cell death in normal tissues following radiation exposure (Carruthers *et al.*, 2016). This means that survivin can only be down-regulated rather than being totally inhibited in both malignant and non-malignant tissues. In addition, this is a good strategy because survivin can then be used to protect normal cells against radiation while radiation can be targeted to destroy cancer cells using monoclonal antibodies.

1.2.2. Diversity of survivin gene products

Survivin has been earmarked as an essential molecular marker and target in both cancer diagnosis and therapeutics (Werner *et al*., 2016). However, it remains obscure how the six survivin splice variants are regulated. The expression of the different newly discovered survivin splice variants is not well-understood, especially during arsenic trioxide-induced cell cycle arrest and apoptosis in breast cancer cell lines.

For a long time, research focus was mainly on the wild type variant but the discovery of splice variants has opened a new avenue to discover new therapeutic targets due to their diagnostic significance. The wild-type variant is highly expressed in embryonic stem cells (Mull *et al*., 2014) and human cancer cells (Faversani *et al*., 2014). However, its down-regulation has been shown to competently inhibit tumour cell growth and also improve the treatment- induced apoptosis of breast cancer MCF-7 cell line (Wang and Ye, 2015; Osterman *et al*., 2016).

Arsenic trioxide has been shown to exert anticancer activities against solid cancers, including breast cancer (Hoffman *et al*., 2015; Liu *et al*., 2015). Arsenic trioxide has also been demonstrated to inhibit growth of other cells, including lung adenocarcinoma cell line (H1355), Glioblastoma multiforme (GBM) and Hepatocellular carcinoma (HCC) by down-regulating survivin expression and through the activation of p38 and JNK pathways (Cheng *et al.,* 2006; Zhou *et al*., 2015; Sadaf *et al*., 2018). Interestingly, there is no study which had proven that arsenic trioxide has any effect on the splicing machinery of survivin and its splice variants.

1.2.3. Regulation of survivin

Regulation of survivin and its variants remains poorly understood. The discovery of the regulatory biomolecules, microRNAs (MiRs) present an interesting opportunity to study how survivin and its variants are regulated in cancers, especially, breast cancer. MicroRNAs are small noncoding RNA molecules which interfere with the expression of specific genes by binding to the 3'- untranslated region of mRNA and thereby alter protein translation or induce mRNA degradation. Recent data suggests that a class of microRNAs also play an important role in survivin dysregulation in human cancers (Huang *et al*., 2015). Several microRNAs such as MiR-34a (Cao *et al*., 2013), MiR-16 (Ma *et al*., 2013), MiR-203 (Xu *et al*., 2013), and MiR542-3p (Zhang *et al*., 2016) have been demonstrated to decrease the expression of survivin wild-type in human cancer cells but none of the MiRs have been reported to be specific to the other variants. High expression of certain MiRs results in cancer progression (Valeri *et al*., 2013; Donnarumma *et al*., 2017) whereas over-expression of others inhibits tumour progression (Fiore *et al*., 2015; Mudduluru *et al*., 2016). Various kinds of approaches for finding new therapeutics are emerging hence, this study was aimed at investigating the role of arsenic trioxide on the expression of survivin splice variants and their target microRNAs during cell cycle progression and apoptosis of human breast cancer cells.

1.3. Problem Statement

Breast cancer is the most frequently diagnosed cancer among females worldwide and most women never reach their life expectancy due to this disease (Siegel *et al*., 2015). Breast cancer alone accounts for 25% of all cancer cases and 15% of all cancer deaths, worldwide (Walker *et al.*, 2004; Ryane *et al*., 2017). Treatment options for this disease include chemotherapy, radiotherapy and surgery. However, all of these have not been completely effective in destroying the cancerous cells. Although several efforts have been made to reduce the death rate associated with breast cancer, to date, there has been no chemotherapeutic drug effective and available to treat this disease. Studies in search of alternative and better therapeutic strategies for breast cancer treatment has intensified over the years, including exploration of compounds from natural phytochemicals (Gavamukulya *et al*., 2014; Kumar and Chauh, 2016). Strategies such as gene therapy whereby the expression of anti-apoptotic genes such as oncofoetal survivin is suppressed using the anti-cancer drugs could be useful in destroying breast cancer cells. Down-regulation of the wild type survivin has been shown to competently inhibit tumour cell growth and also improve treatment- induced apoptosis of breast cancer MCF-7 cell line (Wang and Ye, 2015; Osterman *et al*., 2016). Targeting biomolecules that regulate molecular mechanisms has become popular and survivin has attracted substantial research interest across the globe. Arsenic trioxide has been shown to exert anticancer activities against tumour cells, including breast cancer (Liu *et al*., 2012; Hoffman *et al*., 2015), bladder cancer cells (Jutooru *et al*., 2010) and lung H1355 adenocarcinoma cells by down-regulating survivin expression (Cheng *et al.,* 2006). Therefore, targeting anti-apoptotic and cell cycle regulatory splice variants could be useful in the search and development of new cancer diagnostics and therapeutics tool.

1.4. Motivation

Survivin is the unique member of the inhibitor of apoptosis proteins (IAPs) family, which is alternatively spliced into six splice variants (Khan *et al*., 2014). The discovery of other survivin splice variants have opened up many opportunities for discovering new

therapeutic targets. Survivin variants have been implicated to play different roles in carcinogenesis (Mishra *et al*., 2015).

Survivin has been acknowledged as an essential molecular marker and target in both cancer diagnostic and therapeutic strategies (Werner *et al*., 2016). Expression of survivin wild-type has been studied using various synthetic inhibitors, including GPD566 (Shi *et al*., 2010), FL188 (Ling *et al*., 2012) and YM155 (Rauch *et al*., 2014). Currently, to the best of our knowledge, there is no study reporting or implicating the newly discovered survivin splice variants in arsenic trioxide-induced cell cycle arrest and apoptosis in breast cancer cells. Furthermore, regulation of the newly discovered splice variants has not been studied, hence their roles in apoptosis, cell cycle and carcinogenesis are poorly understood.

Compounds such as arsenic trioxide, as well as microRNAs (MiRs) specific to survivin variants can be used to reduce the expression of cancer promoting survivin variants in breast cancer cells. Recent data suggests that a class of MiRs play an important role in survivin dysregulation in human cancers (Huang *et al*., 2015). These MiRs, include MiR-34a (Cao *et al*., 2013); MiR-16 (Ma *et al*., 2013); MiR-203 (Xu *et al*., 2013) and MiR542-3p (Zhang *et al*., 2016). Blocking survivin expression in tumour cells by various approaches is now emerging as a promising therapeutic strategy in cancer. Arsenic trioxide (As_2O_3) has been used to treat acute promyelocytic leukaemia (APL) by the Chinese for decades and has been shown to possess anticancer activities *in vitro* against numerous solid tumour cell lines (Hai *et al*., 2015). However, no study has reported on the role of arsenic trioxide on the expression of the six survivin splice variants and their specific MiRs in breast cancer cells.

While the role of survivin in biological pathways leading to carcinogenesis has been confirmed, the role of some of the splice variants in this process is less clear. Indeed, whether these variants are expressed at high levels to exercise biological activity remains unknown. Due to the massive expression of survivin in cancer and its causal role in cancer progression, survivin has undergone intensive investigation as a possible tumour marker (Chieffi, 2011; Adamkov *et al*., 2012). Arsenic trioxide has been investigated as a potential drug against several solid cancers, including breast cancer, therefore, it is important to

further explore its mode of action. Understanding the role it plays in the regulation of the newly discovered survivin splice variants may yield new effective therapeutic targets.

1.5. The Aims of the study

The aims of the study were, firstly, to determine the effect of arsenic trioxide on the expression of survivin splice variants and their specific MiRs during cell cycle progression and apoptosis in breast cancer MCF-7 cell line and secondly, to determine the cytotoxicity and efficacy of using coal fly ash-derived *β*-cyclodextrin carbon nanospheres to deliver arsenic trioxide into breast cancer cells.

1.6. Objectives of the study

The objectives of the study were to:

I. Determine the safety and potential of using carbon nanospheres as a drug delivery vehicle in normal skin KMST-6 cells.
II. Deliver arsenic trioxide into MCF-7 breast cancer cells using the *β*-Cyclodextrin Carbon Nanopheres.
III. Determine the effect of arsenic trioxide on the viability of MCF-7 breast cancer cell line using 3-(4, 5-Dimethylthiazol-2-yl)-2, 5-Diphenyltetrazolium bromide) [MTT] and MUSE® Cell Count and Viability Assays.
IV. Analyse the effect of arsenic trioxide on MCF-7 cell cycle progression, apoptosis, mitochondrial membrane integrity, activation of Multi-Caspases, MAPK and PI3K pathways using flow cytometry.
V. Evaluate the impact of arsenic trioxide on the expression of survivin splice variants using semi-quantitative Reverse Transcription Polymerase chain reaction (RT-PCR) and immunocytochemistry.
VI. Predict and evaluate the survivin variants specific MiRs using Bioinformatics platforms and literature surveys.

1.7. Organization of the dissertation

This dissertation is structured into six chapters and they are described as follows:

Chapter one

This chapter introduces the study.

Chapter two

This chapter covers the literature review addressing important information relevant to the study. This chapter also highlights knowledge and gaps that exist in the understanding the role of survivin splice variants and the mechanisms may play a roles in. It also covers the relevant developments about survivin splice variants, breast cancer and nanomedicine were also reviewed.

Chapter three

The chapter contains all the experimental procedures, equipment and all the reagents that were employed in order to carry out the study.

Chapter four

This chapter covers the safety and efficacy of using coal fly ash-derived *β*-cyclodextrin carbon nanospheres as delivery vehicle for therapeutical purposes. Analyses of the morphological and elemental structure of *β*-cyclodextrin CNSs (Section 4.1), the effect of *β*-cyclodextrin CNSs on cell viability of KMST-6 (Section 4.2), as well as morphology of KMST-6 (Section 4.4) were shown. This chapter the ended with the discussion (Section 4.5) and conclusion (Section 4.6).

Chapter five

Chapter four, the *β*-cyclodextrin CNSs were shown to be safe against normal skin cells and could be used as potential drug delivery vehicles. This chapter covers the cytotoxicity and efficacy of using coal fly ash-derived *β*-cyclodextrin carbon nanospheres to deliver arsenic trioxide into MCF-7 breast cancer cells. Firstly, analysis of the morphological and elemental structure of *β*-cyclodextrin CNSs (Section 5.1), followed by determining the effect of β-cyclodextrin CNSs and arsenic trioxide-*β*-cyclodextrin CNSs on the viability of MCF-7 cells (Section 5.2), morphology (Section 5.3 and 5.4) and cellular apoptosis of MCF-7 cells (Section 5.5). This chapter ended with the discussion (Section 5.6) and conclusion (Section 5.7).

Chapter six

The chapter contains findings of the effect of arsenic trioxide on the expression pattern of survivin splice variants and their specific MiRs during cell cycle progression and apoptosis in breast cancer MCF-7 cell line. Cell cytotoxicity (MTT) Assay was used to assess viability (Section 6.1). Muse® Count and Viability Assay (Section 6.2) was used to confirm the MTT Assay results. Morphological observations were performed (Section 6.3 and 6.4). The Muse® Cell Cycle Analyser was used to analyse cell cycle progression (Section 6.5), cellular apoptosis (Section 6.6), mitochondrial membrane integrity (Section 6.7), multi-caspase activation (Section 6.8) MAPK, (Section 6.9) and PI3K (Section 6.10) signalling pathways. The expression pattern analysis of the survivin splice variants was investigated using conventional PCR (Section 6.11). Expression of survivin was detected using immunocytochemistry (Section 6.12). The prediction and evaluation of MiRs specific to survivin splice variants were shown in Section 6.13 were done. Lastly, discussion (Section 6.14) and conclusion (Section 6.15) were provided.

Chapter seven

This chapter summarizes the main findings of the study. It also covers the limitations of the study.

Chapter eight

The last chapter is chapter eight, which covers the reference for all the citations done throughout the dissertation. Lastly, the appendices are provided at the end of the dissertation.

Chapter Two: Literature Review

2. Introduction

This literature review provides an overview of breast cancer, which is the most commonly diagnosed cancer among women in the world. The development of many tumours involves the over-expression of anti-apoptotic proteins such as survivin, the most studied member of the inhibitor of apoptosis protein (IAP) family. This literature review covers how survivin is associated with cancer progression and biological pathways. Studies are continuously published recommending survivin as a therapeutic target for most cancer treatment. The chapter also looks on how arsenic trioxide is overlooked, while it has been used for ages to treat acute promyelocytic leukaemia (APL), as well as its importance use as anti-cancer agent and its delivery into cancer cells using nanomaterials.

2.1. Breast Cancer

According to the National Cancer Registry (NCR), more than 100 000 South Africans are dignosed with cancer each year, of which 21% is attributed to breast cancer (Van Vuuren *et at*., 2015). Breast cancer is a disease that begins in the cells of the breast due to uncontrolled cell proliferation and spread to other parts of the body in a process called metastasis (Tabaries *et al*., 2015). Cancer is a group of heterogeneous diseases that show substantial variation in their molecular and clinical characteristics, comprising multiple entities associated with distinctive histological and biological features, clinical presentations as well as behavior and responses to therapy. The impaired cells can spread to nearby tissue, but with early diagnosis and treatment, most people continue to live their normal lives. The malignant cells originate in the epithelial tissues in the lining of the milk ducts. The primary tumour begins in the breast itself, but once it becomes aggressive, it may spread beyond the breast to local lymph nodes or metastasize to other organ systems in the body (Pantel and Alix-Panabières, 2010). A lump in the breast is often about a centimeter in size and comprises roughly a million cells. It is estimated that a tumour of this magnitude may take up to a year or five years to mature (Jemal *et al*., 2011). Development of breast cancer is characterized by deregulation of cell cycle control

and resistance to apoptosis. Tumour cells acquire resistance to apoptosis by expressing a number of anti-apoptotic proteins such as the Inhibitors of Apoptosis Protein (IAP) family of proteins that include survivin (Garg *et al*., 2016).

2.1.1. Causes of breast cancer

Risk factors that control the development of breast cancer include mutations, age, geographic location (country of origin) and socioeconomic status, reproductive events, exogenous hormones, lifestyle risk factors (alcohol, diet, obesity and physical activity), familial history of breast cancer associated with mutations, history of benign breast disease, ionizing radiation, bone density and chemo preventive agents (Dumitrescu and Cotarla, 2005). Certain factors known to be important in the epidemiology of breast cancer that are unique to black women include late menarche, relatively early age at birth of the first baby, high parity and prolonged lactation (Vorobiof *et al*., 2001; Bauer *et al*., 2007). Up to 10% of breast cancer is due to genetic predisposition. This means that it can be transmitted through either sex and that some family members may transmit the abnormal gene without developing cancer themselves (McPherson *et al*., 2000). So far, at least five germline mutations that predispose people to breast cancer have been identified. These include mutations in the genes such as *breast cancer 1* and *2* (*BRCA1* and *BRCA2)* and *p53*. Mutations in *BRCA1* and *BRCA2* which are located on the long arms of chromosomes 17 and 13, respectively, have been identified and are associated with high risks of breast cancer (Easton, 1999; King *et al*., 2003). Germline mutations in *p53* predispose an individual to the Li-Fraumeni cancer syndrome (including childhood sarcomas and brain tumours, as well as early-onset of breast cancer) while mutations in *PTEN* genes are responsible for Cowden disease (of which breast cancer is a major feature) [Key *et al*., 2001].

2.1.2. Types of Breast Cancer

The difference between breast cancer types is due to the site at which the tumor began expressing receptors. Triple-negative breast cancers, are those tumours that lack expression of oestrogen receptor (ER), progesterone receptor (PR), and receptor

tyrosine-protein kinase erbB-2 (HER2) [Navratil *et al*., 2015]. These have a more aggressive clinical course than other forms of breast cancer (Foulkes *et al*., 2010). Ductal carcinoma *in situ* (DCIS) is a non-invasive cancer where abnormal cells have been found in the lining of the milk duct. The typical cells of this type do not spread beyond the ducts into the surrounding breast tissue. Ductal carcinoma *in situ* is an early stage cancer that is highly treatable (Rakha *et al*., 2010). The invasive ductal carcinoma (IDC) has abnormal cancer cells that start developing in the milk ducts and spread beyond the ducts into other parts of the body. IDC is the most common type of breast cancer, making up nearly 70 to 80% of all breast cancer diagnoses (Kerlikowske, 2010). Inflammatory breast cancer is an aggressive and fast growing breast cancer whereby cancer cells infiltrate the skin and lymph vessels of the breast. It often produces no distinct tumour or lump that can be felt and isolated within the breast. As soon as the lymph vessels become blocked by the breast cancer cells, symptoms begin to appear (Robertson *et al*., 2010). Metastatic breast cancer is also classified as Stage 4 breast cancer meaning the cancer has spread to other parts of the body such as the lungs, liver, bones or brain (Dawson *et al*., 2013).

2.1.3. Breast cancer treatment

Current treatment strategies for breast cancer include surgery, radiotherapy and a range of chemotherapeutic strategies using traditional non-targeted drugs. In early breast cancer, surgery can get rid of any disease that has been detected in or around the breast or regional lymph nodes, but hidden deposits of disease may remain either nearby (i.e. in the residual breast tissue, scar area, chest wall, or regional lymph nodes) or at far sites that could, if untreated, develop into life-threatening recurrence (Early Breast Cancer Trialists' Collaborative Group, 2005). Gene therapy can be defined as the transfer of genetic material into a cell for therapeutic purposes. Although originally intended as a means of compensating for heritable genetic diseases, gene therapy may also be used to treat acquired diseases, with gene transfer used as a type of drug-delivery system (Zarogoulidis *et al*., 2012). Gene therapy involves genetic and epigenetic dysregulation of a wide range of genes and may be caused by drug efflux transporters such as P-glycoprotein, breast cancer resistant protein (BCRP) or multiple resistance protein-1

(MRP1) [Gu *et al*., 2015; Chen *et al*., 2016]. To the best of our knowledge, there has been no report of survivin as a target for gene therapy.

Currently, the drug delivery system is used and it seems to improve pharmacokinetics, increase efficacy, specificity and bioactivity against human cancers without causing any harm to healthy tissues. Nanomaterials-based drug delivery systems have been successfully used in breast cancer treatment (Al Faraj *et al*., 2015; Kossatz *et al*., 2015; Alyafee *et al*., 2018). Other applications for delivery systems in breast cancer include the permitted chemotherapy drugs such as vinca alkaloids, platinum, and camptothecins (De Laurentiis *et al*., 2010; Munari *et al*., 2014). The increasing repertoire of sophisticated delivery systems may thus allow new classes of potent anticancer agents like arsenic trioxide to reach clinical application.

2.2. Survivin

Survivin is the fourth member of the chromosomal passenger complex (CPC), a regulatory of chromosome microtubule attachment, spindle assembly checkpoint, and cytokinesis during cell division (Carmena *et al*., 2012). It is also the smallest member of the inhibitor of apoptosis proteins (IAPs) family (Martini *et al*., 2016). Survivin is involved in regulation of cell division, inhibition of apoptosis and promotion of angiogenesis. Survivin is expressed during embryonic and foetal development but rarely in differentiated normal tissues (Faversani *et al*., 2014; Mull *et al*., 2014). Survivin has been regarded as an essential guardian of embryonic gut development and adult gut homeostasis protecting the epithelium from cell death and promoting the proliferation of intestinal stem and progenitor cells (Martini *et al*., 2016). It is however, upregulated in transformed cell lines and most common types of human cancers including bladder, breast, oesophageal, uterine (Adamkov *et al*., 2010) and colorectal cancers (Hernadezn *et al*., 2011).

Alternative splicing of survivin pre-mRNA results in six survivin mRNA transcripts (Khan *et al*., 2014). The six splice variants include the wild type survivin, survivin 2B, survivin 2α, survivin 3B, survivin 3α and survivin ∆Ex3. For a long time, the focus was mainly on the wild type variant but the discovery of the new splice variants has opened a new avenue to discover new therapeutic targets. Down-regulation of the wild type survivin has

been shown to competently inhibit tumour cell growth and also improve the treatment-induced apoptosis of breast cancer MCF-7 cell line (Wang and Ye, 2015; Osterman *et al*., 2016).

2.2.1. The survivin “cousins” and splice variants

As a member of IAPs, survivin has been documented to precisely inhibit caspases- 3, 7 and 9 and consequently, inhibits caspase-dependent apoptosis (Khan *et al*., 2014). As shown in Table 2.1, the IAP family consists of eight members: survivin, XIAP, NAIP, c-IAP1, c-IAP2, livin, ILP2 and BRUCE (Cheung *et al*., 2013). Proteins of the IAP family are described by the existence of 1–3 copies of a baculovirus IAP repeat (BIR) motif at its amino terminus. This domain contains 70–80 amino acid residues and was first identified in baculovirus anti-apoptotic proteins (Srinivasula and Ashwell, 2008). Some, but not all IAPs also possess a RING finger domain which is defined by seven cysteine and one histidine residues that coordinates two zinc atoms. Other motifs found in specific IAPs include a caspase recruitment domain (CARD), an ubiquitin conjugating motif and a nucleotide P-loop sequence of the dissimilar IAPs. Survivin is the smallest with 142 amino acid residues and a molecular mass of 16.5 kDa (Obexer and Ausserlenchner, 2014). It displays a single BIR domain but lacks the RING finger present in some other IAP members. In survivin, the RING domain is substituted by a long amphipathic alpha-helical region. Studies with X-ray crystallography have shown that wild-type survivin exists primarily as a homodimer (Gayathri and Rao, 2017).

Table 2.1: IAP Family members and their domain arrangements

Member	Number of BIR motifs	Presence of a RING finger	Presence of CARD	References
Survivin	1	No	No	Sah *et al*., 2006
XIAP	3	Yes	No	Eckelman *et al*, 2006
cIAP-1	3	Yes	Yes	Salvesen and Duckett, 2002
cIAP-2	3	Yes	Yes	Salvesen and Duckett, 2002
ILP-2	1	Yes	No	Saleem *et al*., 2013
Livin	1	Yes	No	Ashhab *et al*., 2001
NAIP	3	No	No	Liston *et al*., 2003
Bruce	1	No	No	Hou *et al*., 2008

Survivin proteins are encoded by the *baculoviral inhibitor of apoptosis repeat-containing 5* (*BIRC5)* gene, which contains four exons (Moore *et al*., 2014; Mull *et al*., 2014). Due to alternative splicing, the *BIRC5* gene is transcribed into six dissimilar mRNA transcripts: wild-type survivin, survivin-2B, survivin-ΔEx3, survivin 3B, survivin 3α and survivin 2α (Khan *et al*., 2014). As shown in figure 2.1, a complete wild-type survivin transcript consists of all the four exons that code for a protein made of 142 amino acids. Survivin 3B transcript consists of exons 1 to 4 and an extra exon 3B; the extra exon consists of an in-frame UGA stop codon that results in an open reading frame of 363 nucleotides, predicting a truncated 120 amino acids protein. On the other hand, survivin ΔEx3 lacks exon 3, resulting in a protein of 137 amino acids with a truncated C-terminus (Caldas *et al.*, 2005). Survivin 2B is made of all the four exons, including an extra exon 2B between exon 2 and exon 3. The inclusion of exon 2B generates the longest polypeptide of 165 amino acids. Survivin 2α comprises of the first two exons, of the *BIR5* gene as well as a small piece of intron 2. Survivin 2α is transcribed and translated into the smallest survivin protein of 74 amino acids among all variants (Badran *et al*., 2004). Survivin 3α contains 1–73 amino acids of the wild-type survivin protein, but the remaining (74–142) are replaced by five amino acids (MRELC), creating a new protein of 78 amino acids (de Nicochea-campion *et al*., 2013; Sah and Seniya, 2015).

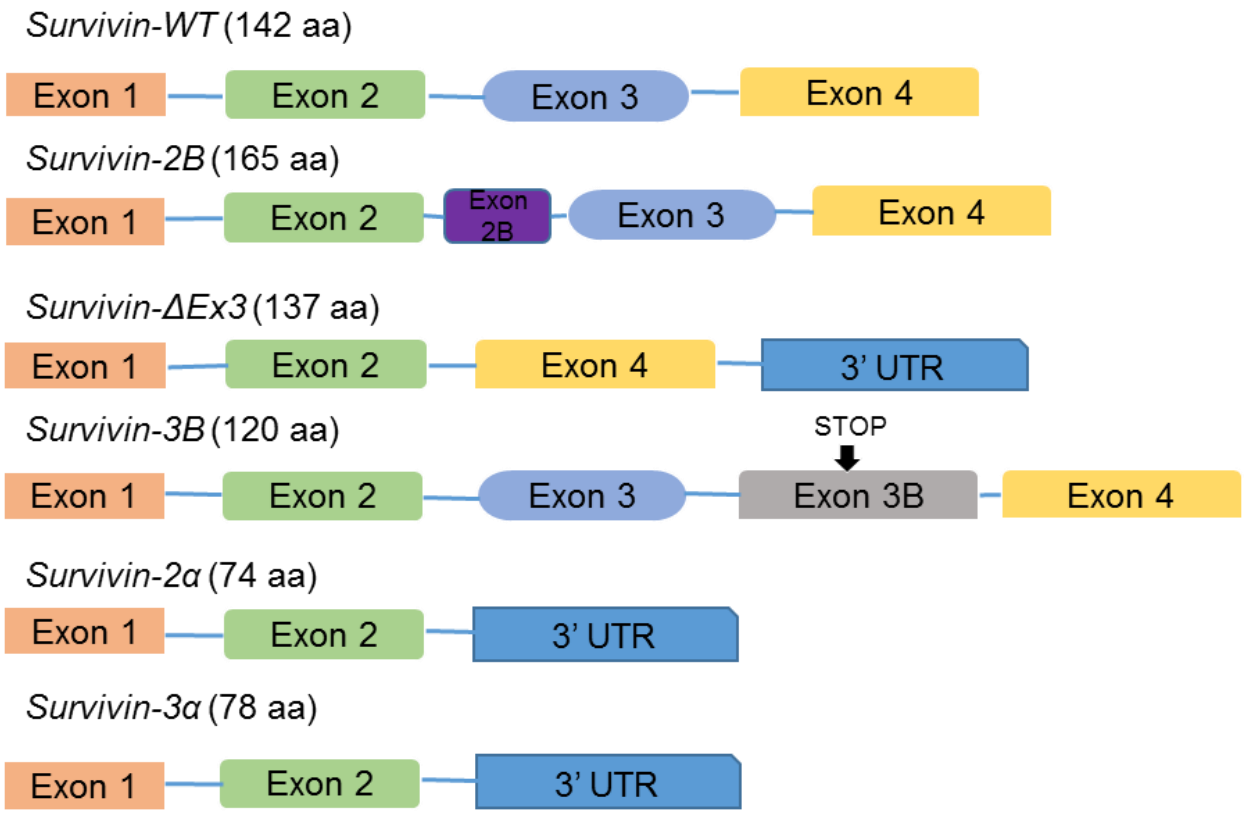

Figure 2.1 – Schematic illustration of the six known survivin isomers due to alternative splicing: The figure is adapted from Khan *et al*. (2014).

2.2.2. Molecular functions of survivin isoforms

The diversity in survivin function suggests complexity in the function of the survivin isomers, even though their respective functions are not fully understood. Survivin wild type is the most studied with its high expression associated with most cancers, if not all. There are observations showing tumour-specific expression of certain splice variants (Cho *et al*., 2011; Mishra *et al*., 2015). Some of these isomers, survivin 2B may be used for cancer staging. There is still a lot of work that needs to be done in order to fully understand the role of the survivin isomers.

Survivin 2B has pro-apoptotic function by neutralizing anti-apoptotic effects of wild type survivin and survivin ΔEx3 (Ling *et al*., 2007). Based on literature data, it can be said that survivin 2B expression is dependent on the nature and stage of cancer. Early stage breast

cancer has been shown to express high levels of survivin 2B, while late stages of breast cancer showed low or no expression of this variant. (Khan *et al*., 2014). Therefore, survivin 2B functions by opposing the role of the wild type survivin or survivin ΔEx3. This variant can be a useful anticancer target but there is little information about its function.

Survivin 2α has been documented to be pro-apoptotic in most human cancer cells (Caldas *et al*., 2005; Kyani *et al*., 2014) including breast cancer (Vegran *et al*., 2011). The pro-apoptotic nature of survivin 2α is attributed to its lack of the third coil in the BIR domain, which is for the necessary in inhibition of apoptosis (Vegran *et al*., 2007).

The survivin ΔEx3 isoform has been shown to be anti-apoptotic and implicated in many cancers including gastric cancer (Krieget *et al*., 2002), breast cancer (Ryan *et al*., 2005; Khan *et al*., 2014), bladder cancer (Atlasi *et al*., 2009), thyroid cancer (Waligorska-Stachura *et al*., 2014) and oral cancer (Mishra *et al*., 2015). The survivin ΔEx3 isoform dimerizes with the wild type survivin, which consequently results in the inhibition of apoptosis and induction of angiogenesis (Caldas *et al*., 2005; Athanasoula *et al*., 2014; Mishra *et al*., 2015). This isoform has also been suggested to associate with Bcl-2 and activated caspase-3 proteins, thereby inhibiting apoptosis (Mahotka *et al*., 2002; Malcles *et al*., 2007).

Survivin 3B is an anti-apoptotic isoform that has been shown to possess a complete BIR domain, which is associated with its anti-apoptotic functionality (Pavlidou *et al*., 2011). Studies based on breast cancer cell lines confirmed the significance of the expression of the variant 3B (Ryan *et al*., 2005; Vegran *et al*., 2007). The suppression of this protein resulted in induced apoptosis (Knauer *et al*., 2007). The ectopic expression of survivin 3B potentiates tumorigenic activities through evasion of immune surveillance (Vegran *et al*., 2013). This variants also augments resistance against chemotherapy through an engagement of pro-caspase-6 in spite of mitochondrial depolarization and caspase-3 activation (Sah *et al*., 2015).

Lastly, survivin 3α, which is also believed to be anti-apoptotic (de Nicochea-campion *et al*., 2013) by an additional of 32 nucleotides from intron 2 as a cryptic exon (Mola *et al*., 2007). There is very little information about this variant. The anti-apoptotic proteins that counteract apoptosis signalling signify promising new therapeutic targets to impair cancer

cell growth and enhance treatment response (Pennati *et al*., 2012). Therefore, further work on the expression and function of these variants in various types of tumour tissue, is of paramount importance. Table 2.2 summarizes the general understanding of the roles of the different survivin isoforms.

Overall, survivin is essential for the integrity of stem/progenitor cells. This has been demonstrated for pluripotent stem cells, where expression and subcellular localization of survivin and its splice variants (2B, ΔEx3 and 3B) may be controlled by microRNAs (Mull *et al*., 2014). Stem cells have been reported to predominantly depend on the expression of survivin for protection against apoptosis (Wen *et al*., 2013; Lee *et al*., 2013). Even though this is a unique field of investigation, it is fascinating that survivin expression in CD34+38−myeloblastic stem cells is related to extensive transcriptional reprogramming and upregulation of regulators of cell proliferation, phosphatidylinositide 3-kinases (PI3K), and cell migration/invasion (Carter *et al*., 2012). Conversely, deletion of survivin in hematopoietic stem cells disrupts virus integration site 1 (Evi-1)-dependent transcriptional program, resulting in loss of downstream target genes such as *Gata2*, *Pbx1* and *Sall2*, which regulate proliferation, differentiation and apoptosis in many cell types (Fukuda *et al*., 2015).

Table 2.2: The molecular functions of survivin splice isomers.

Survivin variant	Function	Reference
Survivin wild-type	Anti-apoptotic	Mishra *et al.*, 2015
Survivin 2B	Pro-apoptotic/Anti-apoptotic	Zhu *et al.*, 2004; Ling *et al.*, 2007
Survivin ΔEx3	Anti-apoptotic	Yedjou *et al.*, 2009; Gaytan-Cervantes *et al*., 2017
Survivin 3B	Anti-apoptotic	Knauer *et al.*, 2007, Pavlidou *et al*., 2011
Survivin 2α	Pro-apoptotic	Zhu *et al*., 2004; Ling *et al*., 2007; Mishra *et al.*, 2015
Survivin 3α	Anti-apoptotic	de Nicochea-campion *et al*., 2013

2.2.3. Localization and subcellular distribution of survivin variants

Different survivin variants have been localized in different subcellular compartments, further demonstrating the diversity in survivin functions. Survivin wild-type, the main transcript has capability to interfere with the cellular death pathways, which appears to reside in the cytoplasm (Serrano-López *et al*., 2013). Survivin wild type localizes to the mitochondria and it has been proven that cellular stress enhances its expression and localization (Chen *et al*., 2012). In addition, upon the apoptotic stimulation using drugs or any stimulus, mitochondrial survivin is quickly freed to the cytosol where its cytoprotective effects prevent the activation of the initiator caspase-9 (Dohi *et al*., 2004). In normal tissue, survivin is not detected in the mitochondria, thus suggesting that it is exclusively connected with tumour transformation. Survivin subcellular compartmentalization in mitochondria seems to play a role in anti-apoptotic function of protein (Pennati *et al*., 2007).

Survivin ΔEx3 was shown to be mostly localized in the nucleus during G1 and G2 cell cycle phases while only about 22 % is localized in the cytoplasm and very little is found in the mitochondria in cervical cancer cells (Futakuchi *et al*., 2007). Other types of human cancers (breast, oral, acute myeloid leukaemia, and thyroid) have shown nuclear

expression of this isoform (Serrano-López *et al*., 2013; Khan *et al*., 2014; Waligórska-Stachura *et al*., 2014; Mishra *et al*., 2015).

The greater portion (76.3-78%) of survivin 2B has been estimated to be localized in the cytoplasm whereas about 22 %-37.7 % is found in the nucleus. A smaller fraction of the protein remains localized in the mitochondria (Caldus *et al*., 2005; Serrano-López *et al*., 2013). The subcellular localization of survivin 3B remains to be determined, whereas survivin 2α has been detected in cytoplasm and also resides in the nucleus (Kahn *et al*., 2014; Mishra *et al*., 2015). However, the exact location of survivin 3α remains unknown.

These localization patterns are summarized in Table 2.3. Nuclear survivin expression is an unfavourable prognostic indicator in oesophageal, hepatocellular, non–small-cell lung, and ovarian cancers, mantel cell lymphoma, cholangiocarcinoma and endometrial cancers (Fields *et al*., 2004; Li *et al*., 2005; Shinohara *et al*., 2005). In contrast, an advantageous outcome associated with nuclear survivin has been reported for gastric, bladder, and breast cancers, ependymoma, and osteosarcoma. Nuclear survivin may regulate cell proliferation while cytoplasmic survivin may be involved in cell survival but not cell proliferation (Li *et al*., 2005).

Table 2.3: The localization and subcellular distribution of survivin isomers.

Survivin variant	Subcellular distribution	Reference
Wild-type survivin	Cytoplasm and Mitochondria	Barnes *et al.*, 2006; Pennati *et al.*, 2007; Mull *et al*., 2014; Adamkov *et al*., 2011; Balakier *et al*., 2013
Survivin 2B	Cytoplasm	Mahotka *et al*., 2002
Survivin ΔEx3	Nucleus	Mahotka *et al.*, 2002; Badran *et al*., 2004; Mull *et al*., 2014; Lopergolo *et al*., 2012
Survivin 3B	Nucleus	Yedjou *et al.*, 2009
Survivin 2α	Cytoplasm and nucleus	Badran *et al*., 2004
Survivin 3α	Not known	Mishra *et al.*, 2015

2.2.4. Survivin variants and cancer

High expression of survivin isomers has been reported in most type of cancer cells. In cancer cells, increased survivin is usually associated with high cell proliferation (Sui *et al*., 2002; Takai *et al*., 2002; Fields *et al*., 2004), reduced levels of apoptosis (Tanaka *et al*., 2000; Kawasaki *et al*., 2001), resistance to chemotherapy (Tran *et al*., 2002; Zaffaroni *et al.*, 2002) and increased rate of tumour recurrence (Swana *et al*., 1999). Studies have assessed the connection between survivin, disease variables, and clinical outcomes. Elevated survivin expression has been reported as a significant indicator of favourable outcome in patients with gastric (Okada *et al*., 2001) or non–small cell lung cancer (Vischioni *et al*., 2004) and osteosarcoma (Wang *et al*., 2006). Survivin ΔEx3 predominates over 2B in patients with acute lymphoblastic leukaemia (Nakagawa *et al*., 2004). The anti-survivin antibodies used in these studies do not distinguish between the survivin isomers with similar and opposing functions, hence molecular characterization of function and localization of multiple survivin forms may be required to clarify the true prognostic value of survivin and, from a therapeutic standpoint, may help to identify optimally selective survivin-targeted strategies.

Two additional survivin splice variants, survivin 2α (Caldas *et al*., 2005) and survivin 3B (Badran *et al*., 2004) have been identified. Survivin 2α can bind to survivin and antagonize wild type survivin function, suggesting that survivin 2α may alter the anti-apoptotic activity of survivin in tumour cells (Caldas *et al*., 2005). Khan *et al*. (2014) reported that anti-apoptotic forms, survivin wild type and survivin ΔEx3 were highly expressed in breast cancer patient tissues, while expression of the pro-apoptotic variant 2B was found to be low and undetectable in later stages of the tumour. Mishra *et al*. (2015) reported expression of the six survivin splice variants in oral cancer. Wild-type survivin, survivin 3B, and survivin Δ-Ex3 were highly expressed, while survivin 2B, survivin 2α and survivin 3α were downregulated. Wild-type survivin was shown to require dimerization to perform its anti-apoptotic function. The study also showed that dimerization of survivin wild type with either survivin 3B or survivin-ΔEx3 retained its anti-apoptotic properties whereas dimerization with survivin 2α or survivin 2B, attenuate its anti-apoptotic effect. The function of survivin 3α is not yet known, while the function of other variants have been reported in breast cancer.

Survivin is possibly of great value in the prognosis of breast cancer patients. Survivin, an anti-apoptotic protein, was described as strongly expressed in human cancers including breast cancer (Ye *et al*., 2014; Wang *et al*., 2015). Differential expression of survivin and its splice variants in tumour tissues introduces it as a candidate molecular marker for cancer. However, its prognostic relevance to breast cancer patients has long been a matter of debate (Cheng *et al*., 2015; Parvani *et al*., 2015). Survivin and its splice variants were differentially expressed in tumour samples compared with normal adjacent tissues (Khan *et al*., 2014; Mishra *et al*., 2015). The expression of survivin-3B and survivin-3α was precisely detected in tumour tissues (53%) compared to normal adjacent (5%) and 65% in tumour tissues and 0.0% in normal adjacent tissues for survivin-3α. Survivin wild-type and survivin-ΔEx3 were both upregulated in both benign (cancer cells that remain in their site of origin) and malignant (cancer cells that spread from the primary tumour to the other parts of the body) tumours. Additionally, survivin and survivin-ΔEx3 were detected in breast cancer samples while survivin-2B was differentially expressed depending on the aggressiveness of the disease (Khan *et al*., 2014).

Conversely, survivin-2α was the foremost expressed variant of survivin in breast cancer. Differential expression of survivin-2α and survivin-3α splice variants highlights their usefulness as new candidate markers for breast cancer diagnosis and prognosis (Moniri *et al*., 2013). Végran *et al*. (2013) analysed the apoptosis gene signature of survivin and its variant expression in breast cancer; a noteworthy relationship between survivin transcripts and apoptotic genes were found. Interestingly, survivin-3B variant showed major inverse correlations with pro-apoptotic genes. This data suggests survivin-3B contributes to cell survival through the anti-apoptotic pathway and that its expression levels could be an important factor in determining therapeutic strategies for breast carcinoma. Another study revealed that high levels of survivin mRNA were strongly associated with high nuclear grade, positive axillary lymph nodes, negative hormone receptor status, positive Her2 amplification, higher Ki67 labeling index, and presence of vascular invasion (Xu *et al*., 2014).

High mRNA expression of survivin was an independent marker of poor prognosis both in the entire cohort and in the HR-positive/ Her2-negative subtype, whereas the protein expression of survivin was not (Yamamoto *et al*., 2012). The expression of survivin-3B and survivin-ΔEx3 did not vary after an anthracycline-based chemotherapy in breast carcinomas, whereas a significant decrease in the percentage of expression of the remaining variants was observed (Ve´gran *et al*., 2005). These results confirm previous observations that expression of the anti-apoptotic survivin-ΔEx3 and Survivin-3B is higher in p53-mutated breast tumours (Ve´gran *et al*., 2007). However, unlike Ryan *et al*. (2005) results but like Span *et al*. (2006), survivin-ΔEx3 expression increases with histological grade and is more expressed in ER-negative tumours. Survivin-2B is overexpressed in high-grade ER-negative and node-invasive tumours and this seems to indicate that survivin-2B could be a marker of aggressiveness. Interestingly, due to its probable potential pro-apoptotic role, survivin 2α is more present in low-grade and non-invasive tumours. Caldas *et al*. (2005) showed the expression of survivin-3B was associated with tumour resistance after one course of chemotherapy treatment.

Added to this, increased expression of survivin-3B after one course of docetaxel/epirubicin treatment was associated with reduced disease-free survival (DFS) of breast cancer patients. Végran *et al*. (2011) found a significant relationship with either patient's overall or DFS for survivin-3B expression. Indeed, the adverse association between survivin and poor outcome in breast cancer seems to be quite confusing. This can be explained by the fact that the analysis of survivin transcripts with specific primers and probe probably differs from studies that seek to distinguish the different splice variants. A pro-apoptotic role for survivin-2a had been described (Caldas *et al*., 2005); however, it was found to be associated with the worst prognosis of breast cancer patients (Span *et al*., 2006). Taken together, survivin-3B may contribute to cell survival through the anti-apoptotic pathway.

Furthermore, survivin-3B could play a significant role in breast tumour development and could be considered as a new therapeutic target. These differences in survivin splice variant features might explain how survivin mediates both apoptosis and cell division regulation (Yang *et al*., 2006). More so, the association between survivin-2B and survivin

wild-type and oestrogen receptors, further strengthens the fact that this particular variation of survivin mRNA could predict survival of breast cancer patients (Takai *et al*., 2008).

Nectin-4 is a new tumour-associated antigen and a reliable biomarker for breast carcinoma. The *in vivo* association of survivin and Nectin-4 with unfavourable prognostic indicator, and with one another, suggests that these proteins may also interact in breast carcinoma in order to exert their adverse effects. The combined survivin and Nectin-4 expression demonstrates a strong independent association with poor prognosis during cell cycle progression of breast cancer cells (Anthanassiadou *et al*., 2011).

2.3. Survivin and cell-cycle

2.3.1. Cell cycle phases

The cell cycle division is a complex sequence of events that take place during cell division and duplication of cellular genetic material (DNA) to generate two identical daughter cells (Elledge, 1996). In eukaryotic cells, this process includes a series of four distinct phases. These phases consist of the Mitosis phase (M), Gap 1 phase (G1), Synthesis phase (S), and Gap 2 phase (G2). The G1, S, and G2 phases of the cell cycle are collectively referred to as the interphase (Wang and Levin, 2009) as illustrated in figure 2.2. The division cycle of eukaryotic cells is controlled by a family of protein kinases known as the cyclin-dependent kinases (CDKs). The sequential activation of individual members of this family and their consequent phosphorylation of critical substrates promotes orderly progression through the cell cycle (Serrano *et al*., 1993). The dividing cell spends most of its time in interphase as it grows in preparation for cell division. The mitosis phase of the cell division process involves the separation of nuclear chromosomes, followed by cytokinesis (division of the cytoplasm forming two distinct cells) [Morrish *et al*., 2010]. At the end of the mitotic cell cycle, two distinct daughter cells are produced (Maton *et al*., 1997). The time it takes for a cell to complete one cell cycle varies depending on the type of cell. Some cells, such as blood cells in bone marrow, skin cells, and cells lining the stomach and intestines, divide rapidly and constantly. Other cells divide when needed to replace

damaged or dead cells (Cooper, 2000). These cell types include cells of the kidneys, liver, and lungs.

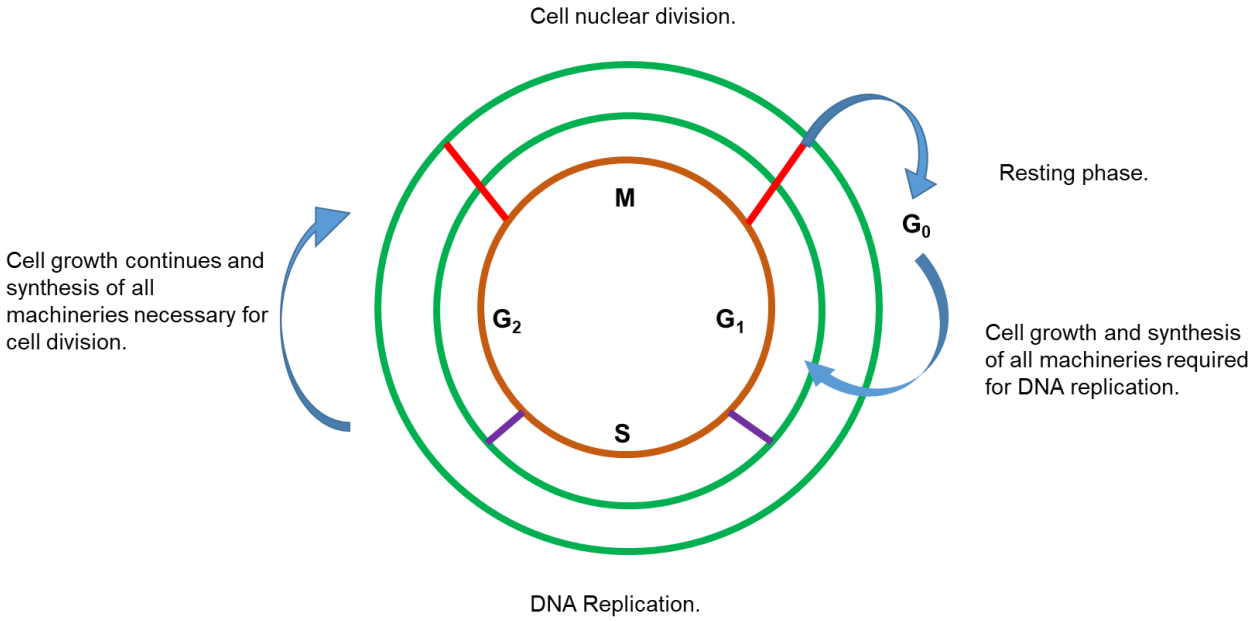

Figure 2.2 – The cell cycle phases: The figure is illustrated as adapted from Lee *et al*. (2013).

Other cell types, including nerve cells, stop dividing once they have matured (Brownell *et al*., 2011). Once a cell has completed the cell cycle, it goes back into the G_1 phase and repeats the cycle again. Cells in the body can also be placed in a non-dividing state called the Gap 0 phase (G_0) at any point in their life. Cells may remain in this stage for very long periods of time until they are signalled to progress through the cell cycle as initiated by the presence of certain growth factors or other signals. Cells that contain genetic mutations are permanently placed in the G_0 phase to ensure that they are not replicated. When the cell cycle goes wrong, normal cell growth control is lost, cancer cells may develop, which gain control of their own growth signals and continue to multiply unchecked (Sakaue-Sawano *et al*., 2008). Overexpression of survivin in cancer may overcome cell cycle checkpoints to facilitate aberrant progression of transformed cells through mitosis (Sah *et al*., 2006).

2.3.2. Expression of survivin during cell cycle progression

Cell cycle progression affects the expression of survivin. High levels of survivin are observed during M-phase while low expression levels of survivin are found in cells arrested in the G_1-phase of the cell cycle (Altieri 2003). Several studies have shown that survivin functions in the inhibition of apoptosis, but substantial evidence exists showing that wild-type survivin is also involved in regulating mitotic progression (Okada and Mak, 2004; Yang *et al*., 2006).

The involvement of survivin splice variants in cell cycle progression is not fully understood. The inhibition of survivin with specific antibodies resulted in delayed metaphase and gave rise to mitotic cells with shorter and less dense mitotic spindle (Li *et al*., 1998). In lung fibroblasts and retinal pigment epithelial cells, depletion of survivin caused defects in cell division but did not affect apoptosis (Yang *et al*., 2006). Inhibition of survivin expression suppressed growth of different types of cells, including gastric orthotopic transplantation tumour cells (Wang *et al*., 2016), colorectal cancer cells (Ye *et al*., 2014) as well as A549 cell growth *in vitro* and *in vivo* (Li *et al*., 2013). It is therefore, clear that the role of survivin in cancer biology far exceeds the simple inhibition of apoptosis.

Since survivin has been implicated in the regulation of the mitotic spindle checkpoint, from kinetocore to spindle assembly, its overexpression in cancer may allow cells with spindle defects or misaligned kinetochores to continue through cell division (Alterieri, 2003). In addition to its direct role in carcinogenesis, survivin may also play a key role in tumour angiogenesis because it is strongly expressed in endothelial cells during the remodelling and proliferative phase of angiogenesis (Luo *et al*., 2006). Survivin wild-type illustrated a cell-cycle dependent expression with a noticeable increase in the G2/M phase (Li *et al*., 1998; Liao *et al*., 2011). In addition, Jha *et al*. (2012) suggested that in metaphase, survivin localizes to kinetochores and then translocates to the central spindle middle zone in anaphase. It accumulates to mid-bodies in telophase. In various cancer cell lines, survivin is up-regulated in G2/M phase. Ruchaud *et al*. (2007) suggested that an alternative likelihood is that survivin stimulates mitosis by acting as an interphase

between the centromere and the chromosomal passenger complex (CPC). It remains less understood if the novel splice variants play part in these processes. Although expression of survivin wild-type during cell cycle progression and apoptosis has been studied, little is known about the expression of spliced variants, especially in arsenic trioxide and cobalt- mediated cell cycle arrest of MCF-7 cells.

2.4. Survivin and apoptosis

Apoptosis or programmed cell death is a naturally occurring process in the body where cells undergo death to maintain cell homeostasis (Ghobrial *et al*., 2005). It involves a controlled sequence of steps in which cells signal self-termination. Apoptosis works to keep the body's natural cell division process in check. It plays important functions in many normal processes ranging from the foetal development to adult tissue maturation. It is differentiated from necrosis by morphological features such as cell shrinkage, nuclear DNA fragmentation and membrane blebbing (Hengartner, 2000; Rich *et al*., 2000).

As demonstrated in figure 2.3, there are two most studied apoptotic pathways that lead to cell demise:the intrinsic (mitochondrial-dependent) and extrinsic (death receptors-dependent). During the intrinsic pathway, a cell initiates the suicide process from inside, which results in the demise of the cell (Wei *et al*., 2013). As a result, the cell suffers a reduction in size as its cellular components and organelles break down and become packed in the cytosol. Bubble shaped balls called blebs appear on the surface of the cell membrane. The cell then breaks down into smaller fragments called apoptotic bodies. These fragments are enclosed in membranes so as not to harm nearby cells. Then phagocytic cells, usually macrophages, engulf and destroy the apoptotic bodies without causing an inflammatory reaction (Ashkenazi, 2008). Apoptosis can also be triggered externally by chemical substances that bind to specific receptors on the cell surface. This is the pathway used by certain white blood cells to activate apoptosis in infected cells and this is called the extrinsic apoptotic pathway (Duiker *et al*., 2010).

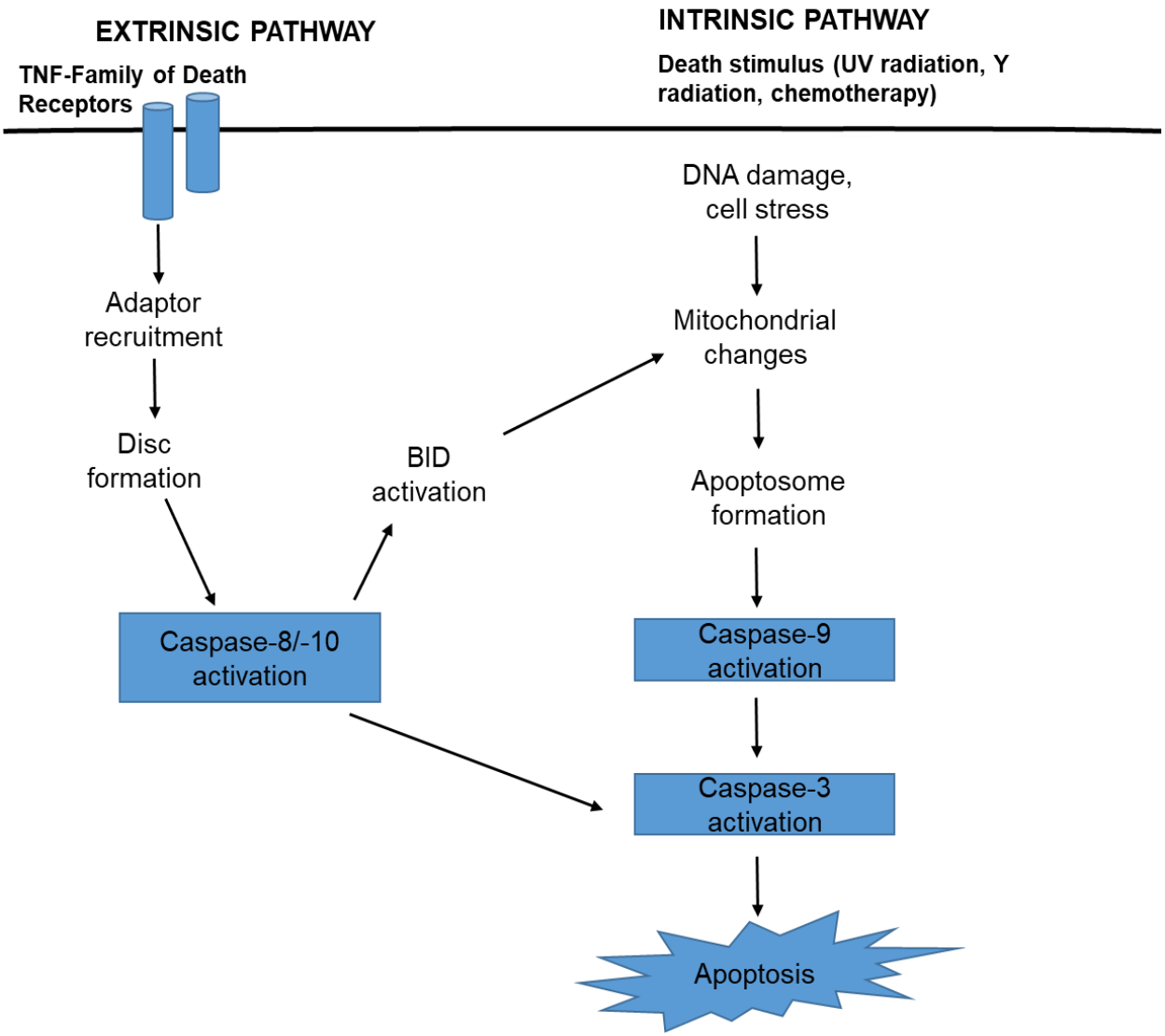

Figure 2.3 – The intrinsic and extrinsic apoptotic pathways: Activation of cell death pathways can be initiated through different mechanisms, including through ligand binding (FasL, TNF) to a death receptor on the cell surface (extrinsic pathway) or via direct mitochondrial signalling (intrinsic pathway). The figure was adapted from Tan *et al*. (2014)

Failings in apoptotic pathways are now thought to contribute to a number of human diseases including malignancy. Balance exists between pro and anti-apoptotic effector molecules, which permits the cell to survive with limited mitochondrial damage, where the IAPs can adequately block caspase activation initiated by a small amount of released cytochrome *c*.

Nevertheless, under circumstances where mitochondrial damage begins to affect multiple mitochondria, IAPs have been shown to be regulated by IAP binding proteins such as second mitochondrial activator of caspases (Smac/ DIABLO) [Dalla *et al*., 2014]. There is growing evidence that cancer cells have a core drive to apoptosis that is held in check by IAPs including survivin (Yang *et al*., 2003). Tumour cells, but not normal cells also expressed high levels of IAPs, suggesting that upregulated IAP expression counteracted the high basal caspase activity selectively in tumour cells (Garg *et al*., 2016).

Therefore, strategies targeting IAPs such as survivin are considered as a promising approach to enhance the efficacy of selective cytotoxic therapies against cancer cells (Ng and Bonavida, 2002; McKay *et al*., 2003). However, translocation of endogenous Smac/ DIABLO into the cytosol during anticancer drug- induced apoptosis does not appear to play a major role under certain conditions, for example, in human lung carcinoma cells upon treatment with etoposide (Bartling *et al*., 2004). On the other hand, survivin inhibits apoptosis by hindering activated caspases, usually the effector caspases-3 and caspase-7 and the initiator caspase-9 (Pisarev *et al*., 2003), leading to survival of damaged cells as demonstrated in figure 2.4. This has profound repercussions for tumour cell viability as expression of survivin is sufficient to promote cell growth and sustain exponential tumour growth (Dohi *et al*., 2004). Various studies have been reported on the regulation of survivin gene expression (Khan *et al*., 2010; Sun *et al*., 2014; Pan *et al*., 2018).

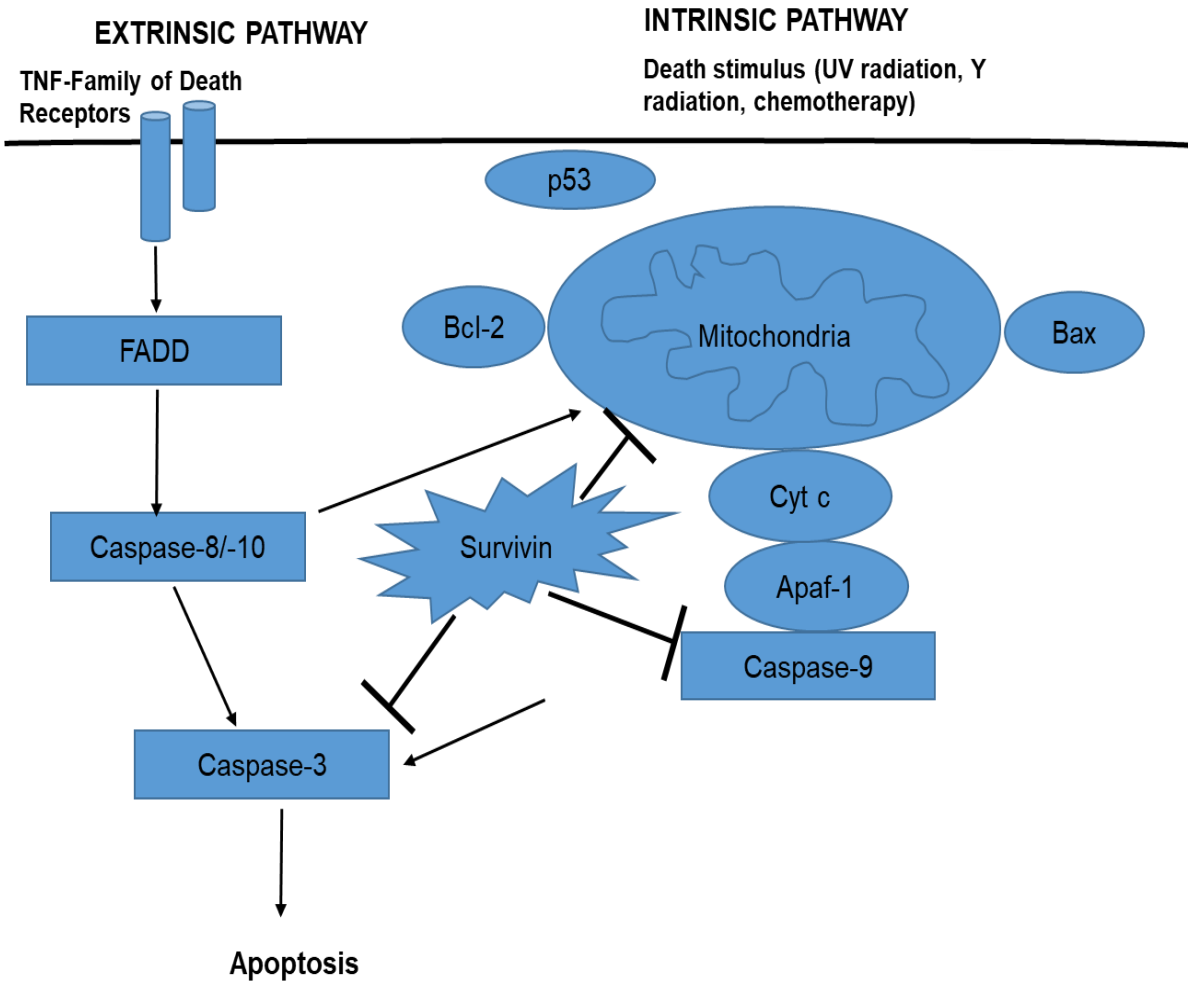

Figure 2.4 – The inhibition of apoptosis by survivin protein: Activation of cell death pathways can be initiated through different mechanisms, including through ligand binding (FasL, TNF) to a death receptor on the cell surface (extrinsic pathway) or via direct mitochondrial signalling (intrinsic pathway). The inhibitors of apoptosis (IAPs) inhibit cell death by physically interacting with caspases. Survivin has been shown to inhibit apoptosis through caspase-dependent and independent pathways. The figure has been adapted from Pisarev *et al*. (2003).

2.5. Regulation of survivin

2.5.1. Small molecule inhibitors

There are several small molecule inhibitors (GPD566, FL188 and YM155), which have been reported to target survivin and interfere with its function (Shi *et al*., 2010; Ling *et al*., 2012; Rauch *et al*., 2014). Despite the challenges associated with small molecule drug development, these inhibitors are important for understanding survivin biology and anticancer drug development. YM155 has been developed as a novel therapeutic agent and it has been used to treat metastatic breast cancer (Yamanaka *et al*., 2011). Interestingly, YM155 suppressed the expression of survivin-2B, ΔEx3 and 3B variants in human triple negative breast cancer (TNBC) cells and the reduced expression was accompanied by spontaneous apoptosis. This small molecule suppresses transactivation of survivin through direct binding to its promoter. It selectively suppresses expression of survivin and induces apoptosis in p53-deficient cancer cells *in vitro* (Feng *et al*., 2013; Wang *et al*., 2014; Cheng *et al*., 2015). YM155 has also been shown to be effective in *in vivo* models of prostate, pancreatic, and lung cancer (Nakahara *et al*., 2007; Giaccone *et al*., 2009; Na *et al*., 2012).

Terameprocol (EM-1421), a plant derived small molecule is a novel transcription inhibitor which suppresses survivin gene expression and induces apoptosis of cancer cells (Ryan *et al*., 2009). GDP366 is a novel small molecule compound, which effectively and selectively suppressed the expression of survivin (Shia *et al*., 2010). Another small molecule that suppresses survivin, FL118, has been shown to have a superior antitumor effectiveness in tumour xenograft models in comparison to standard anti-cancer drugs (Ling *et al*., 2012). MiRs are other small tumour suppressor molecules that have been used to regulate survivin expression (Lyu et al., 2018).

2.5.2. MicroRNAs as inhibitors of survivin

MicroRNAs are small noncoding RNA molecules consisting of about 22 nucleotides and are known to be present in plants, animals and some viruses. MiRs interfere with the expression of specific genes by binding to the 3′- untranslated region of their specific

mRNAs, resulting in mRNA degradation and affecting protein translation (Farazi *et al*, 2013). The MiRs can either act as an oncogene or tumour suppressor. Reports suggest that a class of microRNAs also play an important role in survivin dysregulation in human cancers (Gurtan *et al*., 2013; Markou *et al*., 2013; Huang *et al*., 2015).

Several MiRs such as MiR-203, which is the most studied survivin targeting MiR, directly targets survivin mRNA for degradation (Wei *et al*., 2013). MiR-34a has been shown to decrease the expression of survivin and its mechanism of action in controlling survivin expression varies from one cancer type to another (Cao *et al*., 2013; Ma *et al*., 2013). MiR-542-3p is one of the survivin specific MiRs, which contain multiple binding sites on the 3′- UTR of the survivin mRNA, which directly regulates survivin expression primarily via binding at the second predicted binding site (Zhang *et al*., 2016) and has been demonstrated to decrease the expression of survivin wild-type in human cancer cells. None of these MiRs have been reported to be specific to the other survivin variants. Antisense approaches to block survivin have also been tested. Another specific survivin small interfering RNA (siRNA) have also been shown to inhibit survivin expression in breast cancer MCF-7 cells, induced apoptosis and inhibit proliferation (Wang and Ye, 2015).

Almost all survivin small molecule inhibitors have been designed based on protein-protein interactions between survivin and other partner proteins. Since survivin functions through multiple mechanisms using a variety of partner proteins, hindering one pathway may not completely point to reduction of its signalling. Small molecules are cost effective and have short development time as compared to immunotherapeutic approaches. Therefore, there is enough reasoning to discover and improve existing small molecule inhibitors of survivin. Immunotherapy approaches, although complex in terms of translational development, are specific and have long lasting effects. However, tumour adaption and immune evasion is one bottleneck to the success of immunotherapy strategies. Moreover, small molecule targeting survivin alone has not demonstrated a completely curative response. Therefore, a synergistic combination of small molecules with immunotherapy may be explored to induce and sustain tumour elimination over a course of time. New drug targets are needed and new effective compounds need to be studied or investigated. Arsenic trioxide had shown a great deal of promise against cancers.

2.6. Arsenic trioxide

Arsenic trioxide is an extremely toxic soluble white inorganic compound with the formula, As_2O_3. Even though arsenic can be toxic, with prolonged exposure from industrial or natural sources resulting in serious harmful effects, arsenic has been used therapeutically for decades because of its anticancer properties (Antman, 2001). Arsenic trioxide has been used to treat acute promyelocytic leukaemia (APL) and has activity *in vitro* against numerous solid tumour cell lines where the induction of differentiation and apoptosis are the major effects (Wang *et al*., 2010; Ma *et al*., 2011). Arsenic trioxide at low concentrations (0.1 – 0.5 mol/L) has been reported to induce differentiation of APL cells through degradation of PML (the characteristic APL fusion protein)-RARα (retinoic acid receptor alpha), while at high concentrations (0.5–2 mol/L) induces apoptosis through both PML-RARα-dependent and independent mechanisms (Zhang *et al*., 2010). In contrast, low doses of arsenic trioxide, starting in the 2 mol/L range, combined with U0126 caused considerably improved cell growth inhibition of MCF-7 breast carcinoma cells (Chow *et al*., 2004). Stevens *et al*. (2017) reported that arsenic trioxide induced oxidative stress and cytotoxicity in HT-29 cells through the mitochondria mediated intrinsic pathway of apoptosis. Arsenic trioxide-induced apoptosis in HT-29 cells is associated with malondialdehyde formation, phosphatidylserine externalization, capase-3 activation and the down-regulation of Bcl-2. Several studies have shown that arsenic trioxide has anti-cancer activities against a variety of solid tumour models and cancer cell lines, including lung, liver, ovarian, cervical, breast and prostate cancers, the antitumor activities have been correlated with its ability to inhibit cell proliferation and induce apoptosis (Zekri *et al*., 2013; Lam *et al*., 2014; Wang *et al*., 2014; Yun *et al*., 2016).

Arsenic trioxide has been shown to downregulate survivin via the activation of p38 and JNK in an ubiquitin–proteasome independent pathway that leads to cytotoxicity and apoptosis in the human lung adenocarcinoma cell line, H1355 (Cheng *et al*., 2006). This is somewhat consistent with results that demonstrated that survivin expression inhibits cell death induced by various apoptotic stimuli *in vitro* (Dean *et al*., 2007) and *in vivo*

(Altieri, 2008). In addition, survivin isoforms were upregulated in APL patients, and their expression was diminished during the arsenic trioxide treatment (Zaki Dizaji *et al*., 2017). Treatment of A549 human non-small cell lung carcinoma (NSCLC) cells with arsenic trioxide reduced the expression of survivin and promoted major apoptotic signalling events, namely, the collapse of the mitochondrial membrane potential, release of cytochrome c, and activation of caspases (Jin *et al*., 2006). Arsenic trioxide-induced apoptosis and autophagy via downregulation of survivin. This was suggested by the finding that treatment with survivin shRNA reduced the viability of U118-MG cells and increased apoptotic and autophagic cells compared to control shRNA. In addition, arsenic trioxide treated U118-MG cells that were pre-treated with specific chemical inhibitors of Phosphatidylinositide 3-kinases (PI3K) and Mitogen-activated protein kinase (MAPK) showed significant changes in cytotoxicity and survivin expression. Thus, it is likely that survivin may act as an ideal target for glioma gene therapy treatments as the compound induced autophagy and apoptosis in human glioma cells *in vitro* and *in vivo* through downregulation of survivin (Chiu *et al*., 2011).

2.6.1. Therapeutic strategies using arsenic trioxide alone or in combination

The use of arsenic trioxide as a cancer drug is one of the astonishing developments in clinical oncology where arsenic trioxide changes from being the "king of poisons" to a "broad spectrum anti-cancer drug" (Wang *et al.*, 2012). Regardless of being the backbone of *materia medica* since the past 2,400 years, arsenic trioxide faced an escalating decline in its use as a therapeutic agent in the twentieth century due to an increasing awareness of its toxicity (Evens *et al*., 2004). Its reappearance become known in the late twentieth century when a group of Chinese physicians recognized it as the main anti-leukemic ingredient in traditional Chinese medicine and decided to assess its therapeutic effectiveness in treating patients with acute promyelocytic leukaemia (APL), a subtype of acute myeloid leukaemia (Shen *et al.,* 1997). Clinical trials using arsenic trioxide to treat APL patients as a single agent or in combination with other drugs produced extremely promising results (Shen *et al*., 1997). Arsenic trioxide was consequently approved in the United States of America by the Food and Drug Administration (FDA) as frontline therapy for APL in 2000 (Antman, 2001). Related clinical successes were subsequently translated

for other haematological malignancies, for example, acute myeloid leukaemia, chronic myelogenous leukaemia, Hodgkin's disease and multiple myeloma although not significantly for solid tumours (Zhang *et al*., 1996). Rapid clearance of arsenic trioxide and its products from the blood by the reticuloendothelial system (RES) bounds the therapeutic dose reaching the tumour site. Increasing arsenic trioxide dosage could not be a solution as it led to systemic toxicities such as long-term memory damage, liver failure, cardiac failure and peripheral neuropathy (Swindell *et al.*, 2013). From that time, several attempts have henceforth been carried out to utilize arsenic significant anti-cancer properties for treating solid tumours by increasing its bioavailability and specificity for carcinoma cells while reducing its administered dosage (Kang *et al.*, 2008). These include preparing the cells prior to arsenic trioxide treatment, employing it in combination therapy with other conventional chemotherapeutic agents to explore their synergistic actions or employing nanotechnology to increase bioavailability of arsenic trioxide while reducing its systemic toxicity (Emadi and Gore, 2010; Zhang *et al.*, 2015).

Anti-cancer activity of free arsenic trioxide has been tested on a variety of solid tumour cell lines with positive experimental results but wih limited clinical success. Zhao *et al.* (2008) administered direct intra-tumoral injections of arsenic trioxide to human oesophageal carcinoma xenografts in mice and investigated arsenic trioxide distribution and its efficacy within the tumour. Tumour growth inhibition of 13.56%, 62.37% and 76.92% was observed with administration of 1, 5 and 10 mg/mL of arsenic trioxide, respectively without appreciable systemic side effects. These results provided encouraging evidence for potential clinical utility of direct intra-tumoral injections of arsenic trioxide as one form of treatment for solid cancers. However, there is an escalating need to investigate other approaches where arsenic trioxide can be delivered selectively to its site of action and to penetrate inside the tumour without being toxic to surrounding healthy tissue. Therefore, there is a crucial need for analysing various possible approaches of increasing the bioavailability of arsenic trioxide without raising its dosage.

2.6.2. The potential of nanomedicine-Arsenic trioxide delivery

Nanotechnology is the discipline that deals with the design, characterization, production, and application of structures, devices, and systems by controlled manipulation of size and shape with the size range from a few nanometers (nm) to several hundred nm, depending on their intended use (Peer *et al*., 2007). For the last decade, nanotechnology has been the area of interest for emerging precise drug delivery systems as it offers numerous benefits to overcome the limitations, improve drug efficacy and safety for the treatment of cancer since it can enter the tissues at molecular level. Investigations are being carried out in order to determine more precise nanotechnology based cancer treatment with a reduction in side effects of the conventional ones (Malam *et al*., 2009; Sutradhar *et al*., 2013). Nanotechnology-based drug delivery systems for cancer treatment, which have been marketed and under research and evaluation, include liposomes, nanospheres, nanocapsules, and nanotubes (Praetorius and Mandal, 2007). Recently, it was discovered that fly ash can be used to make carbon nanomaterials (Hintsho *et al*., 2014). The synthesis of carbon nanomaterials (CNMs) has been well documented ever since the landmark paper by Iijima. (1991). Thereafter, more research was geared towards the production of new and better CNMs (Nalwa, 2004). In the last two decades, there has been a great interest in the formation of CNMs such as carbon nanospheres (CNSs) due to the properties they possess. These materials have been used in various applications, such as adsorption, drug delivery, energy storage and catalysis (Tripathi *et al*., 2014; Hintsho *et al*., 2016).

2.6.3. CNSs as drug delivery vehicles

CNSs have been shown to be ideal candidates as drug delivery vehicles because of their biocompatibility, adsorption capacity thus, they are able to adsorb drugs. Polymerization of these CNSs with OH containing groups has been shown to increase the hydrophilicity of the CNSs, thus improving their ability to be ingested by cell lines (Selvi *et al*., 2008; Ruan *et al*., 2014). With the advances in medicine, the need for targeted drug delivery is in demand to reduce the high cost of treatment associated with surgical methods and

other types of treatments. A study by Allen *et al*. (2004) was the first report of the use of CNMs as potential drug delivery vehicles.

CNSs are mostly synthesized from pure catalysts, which include sugar and starch by either using the chemical vapor deposition method (CVD) or the autoclave (Serp *et al*, 2001; Reitz *et al*., 2008; Wang *et al*., 2009; Tang *et al*., 2012; Li *et al*., 2015). Due to their demand, the cost associated with their production has risen, especially in terms of the catalysts that are required. Additionally, the autoclave method that is mostly used when synthesizing from sugar or starch often requires multiple steps, prolonged reaction time and high temperatures to produce CNSs of high quality. However, some studies have shown researchers are moving towards the production of low cost CNMs through the use of waste materials such as coal fly ash (Hintsho *et al*., 2014; Deng *et al*., 2016; Kumar *et al*., 2016). Coal fly ash has been identified as a potential material due to its metal composition (Co, Fe, and Ni) that are normally used in the synthesis of CNMs (Hintsho *et al*., 2014).

2.6.4. Delivering arsenic trioxide using nanomaterial

Delivery of arsenic trioxide, a clinical anticancer drug, has drawn much attention to improve its pharmacokinetics and bioavailability for efficient cancer therapy. Arsenic trioxide can be delivered selectively to its side of action and to penetrate inside the tumour without being toxic to the surrounding healthy tissues, with a low risk of recurrence (Zhao *et al*., 2015). For instance, liposome, polymersome and other nanoparticles have been successfully employed to deliver arsenic trioxide for efficient cancer treatment without escalating its dosage (Maeda *et al*., 2004; Cai *et al*., 2014; Zhao *et al*., 2014). Nonetheless, these single-function drug delivery systems are unable to track drug bio-distribution *in situ*, which is critical for evaluating the delivery and therapeutic efficiency of the drug (Liu *et al*., 2014). For that reason, the rationally designed multifunctional drug delivery systems (MDDSs) for both real-time monitoring of arsenic trioxide drug and efficient tumor treatment are necessary but remain challenging.

Zhao and colleagues (2015) performed a study where they loaded water-insoluble manganese arsenite complexes, the arsenic trioxide prodrug into hollow silica

nanoparticles to form a pH-sensitive multifunctional drug delivery system. Acidic stimuli triggered the immediate release of manganese ions and arsenic trioxide, which intensely increased the T1 signal (bright signal) and enabled real-time visualization and monitoring of arsenic trioxide release and delivery into HeLa, HepG2, SMMC-7721 and H22 cells. Moreover, this smart multifunctional drug delivery system significantly improved arsenic trioxide efficacy and strongly inhibited the growth of solid tumors without adverse side effects. This approach shows a great potential for real-time monitoring of theranostic drug delivery in cancer diagnosis and therapy. Since it has been reported that the coal fly ash can be used to synthesise nanoparticles, this study is aimed at determining the cytotoxicity and efficacy of using coal fly ash-derived *β*-cyclodextrin carbon nanospheres to deliver arsenic trioxide into breast cancer cells.

.

Chapter Three: Methodology

3. Introduction

The chapter covers materials (Chemicals and consumables, solutions and primer sequences) and methodologies (the synthesis and characterization of carbon nanospheres, the cell culture maintenance, 3-(4, 5-dimethylthiazolyl-2)-2, 5-diphenyltetrazolium bromide (MTT) Assay, Muse® Count and Viability Assay, light and fluorescent microscopy morphological observations, Muse® cell cycle analysis, Muse® Multi-Caspase Assay, Muse® Annexin V and Dead Cell Assay, Muse® MitoPotential Assay, Muse® MAPK Assay, Muse® PI3K Assay, RNA extraction, Polymerase Chain Reaction and Immunocytochemistry and the prediction of survivin variants specific MiRs used in this study to achieve the relevant aims and objectives.

3.1. Materials

This section covers all the chemicals and consumables, buffers and solutions and cell lines throughout the project and the companies they were purchased from.

3.1.1. Chemicals and consumables

Consumables and reagents were purchased from different companies as tabulated in Table 3.1, below. The recipes for the preparation of solutions used in this study are given in Table 3. 2.

Table 3.1: The list of chemicals and consumables used in the study.

Reagent/Consumable and Kits	Company and Country of Origin
Cell culture flasks and plates	Cell Star, United States of America (USA)
Bovine Serum Albumin (BSA)	Sigma-Aldrich, Germany
4′,6-diamidino-2-phenylindole (DAPI)	ThermoFischer Scientific, USA
Foetal bovine serum (FBS)	Sigma-Aldrich, Germany
Dimethyl sulfoxide (DMSO)	Saarchem, Republic of South Africa (RSA).
Paraformaldehyde	Sigma-Aldrich, Germany
Triton™ X-100	ThermoFischer Scientific, USA
Ethidium bromide	ThermoFischer Scientific, USA
Agarose	Sigma-Aldrich, Germany
DMEM	Hyclone, USA
Phosphate Buffered Saline (PBS)	Sigma-Aldrich, Germany
Penicillin and streptomycin	Biowest, USA
Arsenic trioxide	Sigma-Aldrich, Germany
Cobalt chloride	Saarchem, RSA
Curcumin	Sigma-Aldrich, Germany
Trypsin	Lonza, USA
Hydrogen, nitrogen and acetylene	Afrox, RSA
ReliaPrep™ RNA Cell MiniPrep System	Promega, USA
AMV II Reverse Transcription System	Promega, USA
EmeraldAmp® GT- PCR Kit	Takara Bio, USA
Muse® Assay Kits (Muse® Count and Viability Assay, Muse® Cell Cycle Assay, Muse® Annexin V and Dead Cell Assay, Muse® MitoPotential Assay, Muse® Multi-Caspase Assay, Muse® MAPK Assay and Muse® PI3k Assay)	Merck-Millipore, Germany
Survivin recombinant rabbit monoclonal antibody (Product # 700387) and Alexa Flour® 488 goat anti-rabbit IgG secondary antibody(Product #A-11008)	ThermoFischer Scientific, USA

3.1.2. Buffers and solutions

Table 3.2: Recipes of all the solutions that were used in the study.

Solution	Preparation/Recipe
10X 3-(N-Morpholino) Propane-Sulfonic acid (10X MOPS)	3-(N-Morpholino) Propane sulfonic acid (209.5 g/mol), Sodium acetate 3H2O (136.1 g/mol) or NaAc, anhydrous dehydrate (82 g/mol) Ethylenediaminetetraacetic acid (EDTA) (372.24 g/mol), Formaldehyde (37 %), 0.1 M Sodium hydroxide (NaOH)
10X Tris-Borate buffer (TBE)	108 g Tris base (121.1 g/mol), 55 g Boric acid 9.3 g EDTA (372.2 g/mol) Dissolved in sterile distilled water up to 1 L 1 X Tris-borate-EDTA (TBE) buffer: Measured 100 mL of the 10x TBE buffer and added 900 mL of sterile distilled water to make 1 L.
Gel loading buffer (#B7025S)	(Biolabs, New England)

3.1.3. Cell Lines

The MCF-7 breast cancer cells were used as the experimental cancer model cell line while the KMST-6 normal skin fibroblast cell line was used as the non-cancer experimental cell line and the colorectal cell line (Caco2) as the positive control cells for the PCR experiments.

3.2. Methods

This section covers the analytical techniques used in the study. The synthesis and characterization of carbon nanospheres which were done to analyse the structure and shape of the nanospheres using Transmission electron microscopy (TEM) and energy-disperive X-ray spectroscopy (EXD). The cell culture maintenance was done using the Biosafety Type-II cabinet and CO_2 incubator at 37°C. The 3-(4, 5-dimethylthiazolyl-2)-2, 5-diphenyltetrazolium bromide (MTT) Assay was done to determine the cytotoxic effect of *β*-cyclodextrin nanospheres, arsenic trioxide-*β*-cyclodextrin nanospheres, arsenic trioxide, cobalt chloride and curcumin. The Muse® Count and Viability Assay was done to confirm the MTT Assay results. The light and fluorescent microscopy were used to analyse morphological changes of KMST-6 cells and MCF-7 cells after treatment. Muse® Cell Cycle Assay was done to measure the DNA content of MCF-7 cells. Muse® Multi-Caspase Assay, Muse® Annexin V and Dead Cell Assay and Muse® MitoPotential Assay were done to analyse the cell death of MCF-7 cells. The Muse® MAPK Activation Dual Assay and Muse® PI3K Activation Dual Assay were done to analyse the mechanism in which arsenic trioxide, cobalt chloride and curcumin inhibit growth of MCF-7 cells. Polymerase Chain Reaction (PCR) and immunocytochemistry were used to assess mRNA and protein expression of survivin splice variants and isomers, respectively. Lastly, bioinformatics platforms were used to predict and evaluate survivin specific MiRs.

3.2.1. Synthesis and purification of *β*-cyclodextrin and arsenic trioxide beta-cyclodextrin carbon nanospheres (ATO-*β*-cyclodextrin CNSs)

All the gases used in this study were purchased commercially from Afrox, South Africa and were used without further purification. Waste coal fly ash was acquired from the Electricity Supply Commission (ESCOM) Research and Innovation Centre (Roscherville, South Africa) and was used without any treatment or modification. The growth of carbon nanomaterials (CNMs) was achieved by the catalytic chemical vapor decomposition of acetylene (C_2H_2) over fly ash (Work was done at the Department of Chemistry, University of Limpopo). In the synthesis reactions, fly ash was used as a catalyst whereas acetylene (C_2H_2) was used as a carbon source; nitrogen (N_2) and/or hydrogen (H_2) were used as transporters or reduction gases to create ideal reaction environments. In a typical synthesis experiment, 500 mg of as-received fly ash was uniformly spread in a quartz boat and placed in the center of a horizontal tube furnace to ensure controlled heating. A gas mixture (99.9%) of C_2H_2, N_2 and H_2 were introduced into the reaction tube through the gas inlet and exhausted through the gas outlet. Gas mixtures of three types (C_2H_2/N_2, $C2H_2/H_2$ and $C_2H_2/H_2/N_2$) with a total flow rate of 100 mL/min were studied. Furthermore, temperatures ranging from 450°C to 750°C were studied with these gas mixtures. The fly ash was first heated at 10°C/min in N_2, H_2 or a mixture of both for periods between 45 to 75 min to reach a desired temperature. Acetylene gas was then introduced into the reaction zone for a period of 45 min afterwards, the flow of C_2H_2 was stopped and the reactor was cooled naturally under N_2 and H_2 to ambient temperature.

For synthesis of arsenic trioxide-*β*-cyclodextrin CNSs, 200 mg of *β*-cyclodextrin CNSs was dispersed in 50 mL of 1 $mg.mL^{-1}$ of the arsenic trioxide solution and stirred at 50°C for 4 hrs. The arsenic trioxide-*β*-cyclodextrin CNSs were collected by centrifugation at 5000 rpm/min for 15 minutes, followed by washing with ethanol and double distilled water three times and dried in the oven overnight at 80°C.

3.2.2. Characterization of *β*-Cyclodextrin CNSs and arsenic trioxide-*β*-Cyclodextrin CNSs

The samples were characterized using the scanning electron microscopy (SEM) [Hitachi High Technologies America, Inc, USA], Energy Dispersive X-ray (EDX) [EAG laboratories, USA], Transmission Electron Microscopy (TEM) [EAG laboratories, USA], X-ray Diffraction (XRD), Laser Raman and Thermogravimetric analysis (TGA) [ThermoFischer Scientific, USA]. For SEM and EDX analysis, FEI Quanta 200 FEG ESEM instrument equipped with a field emission gun was used. To determine the morphology and particle size distribution of a technai G2 spirit, TEM, electron microscope at an accelerating voltage of 120 kV, was used. XRD measurements were conducted on a Bruker D2 phaser, using a Bregg Brenton geometry with a lynex detector using a Cu-K radiation at 30 kV and 10 mA. The structural features were investigated using a Jobin–Yvon T64000 Raman spectrometer. The thermal stability of each sample was determined using a Perkin Elmer Pyris 1 TGA system. For TGA, each sample was heated to 900°C at a rate of 10°C/min under air (20 mL/min). The mass of each sample was kept constant (ca. 10 mg) in order to reduce any effects in the variability of samples.

3.2.3. Cell culture maintenance

The breast cancer MCF-7 cell line (HTB-22™), normal skin cell (KMST-6) and colorectal cancer Caco2 cell line (HTB-37™) were donated by Prof Mervin Meyer from the University of the Western Cape, South Africa. The cell lines were cultured in Dulbecco Modified Eagle Medium (DMEM), supplemented with 10% of foetal bovine serum (FBS) [Hyclone, USA] and 1% antibiotic mixture containing penicillin and streptomycin (ThermoFischer Scientific, USA). The cells were maintained in culture flasks at 37ºC in a humidified incubator containing 5% CO_2.

3 2.4. *In Vitro* cytotoxicity Assay

For *in vitro* cytotoxicity Assay, two Assays were utilized. Firstly, the MTT Assay was used to determine the cell viability of KMST-6 cells in response to *β*-cyclodextrin CNSs and arsenic trioxide and MCF-7 cells in response to *β*-cyclodextrin CNSs, arsenic trioxide-*β*-

cyclodextrin CNSs, arsenic trioxide, cobalt chloride and curcumin. It was then followed by the Muse® Count and Viability Assay which was done to confirm the MTT Assay results.

3.2.4.1. MTT Assay

The effect of *β*-cyclodextrin, arsenic trioxide-*β*-cyclodextrin CNSs, arsenic trioxide, cobalt chloride and curcumin on the viability of the KMST-6 and MCF-7 cells was determined using the 3-(4, 5-dimethyl-thiozol-2-yl)-2, 5-diphenyltetrazolim bromide (MTT) Assay, according to the manufacturer's instructions. Briefly, the cells were cultured in a flask until 70% confluency. The cells were then counted using the Countess Cell Counter (ThermoFischer Scientific, USA) and 2 X 10^3 cells/well were seeded in 96-well plates and incubated overnight to allow the cells to attach. Cells were then exposed to various concentrations of *β*-cyclodextrin CNSs, arsenic trioxide-*β*-cyclodextrin CNSs (0, 125, 250, 500 and 1000 µg/mL), arsenic trioxide (0, 2, 8, 16 and 32 µM), cobalt chloride which was used as the positive control for cell cycle arrest (0, 50, 100, 150 and 200 µM) for 24 hours, curcumin as positive control for apoptosis (0, 25, 50, 75, 100 and 125 µM) while the untreated cells were used as negative control cells. After the 24 hours incubation, the cells were washed with sterile 1 X PBS and 10 µL of MTT reagent (5 mg/mL) was added and incubated for an additional 4 hours. Following incubation, 100 µL of DMSO was added to dissolve the formed formazan crystals and incubated for a further two hours at room temperature (25°C) in the dark. Thereafter, absorbance readings were taken at a wavelength of 560 nm using microtiter plate reader (Promega, USA).

3. 2.4.2. Count and Viability Assay

Cells (2 X 10^5 cells/well) were cultured in six well plates, overnight. Following incubation, the cells were washed with sterile 1 X PBS and the KMST-6 cells were treated with 250 µg/mL of *β*-cyclodextrin CNSs and 32 µM of arsenic trioxide whereas the MCF-7 cells were treated with 11 and 32 µM of arsenic trioxide, 100 µM of cobalt chloride and curcumin 100 µM for 24 hours in appropriate cell culture conditions. The cells were counted and 1 X 10^6 cell/well were used for each sample. Following treatment, the cells were trypsinized and centrifuged at 300 x *g* for 5 minutes. The cells were then re-suspended in 20 µL cell culture medium and 380 µL Muse® Count and Viability Reagent was added to each sample. The samples were incubated for 5 minutes in the dark at room temperature and thereafter analysed using the Muse® Cell Analyser (Merck-Millipore, Germany).

3.2.5. Morphological examination (Normal light and fluorescence microscopy imaging)

MCF-7 cells (5 X 10^4 cells/well) were seeded in 24 well plates overnight. After incubation, the cells were then exposed to various concentrations of *β*-cyclodextrin CNSs, arsenic trioxide-*β*-cyclodextrin CNSs (0, 125, 250, 500 and 1000 µg/mL), arsenic trioxide (0, 4, 11, 16 and 32 µM), cobalt chloride (50 and 100 µM) and curcumin (50 and 100 µM) for 24 hours. After treatment, the cells were washed with sterile 1 X PBS and fixed with 3.7% paraformaldehyde for 10 minutes at room temperature. The cells were then washed twice with sterile 1 X PBS and stained with DAPI (5 µg/mL) for 15 minutes in the dark, at room temperature. After incubation, the cells were washed twice in 1 X PBS. Morphological changes of MCF-7 cells and KMST-6 cells were observed under the Eclipse Ti-U fluorescence microscope (Nikon Instruments Inc., USA) and the Olympus CKX53 Inverted Microscope, (Olympus, Japan), while images were captured using DSRI-1 camera and an LC-30 camera set (Olympus, Japan), respectively.

3.2.6. Cell Cycle Analysis

Cells (2 X 10^5 cells/well) were cultured in six well plates overnight. Following incubation, the cells were washed with sterile 1 X PBS and treated with 11 µM of arsenic trioxide and 100 µM of cobalt chloride for 24 hours in appropriate cell culture conditions, namely, the complete DMEM medium (Section 3.2.3). Following treatment, the cells were trypsinized and centrifuged at 300 x *g* for 5 minutes. The cells were then washed with sterile 1 X PBS and fixed for 3 hours in 70% ethanol at -20ºC. Following incubation, the cells were centrifuged, washed with sterile 1 X PBS and 200 µL of Muse® Cell Cycle Reagent was added and incubated in the dark for 30 minutes. The samples were analysed using the Muse® Cell Analyser (Merck-Millipore, Germany).

3.2.7. Annexin V and Dead Cell Assay

To determine if arsenic trioxide induces apoptosis, an Annexin V and Dead Cell Kit (Merck-Millipore, Germany) was used. Briefly, the cells (2 X 10^5 cells/well) were seeded in six well plates. After overnight incubation, the cells were treated with arsenic trioxide-*β*-cyclodextrin CNSs (0, 125, 250, 500 and1000 µg/mL), 32 µM of arsenic trioxide and 100 µM of curcumin for 24 hours. After incubation, the cells were trypsinized and centrifuged at 300 x *g* for 5 minutes. The cells were re-suspended in 100 µL of DMEM containing 1% FBS and 100 µL of the Annexin V and Dead Cell reagent (Company, Country) was added to each tube. Each sample was vortexed for 5 seconds and incubated in the dark at room temperature for 20 minutes. Samples were analysed using the Muse® Cell Analyser (Merck-Millipore, Germany).

3.2.8. MitoPotential Assay

Mitochondrial membrane depolarization, a marker of the intrinsic apoptosis pathway, was detected using the Muse® MitoPotential Assay according to the manufacturer's instructions. Briefly, cells (2 X 10^5 cells/well) were cultured in six well plates, overnight and then treated with 32 µM of arsenic trioxide and 100 µM of curcumin for 24 hours. After 24 hour treatment, the cells were trypsinized and counted using the Countess Cell counter (ThermoFischer Scientific, USA). Ten thousand (1 X 10^4) cells were used for each sample, which were then centrifuged at 300 x *g* for 5 minutes and re-suspended in 1 X MitoPotential buffer (MCH100110). The cell suspension for each sample was mixed with 100 µL MitoPotential dye (MCH100110) and incubated for 20 minutes at 37ºC. Following incubation, 5 µL MitoPotential 7-AAD (MCH100110) was added and placed in the dark for 5 minutes. The samples were then analysed using the Muse® Cell Analyser (Merck-Millipore, Germany).

3.2.9. Multi-Caspase Assay

Cells (2 X 10^5 cells/well) were cultured in six well plates overnight. The cells were then washed with sterile 1 X PBS and treated with 11 µM of arsenic trioxide and 100 µM of curcumin for 24 hours in appropriate cell culture conditions. The cells were counted and 1 X 10^5 were used for each sample. Following treatment, the cells were trypsinized and centrifuged at 300 x *g* for 5 minutes. The Multi-Caspase buffer (MCH100109) was used to re-suspend the cells and 50 µL of each sample was transferred to a new tube and 5 µL of Multi-Caspase reagent was added. Samples were incubated at 37°C in an incubator containing 5% CO_2 for 30 minutes, followed by addition of 150 µL Multi-Caspase 7-AAD (MCH100109) and placed in the dark for 5 minutes, at room temperature. The samples were analysed using the Muse® Cell Analyser (Merck-Millipore, Germany).

3.2.10. Mitogen-activated protein kinase (MAPK) Assay

The Muse® Mitogen-Activated Protein Kinase (MAPK) Assay was employed to detect the total protein expression and to measure the phosphotransferase activity of the mitogen-activated protein kinase. The cells (1 X 10^5 cells/well) were seeded in six well plates, overnight in a 37ºC humidified incubator containing 5% CO_2. The cells were then treated with 11 and 32 µM arsenic trioxide, 100 µM cobalt chloride and 100 µM curcumin for 24 hours. Following treatment, the cells were trypsinized and centrifuged at 300 x *g* for 5 minutes. The cells were re-suspended in 500 µL of 1 X MAPK buffer (MCH200104) and equal amount of fixation buffer was added. The samples were placed on ice for 5 minutes. The samples were centrifuged at 300 x *g* for 5 minutes, permeabilized by adding 1 mL of ice-cold permeabilization buffer (MCH200104) and placed on ice for 5 minutes. Following incubation, the cells were centrifuged at 300 x *g* for 5 minutes, re-suspended in 1 450 µL of 1 X MAPK buffer and 10 µL of antibody working cocktail (5 µL of anti-phospho-ERK1/2 [Thr202/Thr204, Thr185/Thr187], phycoerythrin and 5 µL of anti-ERK1/2 PECy5 conjugated antibodies) [MCH200104] was added and incubated for 30 minutes in the dark at room temperature. Following incubation step, 100 µL of 1 X MAPK buffer was added to each sample and centrifuged at 300 x *g* for 5 minutes. The cells were re-suspended in 200 µL of 1 X MAPK buffer and analysed using Muse® Cell Analyser (Merck-Millipore, Germany).

3.2.11. Phosphatidylinositide 3-kinases (PI3K) Assay

The Muse® phosphoinositide 3-kinase (PI3K) Assay was performed to detect the extent of Akt phosphorylation relative to the total Akt expression in given cell population. Similar to MAPK Assay, the cells (2 X 10^5 cells/well) were seeded in six well plates overnight in a 37ºC humidified incubator containing 5% CO_2. The cells were then treated with 11 and 32 µM arsenic trioxide, 100 µM cobalt chloride and 100 µM curcumin for 24 hours. Following treatment, the cells trypsinized and centrifuged at 300 x *g* for 5 minutes. The cells were re-suspended in 500 µL of 1 X PI3K buffer (MCH200103) and equal amount of fixation buffer (MCH200103) was added. The samples were placed on ice for 5 minutes. The samples were centrifuged at 300 x *g* for 5 minutes, permeabilized by adding 1 mL of

ice-cold permeabilization buffer and placed on ice for 5 minutes. Following incubation, the cells were centrifuged at 300 x *g* for 5 minutes, re-suspended in 1 450 µL of 1 X PI3K buffer and 10 µL of antibody working cocktail (5 µL of anti-phospho-Akt [Ser473], Alexa, Fluor®555 and 5 µL of anti-Akt/PKB, PECy5 conjugated antibodies) was added and incubated for 30 minutes in the dark at room temperature. Following incubation step, 100 µL of 1 X PI3K buffer was added to each sample and centrifuged at 300 x *g* for 5 minutes. The cells were re-suspended in 200 µL of 1 X PI3K buffer and analysed using Muse® Cell Analyser (Merck-Millipore, Germany).

3.2.12. Total RNA Extraction

In order to analyse the expression of survivin splice variants by conventional Polymerase Chain Reaction, complementary deoxyribonucleic acid (cDNA) from total ribonucleic acid (RNA) was synthesized. Total RNA from treated and untreated MCF-7 cells and caco2 cells was extracted using the ReliaPrep™ RNA Cell MiniPrep System (Promega, USA). According to manufacturer's instructions. In its entirety, the cells were grown in 75 mL cell culture flasks. The cells were treated with the following concentrations 11 µM of arsenic trioxide, 100 µM of cobalt chloride, 32 µM arsenic trioxide and 100 µM of curcumin for 24 hours in cell culture conditions previously described (Section 3.2.3). The media in culture flasks were removed and the cells were washed with sterile 1 X PBS. The BL + TG buffer (Promega, USA) was added to the cells. The cells were lysed by gentle pipetting over the surface several times and the lysates were transferred to sterile RNAse-free 15 mL tubes. This was then followed by the addition of 85 µL of 100% isopropanol and mixing by vortexing for 5 seconds. The lysate was transferred to the ReliaPrep™ Minicolumn Tube assemble and centrifuged at 12, 000 x *g* for 30 seconds at room temperature. This was repeated until all the lysate mixture in the 15 mL was finished. RNA Wash Solution (500 µL) was added to the ReliaPrep™ Minicolumn and centrifuged at 12 000 x *g* for 30 seconds at room temperature. DNase I was prepared in a new sterile tube, following the manufacturer's instruction (24 µL of yellow core buffer, 3 µL manganese (II) chloride ($MnCl_2$) and 3 µL of DNase enzyme were gently mixed by pipetting). To each column, 30 µL of the freshly prepared DNase I incubation mix was then applied directly to the membrane inside the column. Samples were then incubated for 15 minutes at room

temperature. After incubation, 200 µL of Column Wash Solution was added to the ReliaPrep™ Minicolumn tube and centrifuged at 12, 000 x *g* for 15 seconds at room temperature. This was then followed by addition of 500 µL RNA Wash solution and centrifuged at 13, 000 x *g* for 30 seconds at room temperature. RNA Wash Solution (300 µL) was added and centrifuged at 13, 000 x *g* for 2 minutes at room temperature. Each ReliaPrep™ Minicolumn was transferred from its collection tube to a sterile 1.5 mL elution tube and 50 µL nuclease-free water was added to the membrane. The samples were centrifuged at 12, 000 x *g* for a minute at room temperature. The column was removed and discarded. The elution tube was capped and the purified total RNA was stored at -80°until further use.

3.2.13. RNA Agarose Gel Electrophoresis

One gram of Agarose (Sigma-Aldrich, Germany) was weighed and dissolved in 100 mL of 1 X MOPS buffer (Table 3. 2) using a microwave. The gel was allowed to cool for 1 minute and 2µL of (0.0002 µg/µL) ethidium bromide (ThemoFischer Scientific, USA) was added and gently mixed. The gel was poured and allowed to cast in the gel tray with a comb in place. The comb was removed and the gel with formed wells was pre-run for 10 minutes. Before mixing RNA sample with loading dye, the RNA samples were heated at 65ºC for 5 minutes. The samples were then prepared by mixing 5 µL of RNA and 10 µL of gel loading buffer (#B7025S) [Biolabs, New England]. The RNA samples were run for 60 minutes at 90V. The gel was then viewed using the Bio-Imaging System (BioRad, USA).

3.2.14. Reverse Transcription (cDNA synthesis)

The Promega AMV II Reverse Transcription System (USA) was used to synthesize cDNA from the extracted total RNA (Section 3.2.12). The total RNA samples were thawed and used to reverse transcribe RNA following manufacturer's instructions. The reverse transcription components were mixed as tabulated in Table 3. 3.

Table 3.3: The components of the reverse transcription reaction.

Components	Amount	Final concentration
$MgCl_2$ (25 mM)	4.0 µL	5 mM
Reverse Transcription 10 X Buffer	2.0 µL	1 X
dNTP mixture (10 mM)	2.0 µL	1 Mm
Recombinant RNasin Ribonuclease Inhibitor (40 u/µL)	0.5 µL	0.8 u/µL
Oligo $(dT)_{15}$ Primers (500 µg/mL)	1.0 µL	20 µg/mL
Total RNA (1µg)	5.0 µL	0.2 µg
AMV Reverse Transcriptase (160 u/µL)	1.0 µL	6.4u/µL
Nuclease-free Water	4.5 µL	
Total reaction volume	**20 µL**	

After the addition of all the components with the reverse transcriptase added last, the samples were incubated at 42ºC for 15 minutes and then heated at 95ºC for 5 minutes. Finally, the samples were incubated at 4ºC for 5 minutes to inactivate the AMV reverse transcriptase and prevent it from binding to the cDNA. The cDNA samples were stored at -20ºC until further use.

3.2.15. Nucleic acids Quantification

Quantification of both RNA and cDNA was performed using the BeckMan Coulter Life Sciences UV Spectrophotometer (Life Science Instruments, USA). The readings were taken at 260 nm and 280 nm wavelengths. A ratio of 1.8-2.0 for RNA was regarded as pure quality.

3.2.16. Polymerase Chain Reaction (PCR)

The primers were manually designed (Section 3.2.16.1), validated using bioinformatics databases and purchased from Inqaba Biotech, South Africa. Following cell culturing (Section 3.2.3), RNA extraction (Section 3.2.12) and cDNA synthesis (Section 3.2.14) using the extracted total RNA, Polymerase Chain Reaction (PCR) was employed by firstly, optimizing each set of primers in order to get the appropriate annealing temperature at which each primer set works best. Secondly, once the annealing temperatures were obtained, the experimental PCR reactions were performed. After each run, the samples were subjected to DNA agarose gel electrophoresis and images were captured. The band intensity was measured using the Image J software (https://imagej.nih.gov/ij/docs/index.html).

3.2.16.1 Primer design

The primers were designed manually using the complete mRNA sequences (survivin wild-type [NM_001168], survivin 2B [NM_001012271] and survivin ΔEx3 [NM_001012270]) retrieved from National Center for Biotechnology Information (NCBI) database (https://www.ncbi.nlm.nih.gov). There were only coding sequence that were obtained for the other 3 variants (survivin 2α [AY_92772], survivin 3α [DQ_227257] and survivin 3B [AB_154416.]) in NCBI. The amino acid sequences for each variant were then downloaded from UniProt (www.uniprot.com) and then aligned using Muscle Multiple Sequence Alignment tool (www.EMBL.com) to determine the unique region in each variant. The unique nucleotide sequences were then identified and the primers designed manually using general primer design rules (Appendix A). Oligo Analyser 3.1 was used

to assess the properties of the primers; looking at the GC content and their melting temperatures (T_M).

Additionally, the blast tool (https://blast.ncbi.nlm.nih.gov/Blast.cgi) was used to ascertain the specificity of the each primer. The primers were designed in such a way that primer pairs had the same or close (less than 1ºC difference) melting temperatures (T_M). T_M was calculated using the formula: T_M= 4 (G+C) + 2 (A+T) and from the TMs obtained, the annealing temperatures (T_A) of the primers were derived by subtracting 5ºC. The primer pairs which had satisfied all the requirements are tabulated (Table 3.4).

Table 3.4: The primer sequences of all the survivin variants with their melting (T_M), annealing (T_A) temperatures and expected product lengths or sizes.

Survivin variant	Primers	Number of expected products	T_M (ºC)	T_A (ºC)	Product length (bp)
Survivin wild-type	Forward: TAAGAGGGCGTGCGCTCCC Reverse: ATGGCACGGCGCTCTTTCTC	3	64	59	490 (Wild-type) 640 (2B) 426 (Ex3)
Survivin 2α	Forward: GGAAGGCTGGGAGCCAGAT GCATCACCAAGGCACCAGC	1	62	57	120
Survivin 3α	Forward: CAGGGAGGGACTGGAAGCA Reverse: CTCCTGAAACTCCTGGAGGA	1	62	57	195
Survivin 2B	Forward: TGGGAGCCAGATGACGACCC Reverse: CCCTGGAAGTGGTGCAGCCA	1	66	61	329
Survivin 3B	Forward: CGTCCGGTTGCGCTTTCCTTT Reverse: TCAATCCATGGCAGCCAGCTG	1	66	61	400
Survivin ΔEx3	Forward: CTGGGAGCCAGATGACGACC	1	66	61	200

	Reverse: AAGGCTGGTGGCACCAGGGA				
Housekeeping gene					
GAPDH	Forward: AGCTGAACGGGAAGCTCACT Reverse: TGCTGTAGCCAAATTCGTTG	1	59	54	297

3.2.16.2. Polymerase Chain Reaction (PCR) components

The PCR components were thawed on ice and mixed as per manufacturer's instructions (Takara, Japan) [Table 3.5].

Table 3.5: The components of a PCR reaction

Components	Amounts	Final concentrations
EmeraldAmp® GT PCR Master Mix (2X)	12.5 µL	1 x
PCR water	9.5 µL	
Forward primer	1.0 µL	0.2 µM
Reverse primer	1.0 µL	0.2 µM
cDNA sample	1.0 µL	200 ng
Total reaction volume	**25 µL**	

The samples were subjected to Polymerase Chain Reaction using the T100™ Thermal Cycler (BioRad, USA) under different conditions as per primer set (Table 3.4).

The general PCR conditions were as follows:

Step 1: 98ºC for 30 seconds for initial denaturation for one cycle

Step 2: 96ºC for 30 seconds

Step 3: Annealing at T_A for 45 seconds

Step 4: Extension at 72ºC for 1 minute

Steps 2 to 4 were repeated for 25 to 30 cycles.

Step 5: Final extension at 72ºC for 5 minutes for one cycle.

3.2.16.3. DNA Agarose Gel Electrophoresis

One gram of Agarose (Sigma-Aldrich, Germany) was weighed and dissolved in 100 mL of 1 X TBE buffer (Table 3.2) and microwaved for 3 minutes. The gel was allowed to cool

for 1 minute and 2 µL of 0.0002 µg/µL ethidium bromide was added and gently mixed. The gel was poured and allowed to cast in the gel trays with a comb in place. After the gel had set, the comb was removed and the gel with formed wells was pre-ran for 10 minutes. The samples were loaded and ran for 60 minutes at 90 V. The gel was then viewed using the BioRad Bio-Imaging System (BioRad, USA). The band densities from three independent experiments were measure using Quanty-One 4.6.5 software (BioRad, USA).

3.2.17. Immunocytochemistry

The cells (1 X 10^5 cells/well) were seeded in 12 well plates overnight. Following incubation, the cells were washed with sterile 1 X PBS and treated with 11 µM and 32 µM of arsenic trioxide, 100 µM of cobalt chloride and 100 µM curcumin for 24 hours at 37ºC in a humidified atmosphere as described in section 3.2.3. The cells were washed with sterile 1 X PBS and fixed in 4% of paraformaldehyde (Sigma-Aldrich, Germany) for 15 minutes. The cells were then permeabilized with 0.25% Triton™ X-100 (ThermoFischer Scientific, USA) solution for 10 minutes and blocked with 5% Bovine Serum Albumin (BSA) [Sigma-Aldrich, Germany] for 1 hour at room temperature. The cells were labelled with 5 µg/mL of survivin recombinant rabbit monoclonal antibody (Product # 700387) [ThermoFischer Scientific, USA] for 3 hours at room temperature. The full information for the antibody is provided in appendix B. The cells were then washed with sterile 1 X PBS, then survivin proteins were detected with 4 µg/mL of Alexa Flour® 488 goat anti-rabbit IgG secondary antibody (Product #A-11008) [ThermoFischer Scientific, USA] for 30 minutes in the dark. The cell nuclei were identified by counterstaining with 4', 6-diamidino-2-phenylindole (DAPI) for 5 minutes. The samples were examined using an Eclipse Ti-U fluorescence microscope (Nickon Instruments Inc. USA) and images were captured at 20X magnification. The fluorescence intensities for the survivin proteins were measured using the Image J software (https://imagej.nih.gov/ij/docs/index.html).

3.2.18. Prediction and literature survey of survivin splice variants specific MiRs

The survivin variants specific MiRs molecules were obtained from different bioinformatics platforms: MiRTarBase (www.MirTarbase.mbc.nctu.edu.tw), MIRDB (www.MIRDB.org) and TargetScan (www.TargetScan.org). Literature surveys (www.googlescholar.com, www.sciencedirect.com and www.ncbi.nlm.nih.gov) were done to assess the expression of MiRs during cell cycle progression and cellular apoptosis of various cancer cell lines.

3.2.19. Statistical analysis

All the experiments were done in triplicates and three independent experiments results were presented as ± SEM. The graphical data was analysed using Graph Pad Prism Version 6.0 Statistical Software using the Tukey Kramer Multiple Comparison test and the differences between two sets of data were considered significant where (*) $p \leq 0.05$ indicates significant, (**) $p \leq 0.01$ very significant and (***) indicate $p \leq 0.001$ meaning extremely significant, comparing each sample with the control.

Chapter Four: Fly Ash-Derived *β*-Cyclodextrin Carbon Nanospheres as Potential Drug Delivery Vehicles

4. Introduction

This section covers the cytotoxicity and efficacy of using coal fly ash-derived *β*-cyclodextrin carbon nanospheres as delivery vehicles. Firstly, analysis of the morphological and elemental analysis of *β*-cyclodextrin CNSs was done (Section 4.1), followed by determination of the cytotoxic effect of *β*-cyclodextrin CNSs and arsenic trioxide on the viability (Section 4.2 and Section 4.3) and morphology (Section 4.4) of KMST-6 cells.

4.1. Morphology and particle size distribution of *β*-Cyclodextrin CNSs

The scanning electron microscope (SEM) images of coal fly ash-derived showed that the material was spherical in shape, showing a turbostatic structure, demonstrated in figure 4.1a. As shown by the Energy dispersive X-Ray (EDX), coal fly ash-derived CNSs consisted mostly of carbon (Figure. 4.1b) and a few other trace metals (Au, Pd, O), indicating that some parts of the catalyst (fly ash) were unburnt during synthesis. The layered structure of the *β*-cyclodextrin CNSs indicated dangling bonds at the edges of the CNSs, thus making it easy for them to bond with other molecules. Transmission electron microscopy (TEM) in figure 4.1c further showed that coal fly ash-derived CNSs were monodispersed with a particle size distribution of approximately 200 nm (Figure.4.1d). To further confirm the formation of these *β*-Cyclodextrin CNSs and test their thermal stability, Laser Raman spectroscopy and TGA were conducted (appendix C). TGA showed that the *β*-cyclodextrin CNSs materials started decomposing early from 180–500°C, showing a slight decomposition by 20% which could be due to the physisorbed water and the polymeric nature of the material. A further major reduction was observed above 550°C showing that the material was no longer stable at temperatures above (Appendix C).

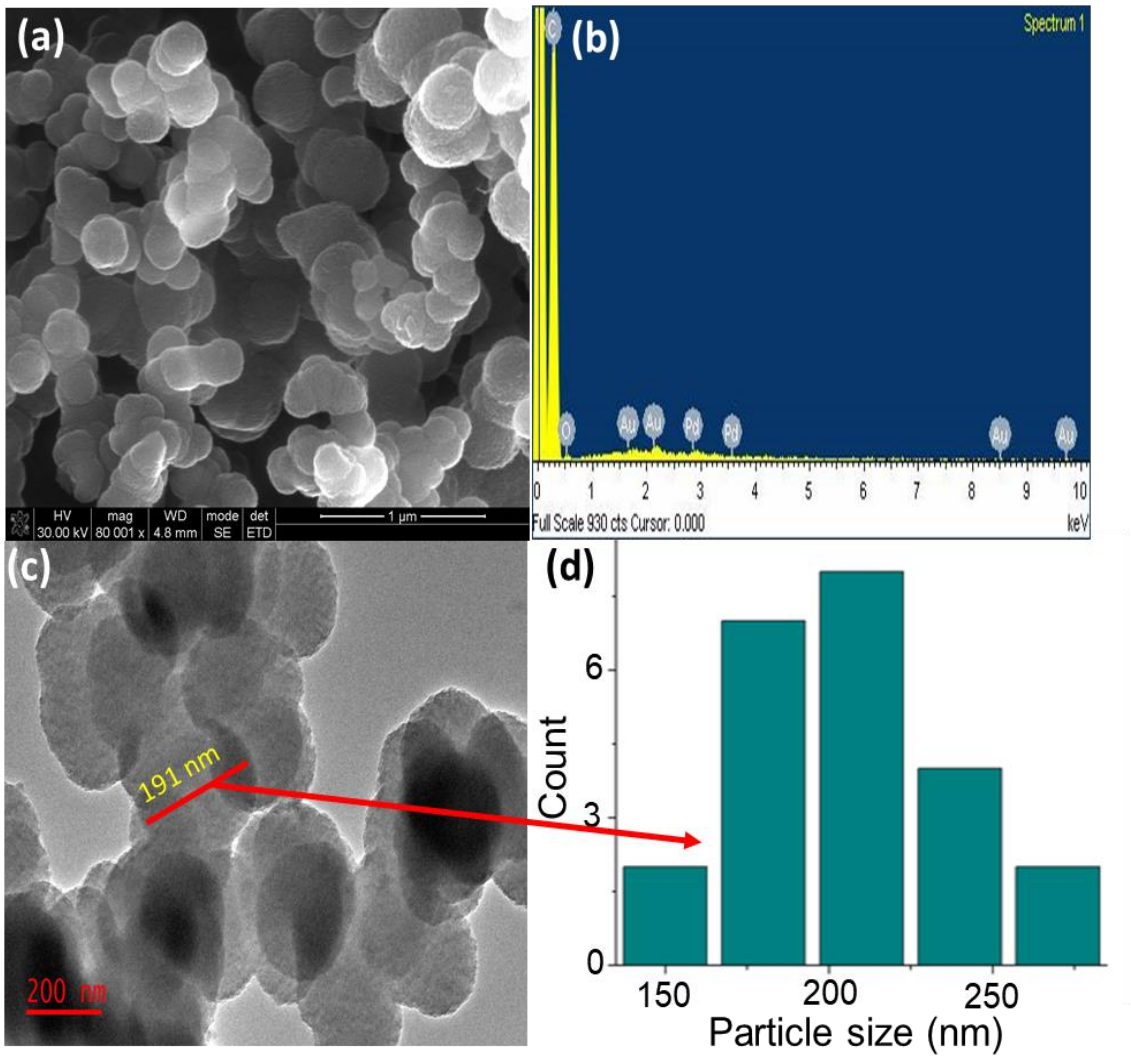

Figure 4.1 – Morphological characterization of the fly ash-derived *β*-cyclodextrin CNSs: SEM (a), EDX micrograph (b) and TEM (c) micrographs with particle size distribution (d) of *β*-cyclodextrin carbon nanospheres (CNSs) synthesized at 650°C.

4.2. MTT Analysis

In order to determine the safety and toxicity of the *β*-cyclodextrin CNSs, KMST-6 cell viability was determined using the standard MTT Assay (section 3.2.4). As shown in figure 4.2a and Table 4.1, the cell viability results showed that the treatment of KMST-6 cells with differing concentrations of the novel *β*-cyclodextrin CNSs had no significant effect on their cell viability with more than 80% cell viability observed across all the concentrations. This trend was also observed after exposing the same cells to different concentration of arsenic trioxide (Figure. 4.2b and Table 4.2).

Table 4.1: The MTT cell viability mean percentages and SEM of KMST-6 cells after 24 h exposure to *β*-cyclodextrin CNSs.

***β*-cyclodextryn CNSs (µg/mL)**	**Mean (%)±SEM**
Control	100.00±0.000
125	85.56±3.215
250	83.97±2.448
500	87.53±2.194
1000	101.11±4.281

Table 4.2: The MTT cell viability mean percentages and SEM of KMST-6 cells after 24 h exposure to arsenic trioxide.

Arsenic trioxide (μM)	**Mean (%)±SEM**
Control	100.00± 0.000
5	91.12± 1.862
10	91.88± 1.983
15	89.47± 2.462
20	91.21±1.688
25	90.43±1.263
32	91.19±1.825
64	90.36±1.999

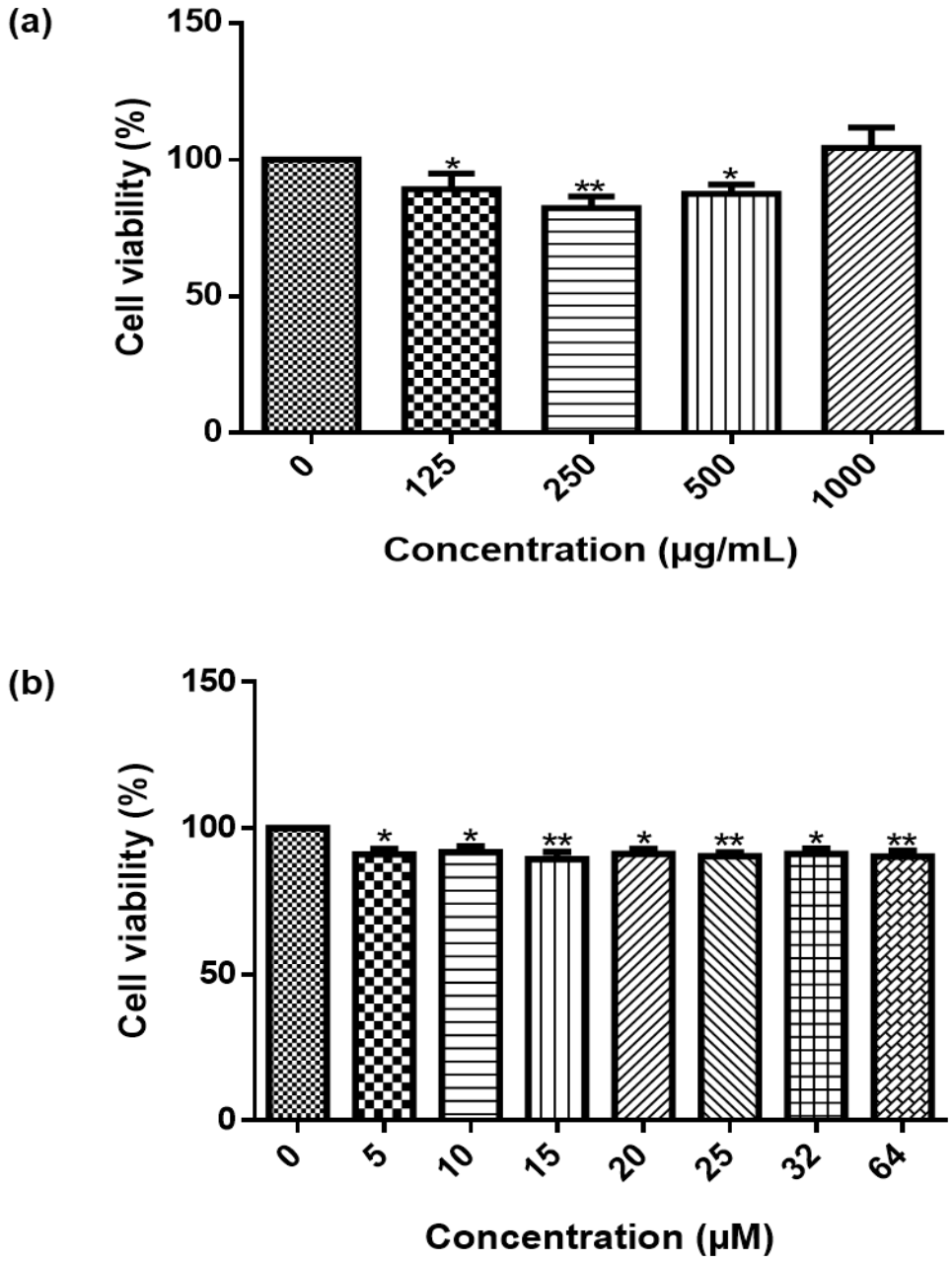

Figure 4.2 – Toxicity of the novel *β*-cyclodextrin CNSs and arsenic trioxide against KMST-6 cells: Cell viability of KMST-6 cells after treatment with (a) *β*-cyclodextrin CNSs at different concentrations and (b) arsenic trioxide at different concentrations after 24 h incubation. Shown are representative data of three independent experiments (percentage mean ±SEM). The difference were found to be statistically significant (* $P<0.05$ and ** $P<0.01$).

4.3. Muse Cell Viability profiles analysis

For further analysis and confirmation of the MTT results (Figure 4.2a-b), Muse® Count and Viability Assay (Figure. 4.3 and 4.4) showed that the *β*-cyclodextrin and arsenic trioxide increased viability of KMST-6 cells. The cell viability of the KMST-6cells was found to be 89.28±1.790 ($p<0.05$) after treatment with 250 µg/mL of *β*-cyclodextrin CNSs (Figure. 4.3a) and 95.16±0.275 ($p<0.001$) after treatment with 32 µM of arsenic trioxide (Table 4.3).

Table 4.3: The Muse® cell viability mean percentages and SEM of KMST-6 cells.

Treatment	**Mean (%)±SEM**	
	Live	**Dead**
Control	83.22±1.769	16.84±1.717
250 µg/mL of *β*-cyclodextrin CNSs	89.28±1.790	10.72±1.790
32 µM As_2O_3	95.16±0.275	4.84 ±0.275

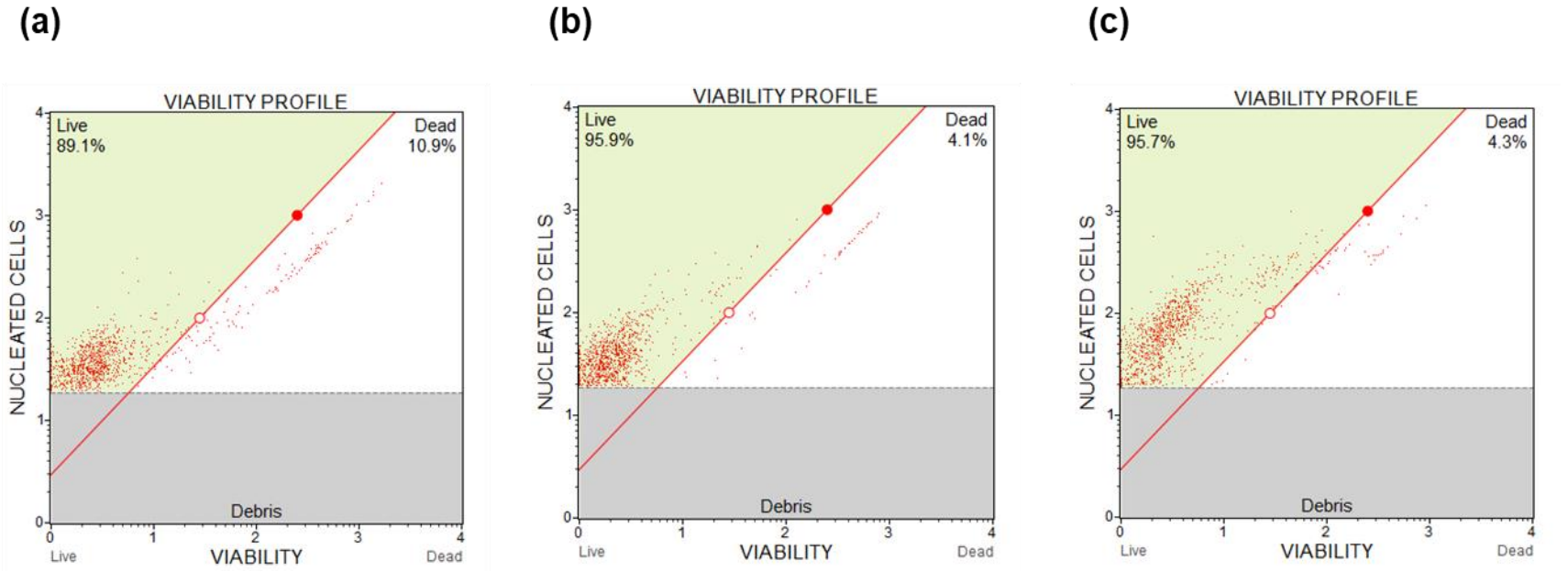

Figure 4.3 – Muse® Count and Viability profiles of the KMST-6 cells after 24 h treatment: (a) Untreated cells, (b) cells treated with 250 µg/mL of *β*-cyclodextrin CNSs and (c) and cells treated with 32 µM of arsenic trioxide. Muse® Cell Analyser was used to analyse the results.

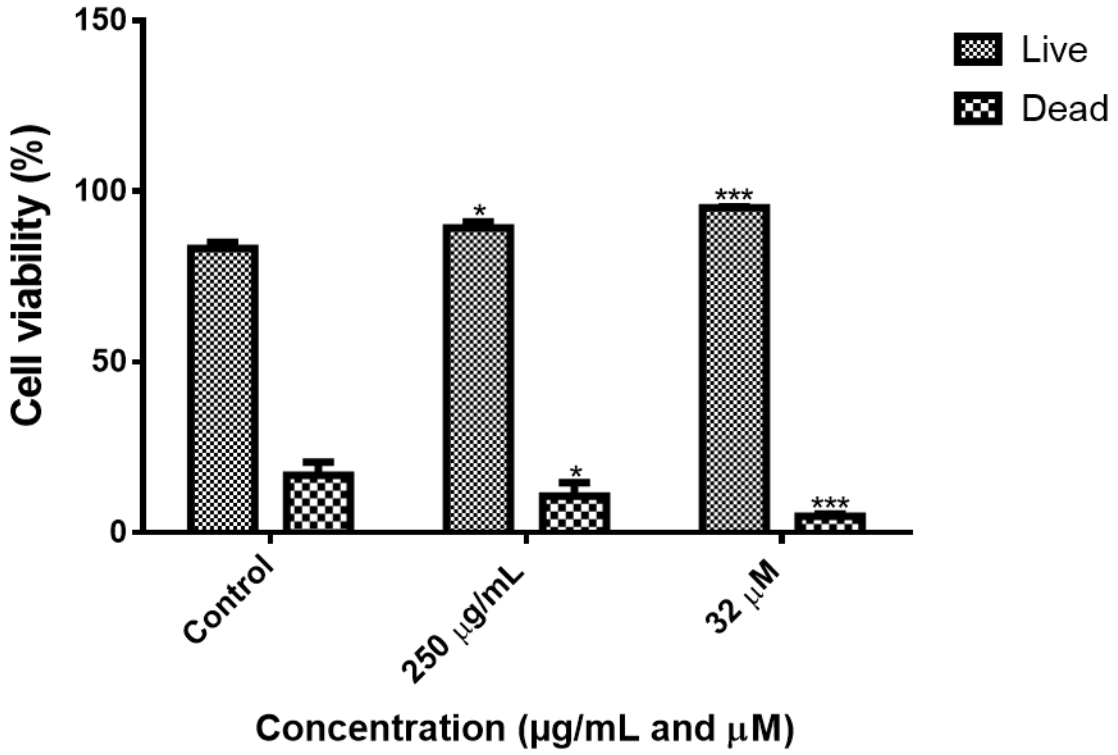

Figure 4.4 – Muse® Count and Viability analysis of the KMST-6 treated cells: The cell viability percentages of the KMST-6 cells treated with 250 µg/mL of *β*-cyclodextrin CNSs and 32 µM of arsenic trioxide for 24 h incubation. Shown are representative data of three independent experiments (percentage mean ±SEM). The difference were found to be statistically significant (* P<0.05 and ***P<0.001).

4.4. Morphological characterization of KMST-6 cells after exposure to *β*-cyclodextrin CNSs

Figure 4.5a-f shows the morphological characteristics of both untreated and treated KMST-6 cells. Both groups maintained the typical epithelial cell shape, as indicated by the yellow circles. In both untreated and treated cells, it was shown that the novel fly ash-derived *β*-cyclodextrin CNSs had no effect on the growth of the KMST-6 cells and this corroborated with the MTT results (Figure. 4.2a). The red cycles indicate the cells that are undergoing apoptosis through cell shrinkage.

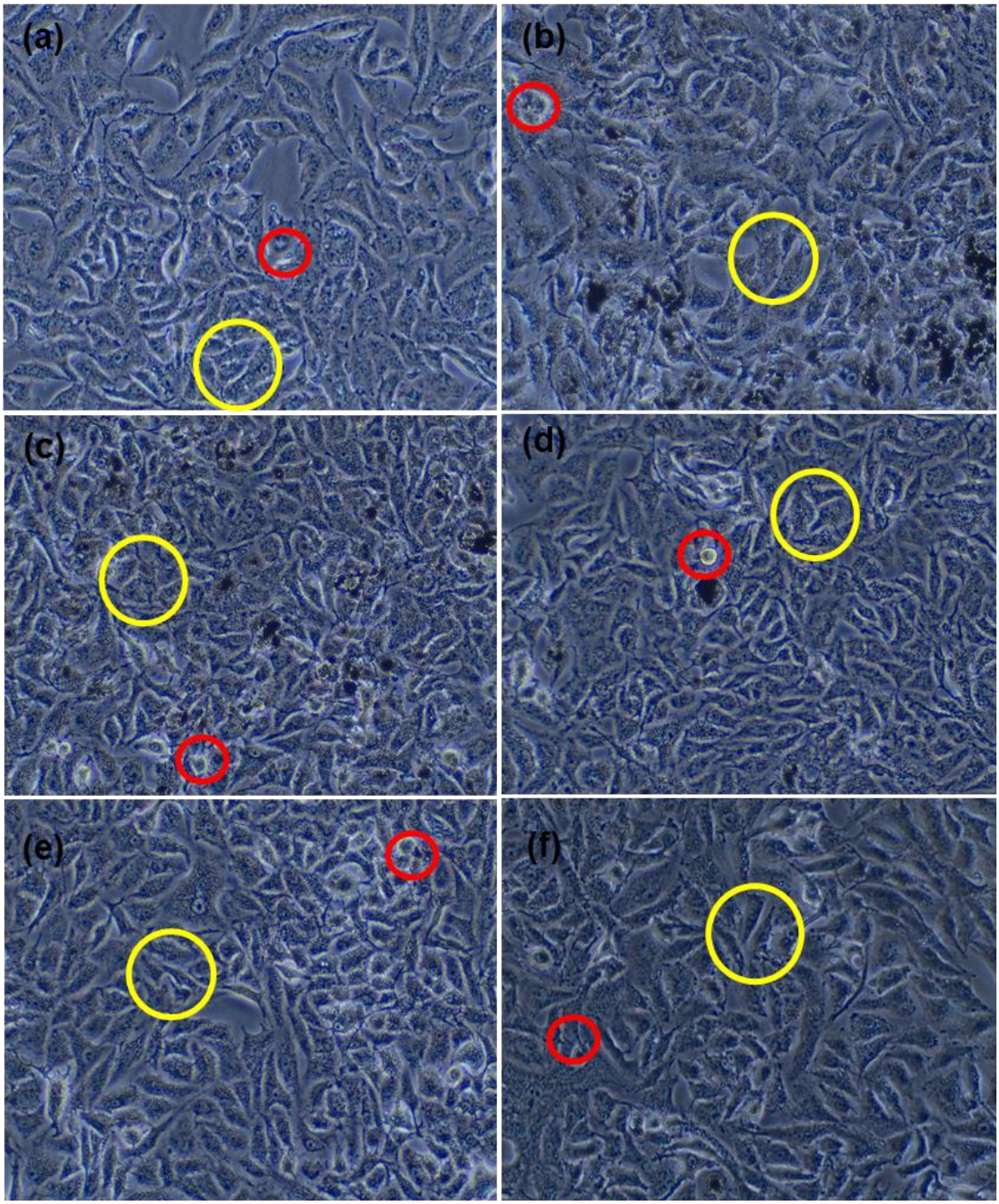

Figure 4.5 – Morphological characterization of the *β*-cyclodextrin CNSs-treated KMST-6 cells: The cells were exposed to various concentrations of nanospheres coated with cyclodextrin (b–f) and images were captured using an Olympus LC-30 camera set (Olympus, Japan).

4.5. Discussion

The synthesis of carbon nanomaterials (CNMs) has been well documented ever since the landmark article by Ijima (1991). In the last two decades, there has been a great interest in the formation of CNMs such as carbon nanospheres (CNSs) due to the properties they possess and hence, these materials have been found in various applications, such as adsorption, drug delivery, energy storage and catalysis (Tripathi *et al*., 2014; Hintsho *et al*., 2016). CNSs have been shown to be ideal candidates as drug delivery vehicles because of their biocompatibility and adsorption capacity, thus they are able to adsorb drugs. To date, there is limited data on the use of carbon nanospheres derived from waste material. The safety and biocompatibility of carbon nanospheres is vital for their biological applications. Carbonaceous nanospheres have been reported to have a good biocompatibility (Anderson and Shive, 1997; Ravi *et al*., 2004). Cytotoxicity of the *β*-cyclodextrin CNSs was evaluated at different concentrations against KMST-6 cell lines to determine their potential as a drug delivery vehicle.

The SEM images of the *β-c*yclodextrin CNSs prepared using coal fly-ash showed that the material was spherical in shape, depicting a turbostatic structure, demonstrated in figure 4.1a. As shown by EDX, they consisted mostly of carbon as shown in figure 4.1b and a few other trace metals (Au, Pd, O) indicating that some parts of the catalyst were unburnt during synthesis. The layered structure of the *β*-cyclodextrin CNSs indicated dangling bonds at the edges of the CNSs thus making it easy for them to bond with other molecules. TEM in figure 4.1c, further showed that these materials were monodispersed with a particle size distribution of approximately 200 nm, shown in figure 4.1d. To obtain more information on the material, structural and thermal stability studies were conducted. To further confirm the formation of these *β*-cyclodextrin CNSs and test their thermal stability, Laser Raman spectroscopy and TGA was conducted as shown in (Appendix A). The D and G bands at 1359 cm−1 and 1531 cm−1 respectively, showed that the materials were indeed carbon nanomaterials as indicated in previous studies (Ferreri *et al*., 2001; Jakka *et al*., 2010; Nath *et al*., 2011).

The safety and biocompatibility of carbon nanospheres is vital for their biological applications. Carbonaceous nanospheres have been reported to have a good biocompatibility (Anderson and Shive, 1997; Ravi *et al*., 2004). For the present study, cell viability studies were used to ascertain the safety and toxicity of these *β*-cyclodextrin CNSs to determine their potential as drug delivery vehicles. To evaluate the toxicity and their potential as delivery vehicles, KMST6 fibroblasts were treated with the coal fly ash-derived *β*-cyclodextrin, this study showed that coal fly ash-derived *β*-cyclodextrin CNSs derived from the coal fly ash have a potential as drug delivery material as shown in figure. 4.2a. The MTT cell viability Assay results showed that the exposure of KMST6 cells to varying concentrations of the novel *β*-cyclodextrin CNSs had no significant effect on their cell viability with more than 80% cell viability observed (Figure 4.3a and 4.4). A standard MTT Assay was also conducted to confirm the safety of arsenic trioxide alone on the KMST-6 cells. As shown in figure 4.2b, the cell viability results showed that the treatment of KMST-6 cells with differing concentrations of arsenic trioxide had no cytotoxic effect on KMST-6 cell viability as more than 90% cell viability was observed across all tested concentrations. Muse® Count and Viability Assay (Figure. 4.3b and 4.4) was conducted. The cell viability of the KMST-6cells was found to be over 90% after treatment with 32 µM of arsenic trioxide.

For further analysis and confirmation of the above results, morphological characterization of these cells was also conducted (Figure. 4). Figures 4a–f shows the morphological shape of both untreated and treated KMST6 cells maintained the typical epithelial cell shape. The few cells that demonstrated typical apoptotic features (red circled in Figure. 4.5) can be attributed to normal cell death when cells reach confluency and start competing for space and scarce nutrients. These results suggested the safety of this material for drug targeting and other applications that require safe materials. This is a good sign as this material can be developed as a safer drug delivery vehicle, because most drug delivery materials tend to be toxic against normal cells. Moreover, selectivity is very important in drug delivery as it is always ideal to target only cancer cells and spare the normal cells (Challa *et al*., 2005; Tiwari *et al*., 2012).

4.6. Conclusion

From this section of the study, novel coal fly ash-derived *β*-cyclodextrin CNSs from a waste material was successfully synthesized. TEM studies showed this material was spherical in shape and had a monodispersed particle size distribution. Thermal stability studies showed the material would be suitable for *in vitro* studies in medical applications. Cell viability studies showed the materials are safe and could be used as potential drug delivery vehicles.

Chapter Five: Delivery of arsenic trioxide using the novel β-Cyclodextrin fly ash-derived carbon nanospheres

5. Introduction

After confirming the safety of β-cyclodextrin CNSs and arsenic trioxide alone on the KMST-6 cells, the study was extended further to investigate the ability of β-cyclodextrin CNSs to funtion as vehicles for the delivery of arsenic trioxide into MCF-7 cells. This chapter covers the morphological and element analysis of the coal fly ash-derived β-cyclodextrin CNSs and arsenic trioxide-β-cyclodextrin CNSs (Section 5.1), followed by the investigation of the cytotoxic effect of coal fly ash-derived β-cyclodextrin CNSs and arsenic trioxide-β-cyclodextrin CNSs on viability (Section 5.2) and morphology of MCF-7 cells (Section 5.3 and 5.4). Lastly, apoptotic cell death was evaluated (Section 5.5).

5.1. Morphologcal and elemental analysis of arsenic trioxide-β-Cyclodextrin CNSs

The shape, morphology and elemental analysis of the β-cyclodextrin CNSs and arsenic trioxide-β-cyclodextrin CNSs were investigated using SEM coupled to EDX. The results, as demonstrated in figure 5.1a-d, showed these materials were both confirmed to be spherically shaped (Figure 5.1a and c) and consist mostly of carbon as shown in the EDX analysis (Figure. 5.1b and d). As depicted in Appendix D, upon testing the thermal stability of these materials, the arsenic trioxide-β-cyclodextrin CNSs started decomposing at a higher temperature (230°C) as compared to β-cyclodextrin CNSs. This can be attributed to the increase in intensity of the G-band that was showed under Raman (Appendix D[a]). Though that was the case, arsenic trioxide-β-cyclodextrin CNSs structure completely collapsed at higher temperatures, whereas the β-cyclodextrin CNSs seemed more stable. The percentage weight loss between 180°C-570°C, was only 20%. A further major reduction was observed above 550°C showing the material was no longer stable at temperatures above 550°C. Arsenic trioxide was successfully introduced as depicted in figure 5.1d as compared to figure 5.1b.

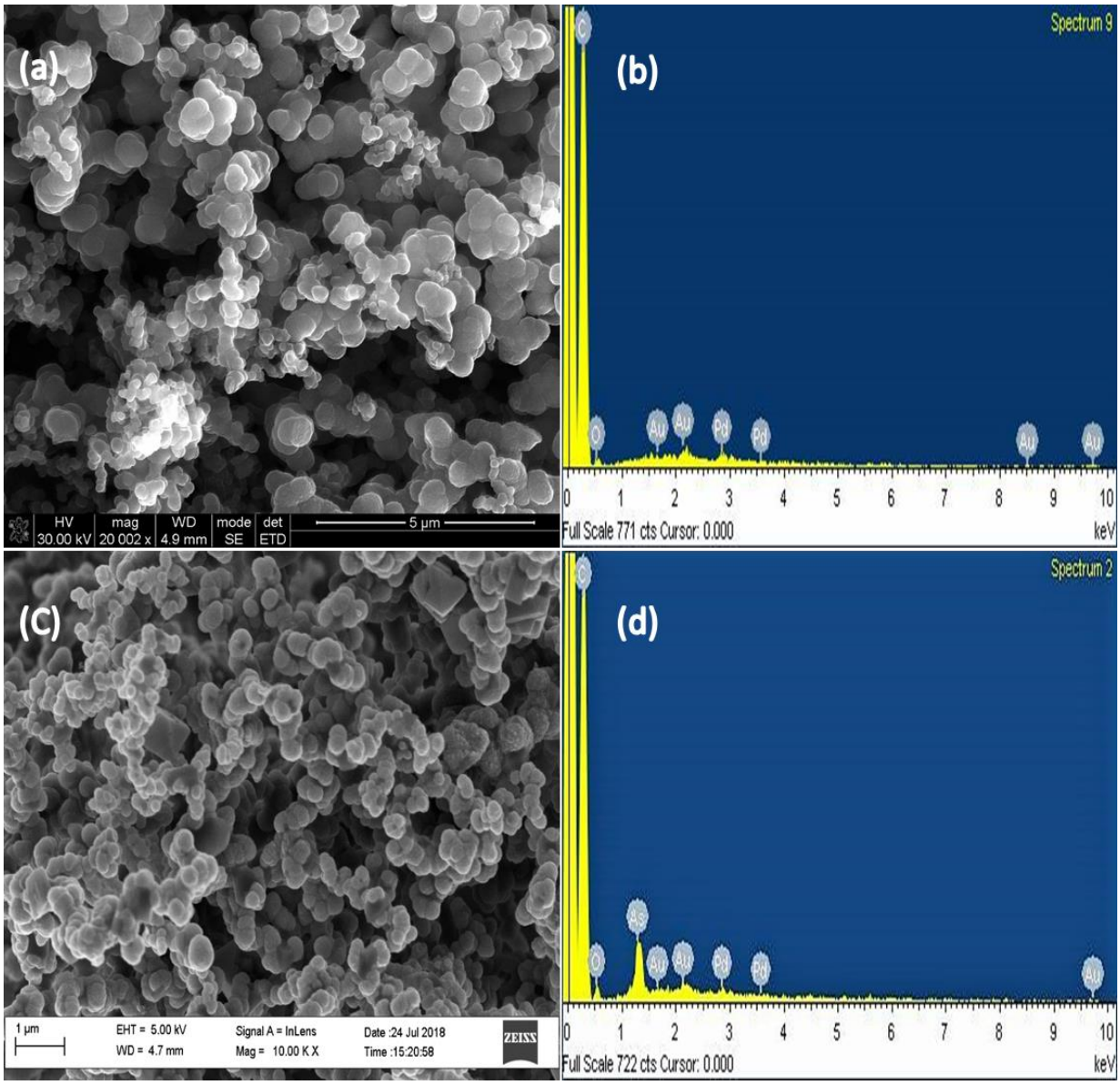

Figure 5.1 – Electron microscopy characterization of the *β*-cyclodextrin CNSs and arsenic trioxide-*β*-cyclodextrin CNSs: SEM micrographs of *β*-cyclodextrin CNSs (a), arsenic trioxide-*β*-cyclodextrin CNSs (c) synthesized at 650ºC. EDX analysis (b and d).

5.2. Cell viability analysis of MCF-7 cells after with *β*-cyclodextrin CNSs and arsenic trioxide-*β*-cyclodextrin CNSs

To determine the potential anti-cancer activity of *β*-cyclodextrin CNSs and the feasibility of using it as drug delivery vehicles, the MCF-7 cells were exposed to varying concentrations of *β*-cyclodextrin CNSs. As shown in Table 5.1 and figure 5.2a, the β-cyclodextrin CNSs showed slightly higher cytotoxicity against breast cancer MCF-7 cells (Figure. 4.2a) compared to the noncancerous skin cells, KMST-6 cells (Figure, 4.5). This suggested that the *β*-cyclodextrin CNSs can be efficient drug delivery vehicles for the treatment of breast cancer and possible other cancers. In this study, it was also showed that the arsenic trioxide-*β*-cyclodextrin CNSs were highly cytotoxic against breast cancer MCF-7 cells (Figure. 5.2b). In order to determine the mode of action, light microscopy was employed (Figure. 5.3). The results are summarized in table 5.1.

Table 5.1: The MTT cell viability mean percentages and SEM of MCF-7 cells.

Treatment (µg/mL)	Mean (%)±SEM (*β*-cyclodextrin CNSs)	Mean (%)±SEM (arsenic trioxide-*β*-cyclodextrin CNSs)
Control	100.00±0.000	100.00±0.000
125	69.00±2.645	39.04±1.841
250	70.08±4.296	32.72±1.906
500	64.82±2.401	36.55±1.958
1000	70.99±3.610	22.92±0.947

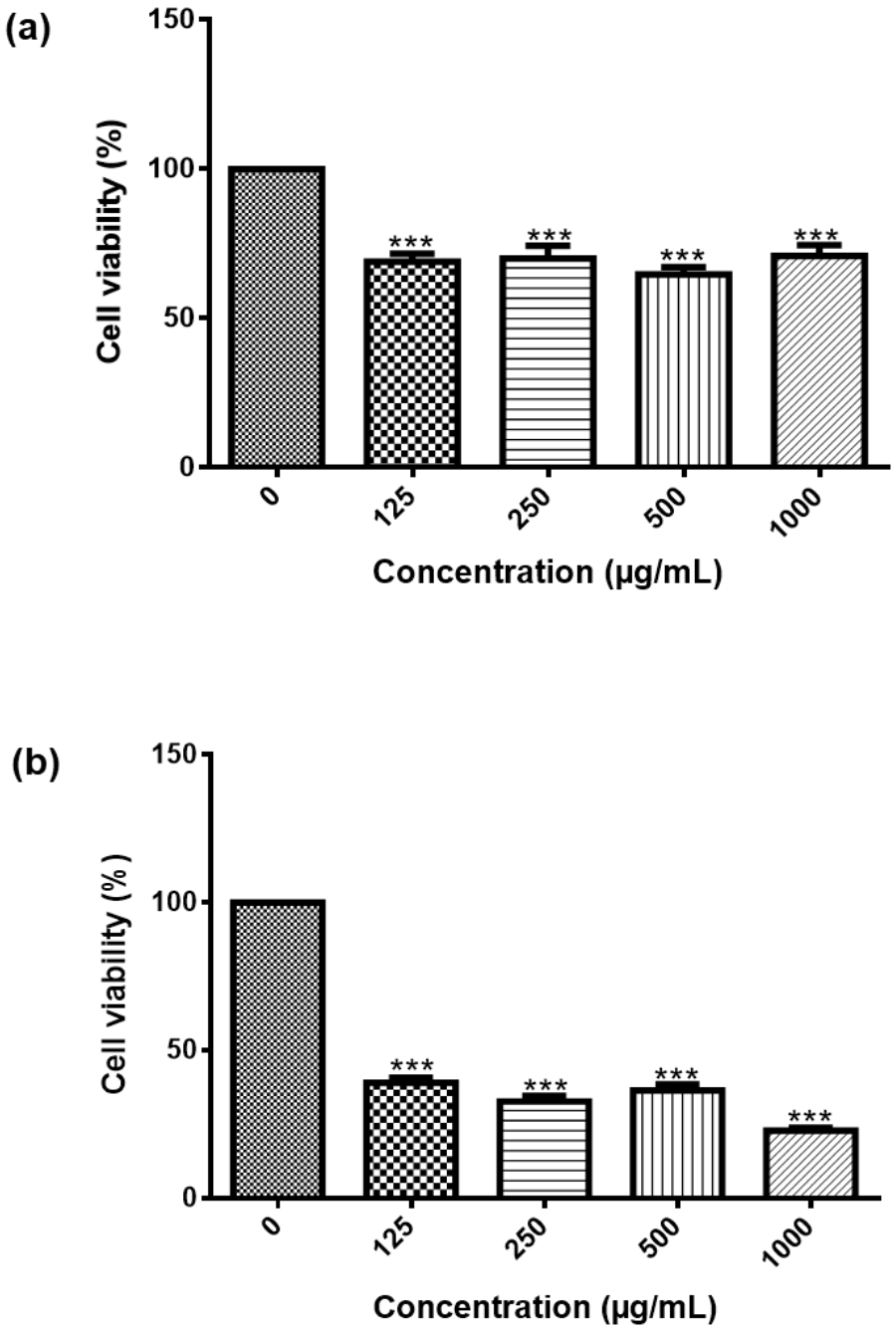

Figure 5.2 – The cytotoxic effect of the novel *β*-cyclodextrin CNSs and arsenic trioxide-*β*-cyclodextrin CNSs against MCF-7 cells: Cell viability of the MCF-7 cells exposed to *β*-cyclodextrin CNSs (a) and arsenic trioxide-*β*-cyclodextrin CNSs (b) at different concentrations for 24 h incubation. Shown are representative data of three independent experiments (percentage mean ±SEM). The difference were found to be statistically significant (***P<0.001).

5.3. Morphological characterization of treated MCF-7 cells

Light microscopy (Figure. 5.3a) showed normal epithelial cell morphology of untreated MCF-7 breast cancer cells. On the contrary, *β*-cyclodextrin CNSs-treated cells (Figure. 5.3b-d) showed reduced MCF-7 cell growth compared to the untreated cells. This reduction corroborates with what was observed with the MTT Assay, which showed that *β*-cyclodextrin CNSs had growth inhibitory effect against breast cancer MCF-7 cells (Figure. 5.3a). Arsenic trioxide-*β*-cyclodextrin CNSs also demonstrated growth inhibition effect against MCF-7 cells (Figure. 5.3f-i) compared to the untreated cells (Figure. 5.3a). Even though *β*-cyclodextrin CNSs treatment resulted in cancer growth reduction, Arsenic trioxide-*β*-cyclodextrin CNSs significantly reduced the growth of the MCF-7 cells (Figure. 5.3f-i). The yellow arrows indicate the normal epithelial cell shape of MCF-7 whereas the red arrows indicate cells with apoptotic features such as membrane blebbing and cell shrinkage.

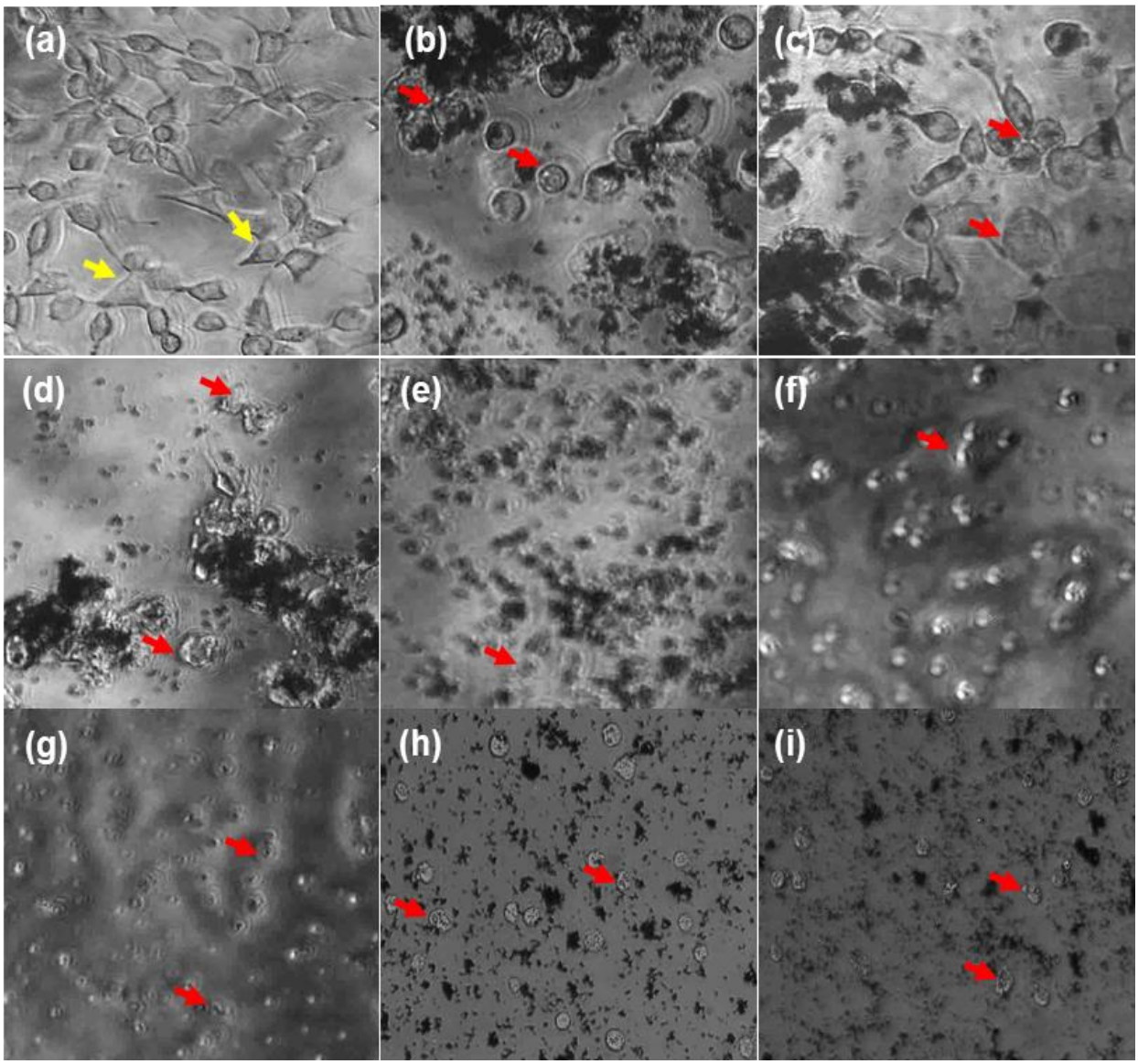

Figure 5.3 – Normal light microscopy images of arsenic trioxide-*β*-cyclodextrin CNSs-treated MCF-7 cells: The MCF-7 cells were exposed to various concentrations of CNSs coated with *β*-cyclodextrin (b-e) and arsenic trioxide-containing carbon nanosphere (f-i). The images were viewed under an inverted light microscope (Nickon Instruments Inc. USA) and captured at 20X magnification using digital DSRI-1 camera.

5.4. Nuclear morphology of treated MCF-7 cells

Figure. 5.4 f-i shows that the cells had a spherical morphological shape, suggestive of apoptotic cells. DAPI staining (Figure. 5.4b-f) also showed nuclear fragmentation, which is typical of cells undergoing or cell that has undergone apoptosis and to confirm these observations, an investigation on whether the cells had undergone apoptosis was carried out using the Muse® Cell Analyser and Muse® Annexin V & Dead Assay (Section 4.9).

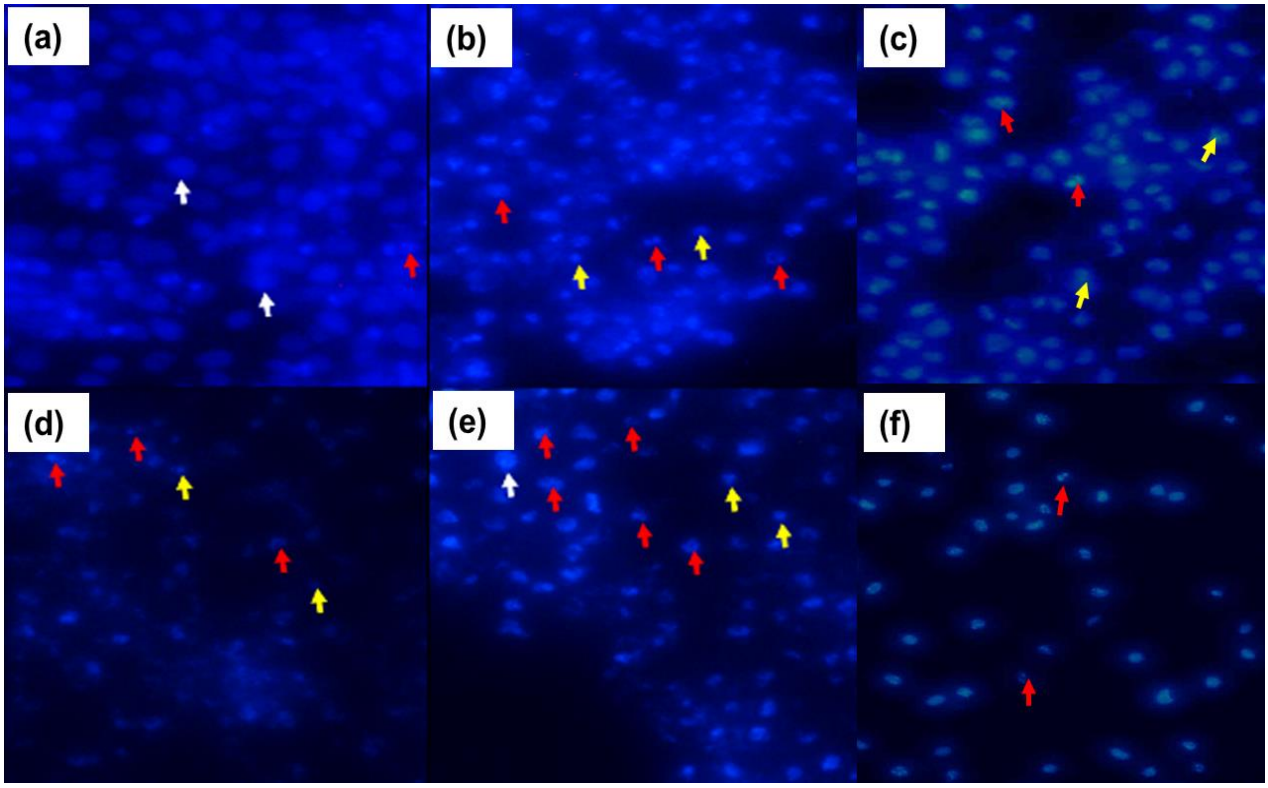

Figure 5.4 – Fluorescent microscopic image of MCF-7 cells: The cells were treated with arsenic trioxide-*β*-cyclodextrin-CNSs at different concentrations (a-untreated, b-125 µg/mL, c-250 µg/mL, d-500 µg/mL, e-1000 µg/mL and f-100 µM curcumin) for 24 h. The images were viewed using fluorescence microscope (Nikon Instruments Inc, USA) and images were captured with a digital DSRI-1 camera. The white arrows indicate the intact nucleus, the yellow arrows show the raptured cell membranes and the red arrows show the fragmented nuclei.

5.5. Apoptosis assesment of arsenic trioxide-*β*-cyclodextrin CNSs treated MCF-7 cells

In order to elucidate the detailed mechanisms of death induced by arsenic trioxide-*β*-cyclodextrin CNSs in MCF-7 breast cancer cells, the MCF-7 cells were treated with arsenic trioxide-*β*-cyclodextrin CNSs at different concentrations (0, 125 µg/mL, 250 µg/mL, 500 µg/mL and 1000 µg/mL) for 24 h. Apoptotic cell death was evaluated using the Muse® Annexin V and Dead Cell Assay. FACS data suggests that arsenic trioxide-*β*-cyclodextrin CNSs- induced apoptosis of MCF-7 after 24 h treatment in a dose dependent manner (Figures. 5.5a-f and 5.6). The results in Table 5.2 and figure 5.6 revealed that the percentage of apoptotic cells reached 98.93±0.492 and 86.80±1.562 as compared to the control 1.03±0.259 after 24 h incubation (Table 5.2).

Table 5.2: The apoptosis mean percentages and SEM of MCF-7 cells.

Treatment (µg/mL)	Mean (%)±SEM				
	Live	Dead	Early apoptotic	Late apoptotic	Total-apoptotic
Control	97.51±0.372	1.45±0.132	0.52±0.192	0.52±0.067	1.03±0.259
125	53.83±2.931	0.30±0.029	24.17±2.325	21.68±1.621	45.85±2.959
250	30.67±0.470	0.12±0.067	49.43±0.555	19.78±0.841	69.22±0.449
500	12.90±1.287	0.00±0.000	63.78±0.945	23.33±0.356	86.80±1.562
1000	1.05±0.477	0.02±0.017	74.00±0.562	24.93±0.797	98.93±0.492

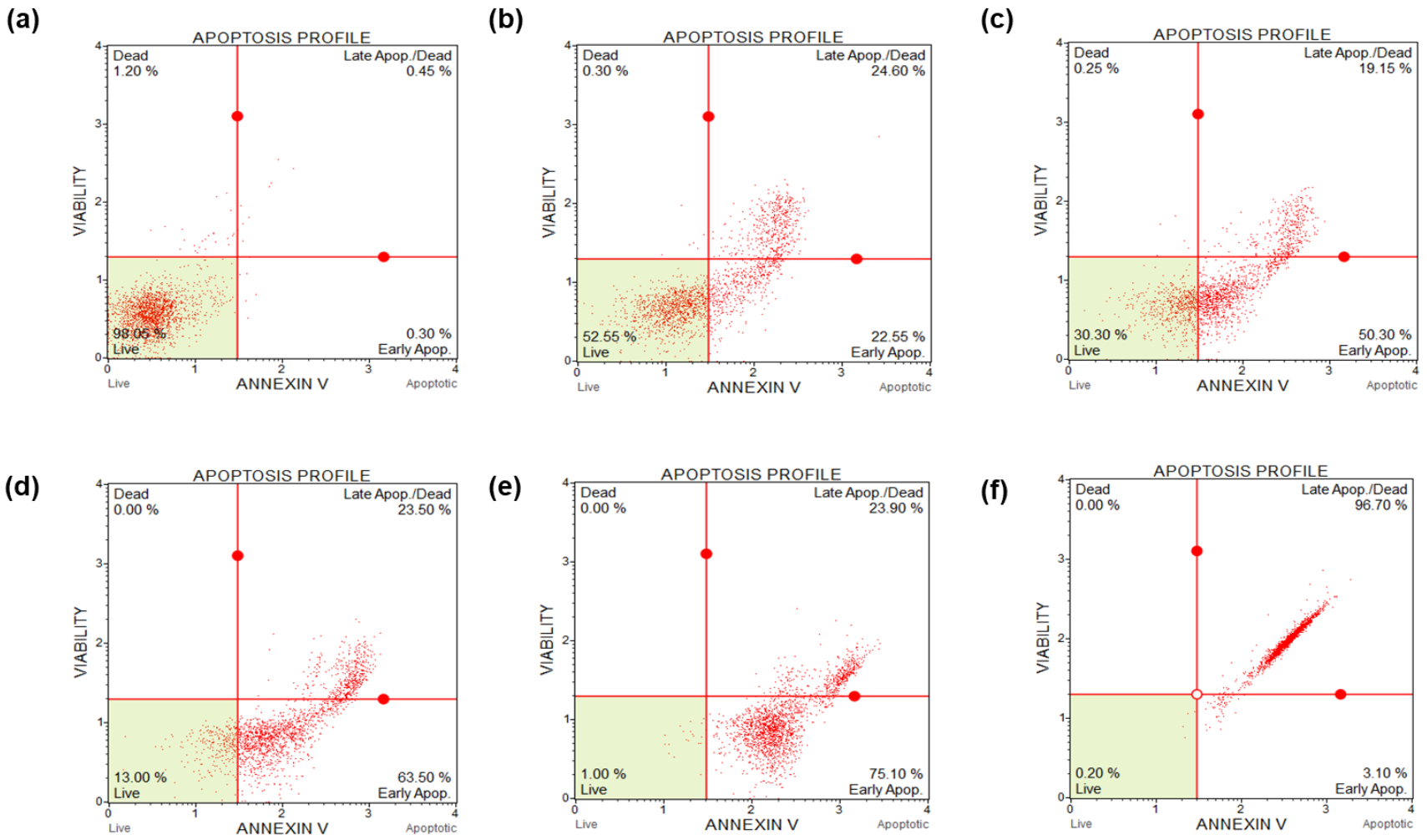

Figure 5.5 – Apoptosis of the MCF-7 cells induced after 24 h treatment with arsenic trioxide-*β*-cyclodextrin CNSs: (a)-Untreated control, (b)-125 µg/mL, (c)-250 µg/mL (d)-500 µg/mL, (e)-1000 µg/mL and (f)-100 µM curcumin. The data was analysed using Muse® Cell Analyser.

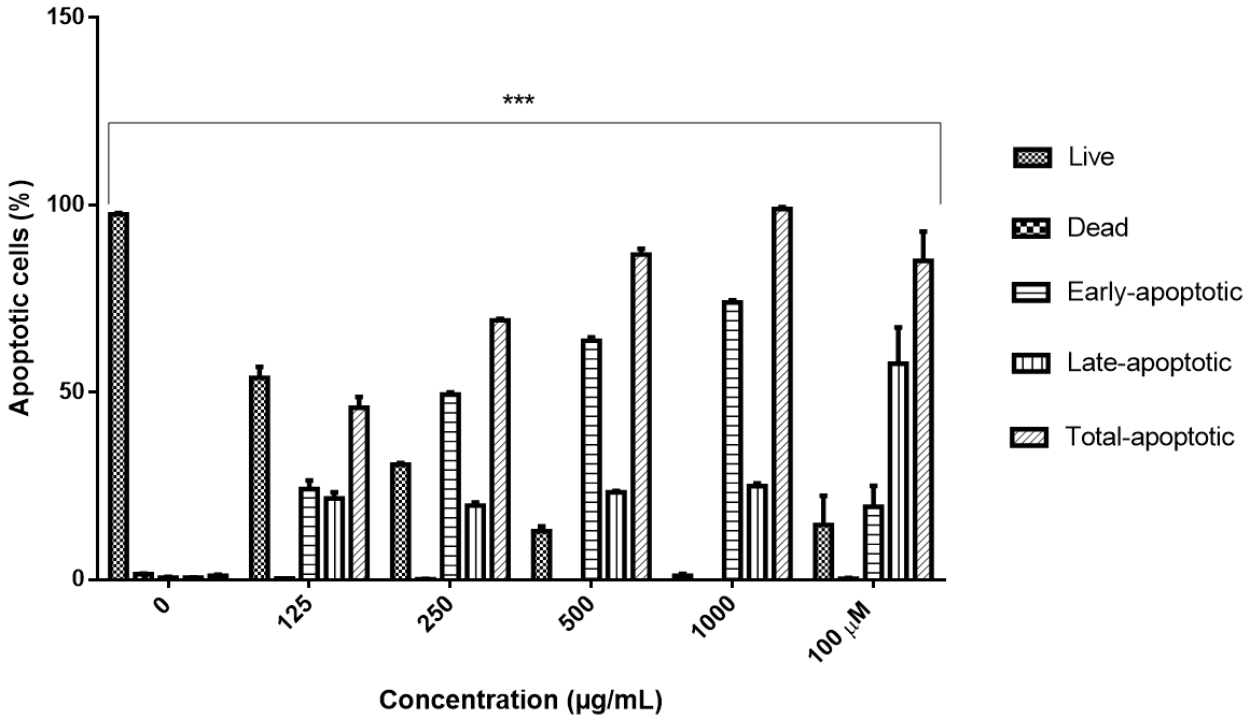

Figure 5.6 – The apoptotic percentages of MCF-7 after 24 h treatment with arsenic trioxide-*β*-cyclodextrin CNSs and 100μM curcumin: Shown are representative data of three independent experiments (percentage mean ±SEM). The difference were found to be statistically significant (***P<0.001).

5.6. Discussion

There is an increasing emphasis on early diagnosis for cancer but the incidence of breast cancer and other cancers continue to rise. In South Africa, the breast cancer incidents are on the rise due to improved accessibility to screening facilities for most people. According to the 2012 National Cancer Registry (NCR) [http://www.nioh.ac.za], breast cancer remains the leading cancer amongst women in South Africa. There is a need for effective cancer drugs and drug delivery systems that will limit the adverse cancer drugs side effects that include non-specific normal cell destruction. Nanotechnology has afforded the scientific community with promising drug delivery materials that may possess both specificity and efficacy. Nanospheres have long been regarded as potential new drug delivery material and according to Singh *et al*. (2010), they possess critical properties that make them suitable material for drug delivery. These include their small size and their ease to penetrate cells and tissues. In this study, the use of *β*-cyclodextrin CNSs derived from the waste material, coal fly ash from South Africa for the delivery of arsenic trioxide for the treatment of breast cancer was investigated.

The shape, morphology and elemental analysis of the *β*-cyclodextrin CNSs and arsenic trioxide-*β*-cyclodextrin CNSs were investigated using SEM coupled to EDX. As shown in figure 5.1a-d, materials were found to be spherical in shape and consisted mostly of carbon as shown in the EDX analysis (Figure. 5.1b and d). In *β*-cyclodextrin CNSs, other metals such as Gold (Au), Palladium (Pd) were also identified in minimal amounts. This could be due to the unburnt portion of the fly ash that was not converted as shown in previous studies where fly ash was used as a catalyst for CNM synthesis (Hintsho *et al*., 2014). On arsenic trioxide-*β*-cyclodextrin CNSs (Figure. 5.1c), the 1% arsenic trioxide that was loaded on the CNSs was also identified, which shows that there was a successful deposition of this anticancer agent. More importantly, the shape of the particles appeared to still be intact. For further analysis in terms of structure and thermal stability, Laser Raman and TGA were conducted respectively. As depicted in Appendix D-(b), upon testing the thermal stability of these materials, the arsenic trioxide-*β*-cyclodextrin CNSs started decomposing at a higher temperature (230^{o}C) as compared to *β*-cyclodextrin CNSs. This can be attributed to the increase in intensity of the G-band that was showed under Raman. Though that was the case, arsenic trioxide-*β*-cyclodextrin CNSs structure

completely collapsed at higher temperatures, whereas the *β*-cyclodextrin CNSs seemed more stable. The percentage weight loss between 180°C-570ºC, was only 20%. A further major reduction was observed above 550ºC showing that the material was no longer stable at temperatures above. The stability of these composites at higher temperatures becomes irrelevant in *in vitro* and *in vivo* set-up when one considers the physiological conditions (37ºC) in which these CNSs will be subjected to as delivery vehicles.

In this study the β cyclodextrin CNSs showed more toxicity against breast cancer MCF-7 cells (Figure. 5.2a) compared to the previous report where these *β*-cyclodextrin CNSs showed insignificant minimum effect against the noncancerous skin cells, KMST-6 cells (Section 4.2). This suggest that these β cyclodextrin CNSs can be efficient drug delivery vehicles for the treatment of breast cancer. Arsenic trioxide-*β*-cyclodextrin CNSs were shown to be highly cytotoxic to breast cancer MCF-7 cells (Figure. 5.1b). In order to determine the mode of action, light and fluorescence microscopy were employed. To determine the feasibility of using *β*-cyclodextrin CNSs as drug delivery vehicles, the MCF-7 cells were exposed to varying concentrations of β cyclodextrin CNSs.

To examine the effect of the arsenic trioxide on the morphology of MCF-7 cells, the cells were exposed to various concentrations of arsenic trioxide-*β*-cyclodextrin fly ash-derived CNSs for a period of 24 hrs. The untreated MCF-7 cells (Figure. 5.3a) maintained their typical normal epithelial shape while, the MCF-7 cells treated with the *β*-cyclodextrin CNSs showed growth reduction and displayed the characteristics of the cells undergoing apoptosis (Figure. 5.3b-d). This reduction in cell growth corroborate what was observed with the MTT Assay (Figure. 5.1a), which showed that *β*-cyclodextrin CNSs inhibited the growth of the breast cancer MCF-7 cells. Arsenic trioxide-*β*-cyclodextrin CNSs also demonstrated inhibitory effect against MCF-7 cells (Figure. 5.3f-i) when compared to the untreated cells (Figure. 5.3a). Even though *β*-cyclodextrin CNSs treatment resulted in cancer growth reduction, arsenic trioxide-*β*-cyclodextrin CNSs significantly enhanced the growth inhibitory effect against MCF-7 cells. As shown in figure. 5.3f-i, arsenic trioxide-*β*-cyclodextrin CNSs treated cells had shrunk and shored spherical shape, suggestive of apoptotic cells. Arsenic trioxide alone changed the morphological features of the cells from polygonal to round shape, including partly condensed chromatin and the appearance of vacuoles (Liu *et al*., 2015). The number of cells decreased with an increase in the

concentration of arsenic trioxide-*β*-cyclodextrin CNSs. Previously, Schwab *et al*. (1994) reported *in vitro* growth inhibition induced by arsenic trioxide against human tumorigenic cells (HBL100ras1), a clone obtained from the human mammary cell line, HBL100. The data further suggest that the decrease in cell number and growth inhibition were due to the induction of apoptotic pathways. DAPI staining (Figure. 5.4b-d) also confirmed the induction of apoptosis where nuclear fragmentation, which is typical of cells undergoing or cell that have undergone apoptosis was observed. It was further confirmed that the arsenic trioxide-*β*-cyclodextrin CNSs- induced apoptosis by using the Muse® Cell Analyser (Merck-Millipore, Germany).

Apoptotic cell death was evaluated using the Annexin V and Dead Cell Kit (Merck-Millipore, Germany). The results showed that the arsenic trioxide-*β*-cyclodextrin CNSs significantly induced apoptosis and both early apoptosis and late apoptosis were detected in MCF-7 cells (Figure 5.5b-e and 5.6), which were significantly higher than those detected in control cells (Figure 5.5a). The same trend of results were observed in cells treated with curcumin (Figure. 5.5f), which was used as positive control. Cellular morphology clearly showed cell shrinkage, which is typical of apoptosis. Arsenic trioxide has previously been shown to induce apoptosis of the MCF-7 cells in a time and dose dependent manner (Baj *et al*., 2002). Arsenic trioxide has also been demonstrated to induce morphologic changes associated with apoptosis, including reduced cytoplasmic volume, membrane blebbing, and nuclear condensation consistent with apoptosis Li *et al*., 2004). This is in line with arsenic trioxide-*β*-cyclodextrin CNSs- induced apoptosis in this study. Moreover, Arsenic trioxide has been shown to induce apoptosis and activate caspase-3 in human mesothelioma cells (Eguchi *et al*., 2011) and myoblasts (Yen *et al*., 2012). Apoptosis is a programmed cell death that depends on caspase activation leading to substrate cleavage and ultimately, cell death (Yen *et al*., 2012). Apoptosis is as much as important in normal cells as much as it is in cancer cells for organogenesis during development, proper function of the immune system, elimination of genetically unstable cells, and for maintenance of cell homeostasis (Fogarty *et al*., 2017). Figure. 5.4b-d and figure. 5.5b-d demonstrated that arsenic trioxide-*β*-cyclodextrin CNSs derived from fly ash are potent against the MCF-7 cells through the induction of apoptosis in a dose-dependent manner as some of the typical apoptotic characteristics were observed.

5.7. Conclusion

In this study, it was shown for the first time that the fly ash-derived arsenic trioxide-*β*-cyclodextrin CNSs can be useful in the treatment of breast cancer. The β-cyclodextrin CNSs have been previously shown to be safe against non-cancer cells, however, in this study *β*-cyclodextrin CNSs exhibited cytotoxicity against the MCF-7 cells. MTT Assay, morphological analysis, and apoptosis analysis showed that novel arsenic trioxide-*β*-cyclodextrin fly ash-derived CNSs extraordinarily reduced cell viability of MCF-7 cells and induced apoptosis in breast cancer cells. Arsenic trioxide is known to be severely cytotoxic against MCF-7 cells (Hoffman *et al*., 2015; Liu *et al*., 2015). Arsenic trioxide-*β*-cyclodextrin fly ash-derived CNSs can be further developed as therapeutics against cancer cells. This is the first study to demonstrate the anticancer activity of coal waste derived nanoparticles.

Chapter Six: The effect of arsenic trioxide on the expression of survivin splice variants during the cell cycle progression and apoptosis of MCF-7 cell line

6. Introduction

The use of arsenic trioxide in medicine dates back to more than 2438 years (Waxman and Anderson, 2001). Arsenic trioxide influences numerous intracellular signal transduction pathways, and consequently affects cellular function (Hoffman et al., 2015; Shen *et al*., 2017). To determine the effect of arsenic trioxide on the expression of survivin splice variants and their specific MiRs during cell cycle progression and apoptosis in breast cancer MCF-7 cell line, various Assays were performed. After the exposure of cells to different concentrations of arsenic trioxide, cobalt chloride and curcumin, cell cytotoxicity (MTT) Assay was used to determine cell viability, ascertain their IC_{50s} and apoptosis inducing concentrations (Section 6.1). Muse® Count and Viability Assay (Section 6.2) was used to confirm the MTT Assay results. Morphological observations were performed by the aid of both light and fluorescence microscopes to analyse the morphological changes as a result of different treatments (Section 6.3 and 6.4). The Muse® Cell Cycle Analyser was used to perform the cell cycle Assay, which was used to confirm the cell cycle phases (Section 6.5). Apoptosis induction was assessed using both the MUSE® Annexin V and Dead Cell Assay (Section 6.6) and the MUSE® MitoPotential Assay (Section 6.7) to evaluate the kind of apoptosis induced by arsenic trioxide. Multi-Caspase activation (Section 6.8) was used to check if apoptosis induced by arsenic trioxide is caspase-dependent or caspase-independent. MAPK (Section 6.9) and PI3K (Section 6.10) Assays were used to evaluate the biological pathways arsenic trioxide inhibits MCF-7 cell growth. Conventional PCR was used to analyse the expression of survivin and its variants during both arsenic trioxide-induced cell cycle arrest and apoptosis (Section 6.11). The protein expression of survivin during arsenic trioxide-induced cell cycle arrest and apoptosis in MCF-7 cells was detected using immunocytochemistry (Section 6.12). The prediction and evaluation of MiRs specific to survivin splice variants (Section 6.13) was done using the Bioinformatics tools. Lastly, the discussion (Section 6.14) and conclusion (Section 6.15) were covered.

6.1. Arsenic trioxide reduced the cell viability of MCF-7 cells in a concentration dependent manner

The MTT Assay and Muse® Count and Viability Assay showed that the treatment of MCF-7 cells with different concentrations of arsenic trioxide (0, 5, 10, 15, 20, 25, 32 and 64 µM), cobalt chloride (0, 50, 10, 150, 200 and 250 µM) and curcumin (0, 25, 50, 75, 100, and 125 µM) for 24 hours significantly ($P<0.001$) reduced the viability of MCF-7 cells in a concentration dependent manner (Figure. 6.1 and Table 6.1 and 6.2). The IC_{50}s for arsenic trioxide and cobalt chloride were found to be 11 µM and 100 µM and the apoptosis inducing concentration for arsenic trioxide was 32 and for curcumin was 100 µM, respectively. The 100 µM of cobalt chloride (Figure. 6.1b) was used as positive control for cell cycle arrest analysis whereas 100 µM of curcumin (Figure. 6.1c) was used as positive control for apoptosis analysis. The MTT cell viability average percentages and standard error of mean are summarized in Table 6.1 and 6.2.

Table 6.1: The MTT Assay average percentages and SEM of MCF-7 cells after 24 h treatment with arsenic trioxide.

Treatment (As_2O_3)	Mean (%)±SEM
Control	100.00 ± 0.000
5 µM	77.41 ± 4.064
10 µM	51.22 ± 3.064
15 µM	42.10 ± 3.747
20 µM	32.58 ± 3.348
25 µM	30.35 ± 2.054
32 µM	23.69 ± 2.193
64 µM	16.61 ± 1.346

Table 6.2: The MTT Assay mean percentages and SEM of MCF-7 cells after 24 h treatment with the positive controls.

Treatments		**Mean (%)±SEM**	
Cobalt chloride	**Curcumin**	**Cobalt chloride**	**Curcumin**
Control	**Control**	100.00 ±0.000	100.00±0.00
50 µM	**25 µM**	61.86± 2.865	77.21±3.408
100 µM	**50 µM**	47.30±2.610	68.35±2.455
150 µM	**75 µM**	43.32±2.963	50.57±3.395
200 µM	**100 µM**	41.50±1.685	50.32±3.213
250 µM	**125 µM**	37.21±2.734	35.91±1.553

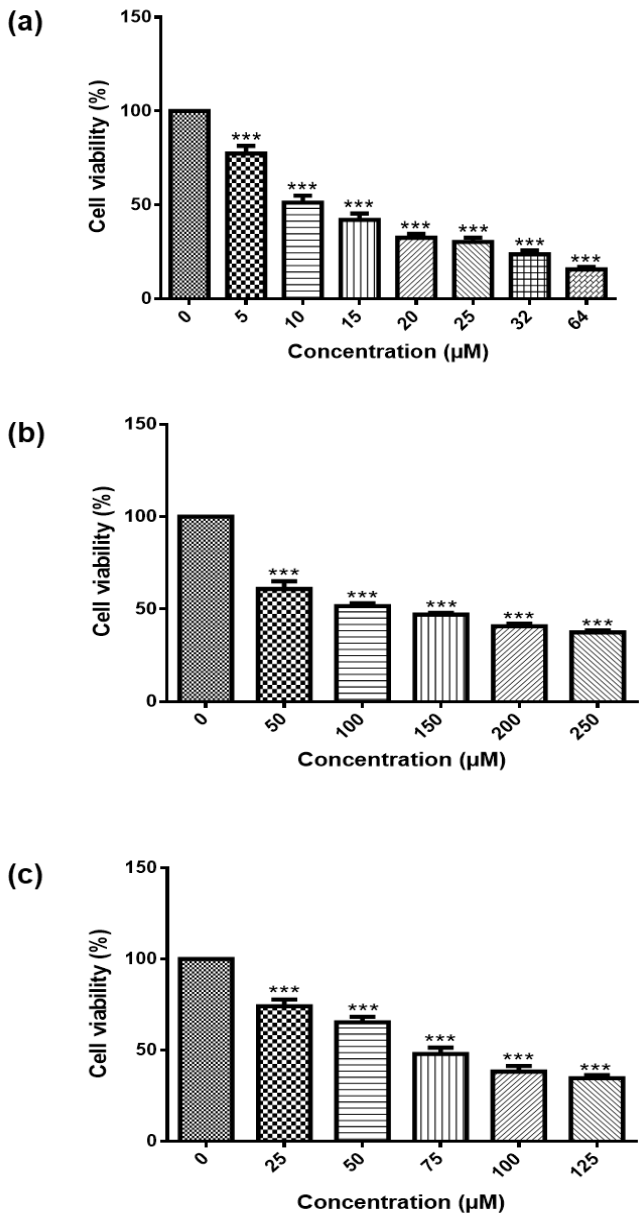

Figure 6.1 – The cytotoxicity effect of Arsenic trioxide, Cobalt chloride and Curcumin on MCF-7 Cell Viability: The figure shows the concentration dependent cytotoxicity effects of arsenic trioxide (a), cobalt chloride (b) and curcumin (c) on the viability of the breast cancer MCF-7 cells. Shown are representative data of three independent experiments (percentage mean ±SEM). The difference were found to be statistically significant (*** P<0.001).

6.2. Confirmation of the IC_{50}s using the MUSE® Count and Viability Assay

The MTT results were confirmed by using the Muse® Count and Viability Assay (Merck Millipore, Germany) [Figure. 6.2]. As shown in Table 6.3, the treatment with arsenic trioxide (11µM and 32 µM), cobalt chloride (100 µM) and curcumin (100 µM) reduced the viability of MCF-7 cells to 51.78% ±1.243 ($p<0.001$) and 29.45% ±2.563 ($p<0.001$), 46.22% ±2.408 and 28.76% ±2.386 SEM, respectively. The results confirm the MTT results obtained (Figure. 6.1)

Table 6.3: The Muse® cell viability average percentages and SEM of MCF-7 cells.

Treatment	Mean (%)±SEM	
	Live	**Dead**
Control	95.08±0.851	4.92±0.851
11 µM As_2O_3	51.78±1.243	48.24±1.240
32 µM As_2O_3	29.45±2.563	70.48±2.610
100 µM Cobalt chloride	46.22±2.408	53.78±2.408
100 µM curcumin	28.76±2.386	71.04±2.465

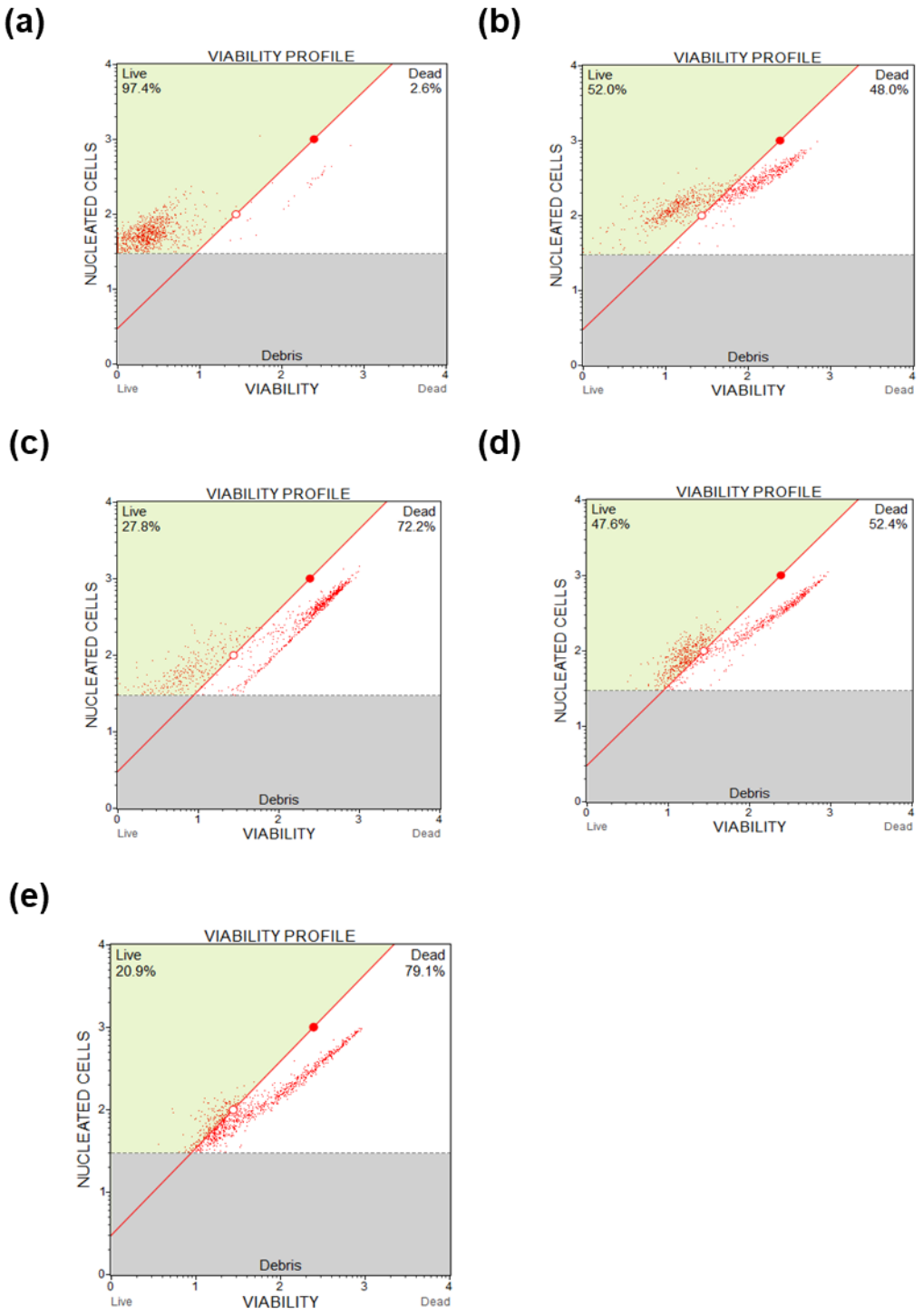

Figure 6.2 – The Muse® cell viability profiles of MCF-7 cells after 24 h treatment: (a) Control, (b) 11 µM and (c) 32 µM arsenic trioxide, (d) 100 µM cobalt chloride and (e) 100 µM curcumin. Muse® Cell Analyser was used to analyse the results.

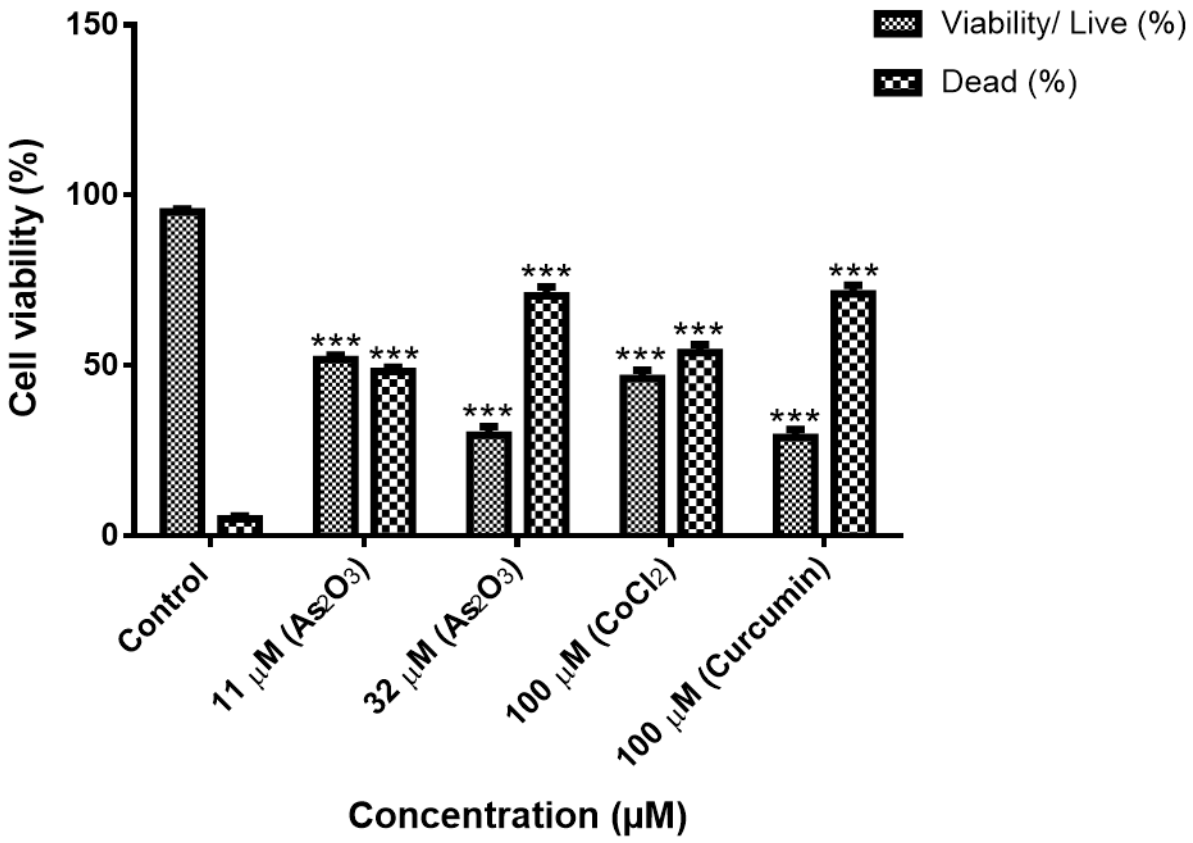

Figure 6.3 – The confirmation of the IC_{50}s using the MUSE® Count and Viability Assay: The cells were expose to 11 µM and 32 µM arsenic trioxide, 100 µM cobalt chloride and 100 µM curcumin for 24 hours. Shown are representative data of three independent experiments (percentage mean ±SEM). The difference were found to be statistically significant (*** P<0.001).

6.3. Arsenic trioxide- induced morphological changes in cultured MCF-7 cells

In order to assess the molecular mechanisms involved in the reduction of viability of MCF-7 cells after 24 hour treatments with arsenic trioxide, cobalt chloride and curcumin, analysed using the inverted light microscope (Figure. 6.4a-i). The untreated cells (Figure. 6.4a) maintained their normal epithelial like shape. However, the cells treated with arsenic trioxide (Figure. 6.4b-e) exhibited morphological changes, typical to apoptosis features such as cell shrinkage (red arrows). Additionally, the cell numbers reduced as the concentration of arsenic trioxide increased. Cells treated with cobalt chloride mantained the epithelial like shape but had damage cell membrane (Figure. 6.4f-g), whereas the cells treated with curcumin exhebited morphological changes and apoptosis features (Figure. 6.4h-i).

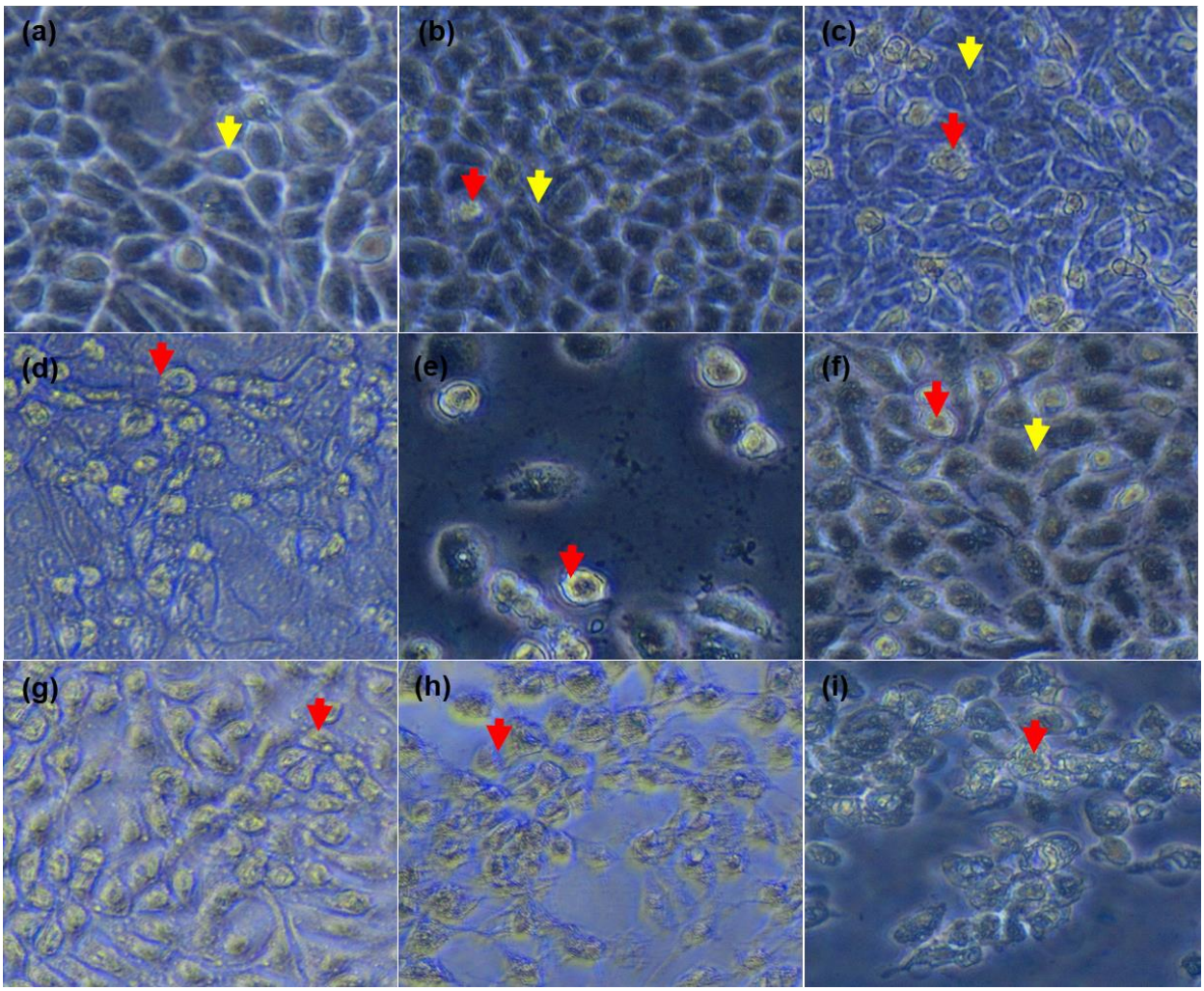

Figure 6.4 – The effect of arsenic trioxide on the MCF-7 cell morphology: The effect of arsenic trioxide on the MCF-7 cell morphology. Normal light microscopy images of MCF-7 untreated cells (a), treated cells with concentrations of arsenic trioxide [(b) - 4 µM, (c) - 11 µM, (d) - 16 µM and (e) - 32 µM], cobalt chloride [(f)-50 µM and (g)- 100 µM] and curcumin [(h)-50 µM and (i)- 100 µM]. The yellow arrows indicate the normal shape of MCF-7 cell and the red arrows show the apoptotic cells. The images were photographed using Olympus CKX53 Inverted Microscope, (Olympus, Japan) and captured with an LC-30 camera set (Olympus, Japan), respectively. The yellow arrows indicate the normal shape of MCF-7 cell and the red arrows shows the apoptotic cells.

6.4. Arsenic trioxide- induced mitotic and apoptotic morphological changes in MCF-7 cells

To analyse the nuclear morphological changes in arsenic trioxide-treated MCF-7 cells, DAPI staining was used. Cells were seeded and exposed to various concentrations of arsenic trioxide, cobalt chloride and curcumin for 24 hours. After incubation, the cells were stained with DAPI. As shown in figure. 6.5a, untreated cells maintained the normal MCF-7 morphology which include intact nuclear structure. Arsenic trioxide- induced cell cycle arrest in MCF-7 cells as demonstrated by accumulation of cells at anaphase (Figure. 6.5c). The cells treated with 16 and 32 µM As_2O_3 showed hallmark features of apoptosis such as chromatin condensation and fragmentation of the nucleus (Figure. 6.5d-e).

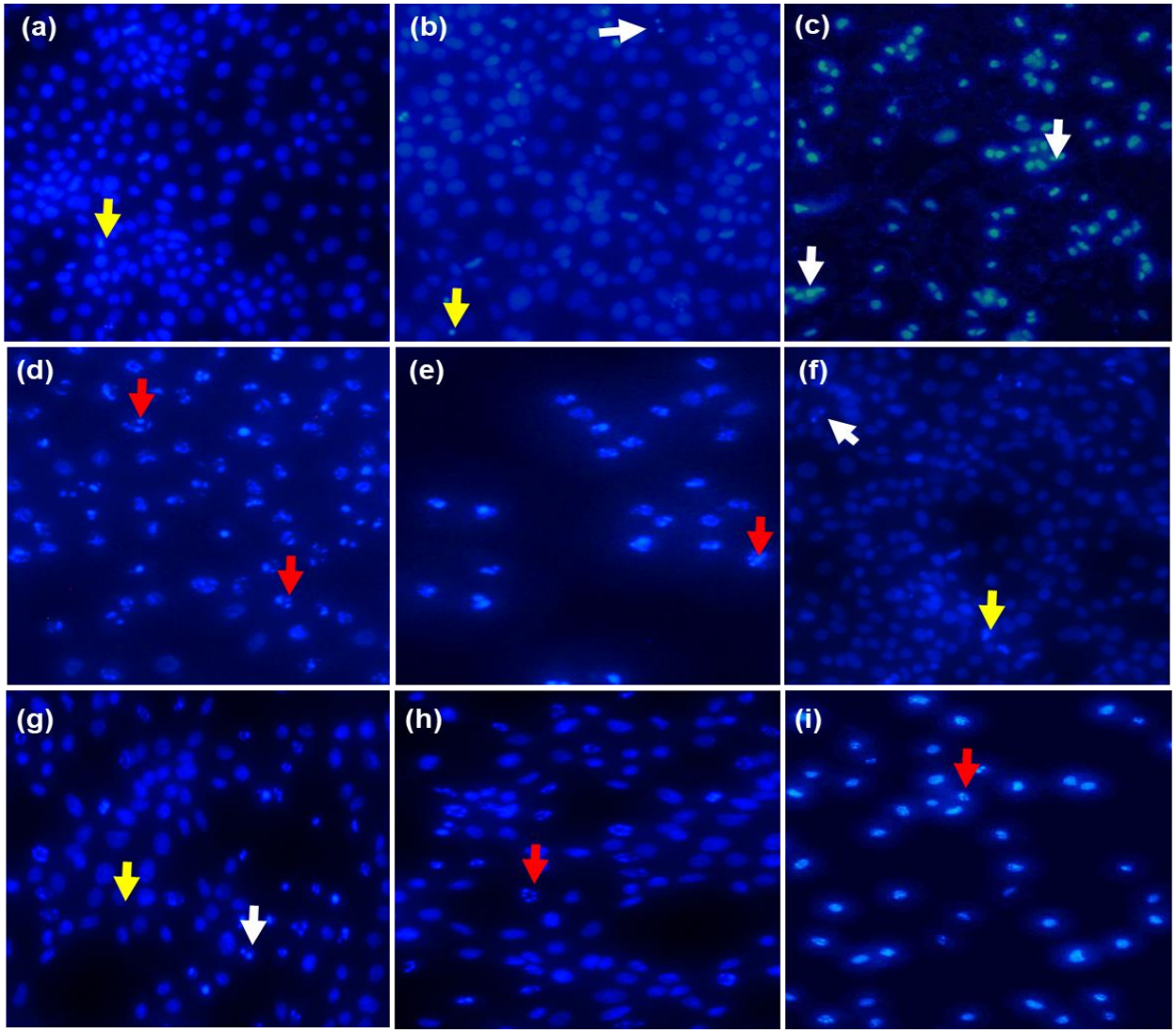

Figure 6.5 – Nuclear morphology of MCF-7 cells after DAPI staining: The fluorescence microscopy images of the untreated MCF-7 cells (a) MCF-7 cells treated with various concentrations of arsenic trioxide [(b)-4 µM, (c)-11 µM, (d)-16 µM and (e)-32 µM], cobalt chloride [(f)-50 µM and (g)-100 µM] and curcumin [(h)-50 µM and (i)- 100 µM] for 24 hours. The samples were analysed using an Eclipse Ti-U fluorescence microscope (Nickon Instruments Inc. USA) and images were captured at 20X magnification. The white arrows indicate intact nucleus, yellow arrows indicate the mitotic cells and the red arrows show the apoptotic cells.

6.5. Arsenic trioxide- induced G2/M cell cycle arrest in treated MCF-7 cells

To confirm the cell cycle arrest induced by arsenic trioxide figure 6.4c, the examination of the DNA content using the Muse® Cell Cycle Assay Kit was done. Arsenic trioxide signifcantly ($p<0.001$) induced the G2/M cell cycle arrest in the MCF-7 breast cancer cells (Figure. 6.6b). As depicted in Table 6.3, as compared to the untreated cells (25.73±1.824), 11 um of arsenic trioxide and cobalt chloride significantly increased the percentage of cells at G2M cell cycle phase to 45.13±0.942 ($p<0.001$) and 35.50±1.428 ($p<0.05$), respectively. The results are summarised in Table 6.4, shows the average percentages of each phase with the standard error of mean and (SEM).

Table 6.4: The cell cycle mean percentages and SEM of MCF-7 cells.

Treatment	**Mean (%)±SEM**		
	G0/G1	**S-phase**	**G2/M**
Control	59.28±1.178	15.38±1.541	25.73±1.824
11 µM As_2O_3	37.57±2.869	17.17±2.419	45.13±0.942
100 µM $CoCl_2$	45.35±3.399	19.20±2.419	35.50±1.428

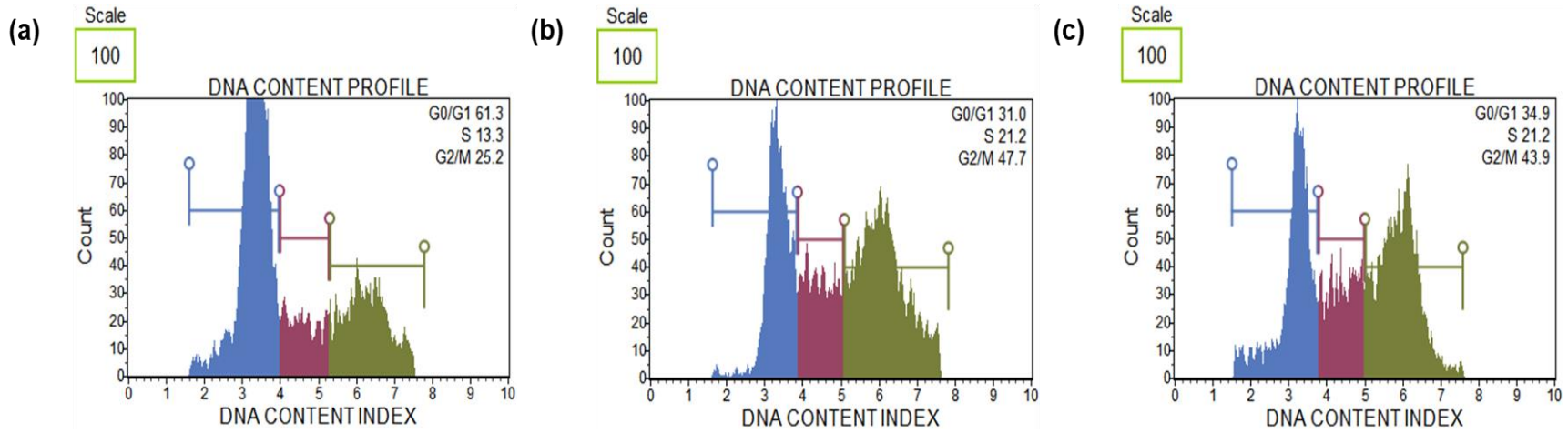

Figure 6.6 – Cell cycle profiles of the MCF-7 cells after 24 h treatment: (a)-Control, (b)-11 µM arsenic trioxide, (c)-100 µM cobalt chloride and (d)-The cell cycle phase percentage. The data was analysed using Muse® Cell Analyzer.

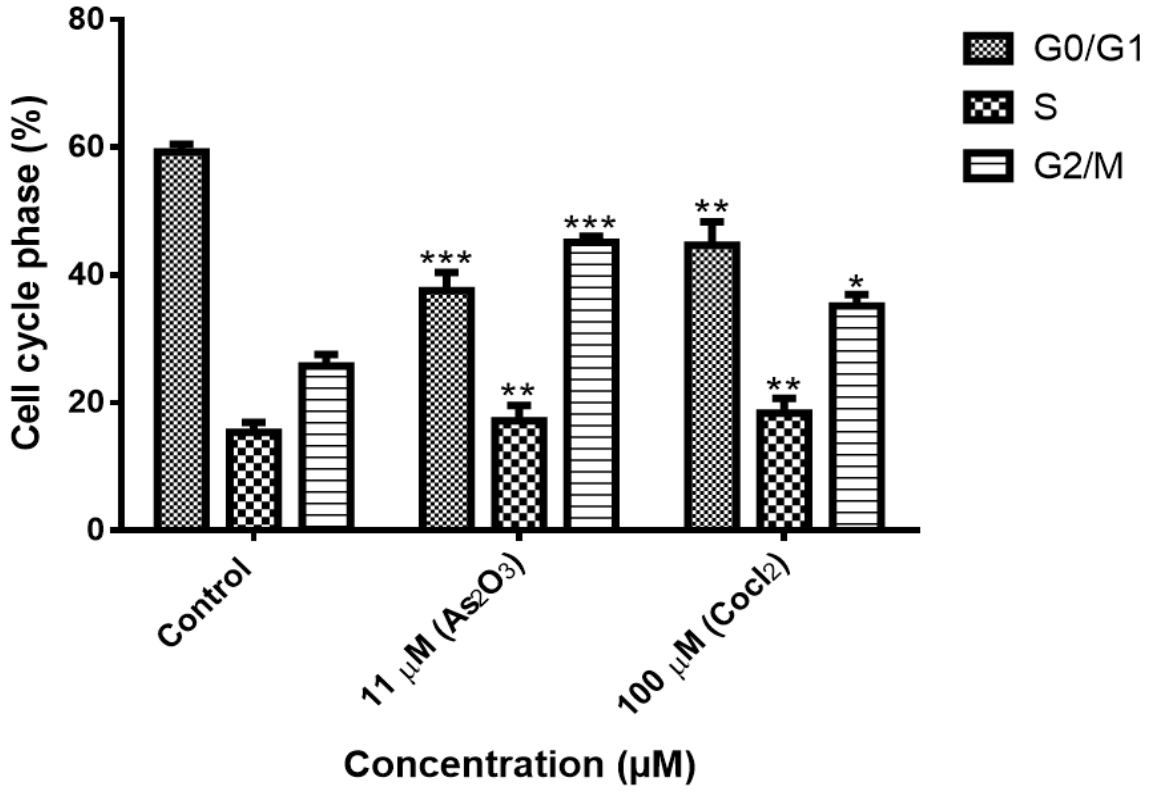

Figure 6.7 – The percentage of MCF-7 cells in the G0/G1, S and G2/M cell cycle phases after 24 h treatment: Shown are representative data of three independent experiments (percentage mean ±SEM). The difference were found to be statistically significant (* $p<0.05$, ** $p<0.01$ and *** $p<0.001$).

6.6. Arsenic trioxide promoted programmed cell death of MCF-7 cells

To further determine whether arsenic trioxide-induced cell apoptosis of MCF-7 cells, the Annexin V and Dead cell kit and Muse® Cell Analyser were used. Arsenic trioxide-induced apoptosis of MCF-7 breast cancer cells after 24 hours treatment (Figure. 6.8). Arsenic trioxide and curcumin significantly ($p<0.001$) induced apoptosis up to 73.43±6.045 and 85.11±7.819 when compared with the untreated cells with value of 10.69±1.451, respectively. The results are summarised in Table 6.5.

Table 6.5: The apoptosis mean percentages and SEM of MCF-7 cells.

Treatment	**Mean (%)±SEM**				
	Live	**Dead**	**Early apoptotic**	**Late apoptotic**	**Total-apoptotic**
Control	87.61±1.681	1.39±0.335	3.51±0.695	7.80±1.732	10.69±1.451
32 µM As_2O_3	23.62±5.394	3.78±1.113	29.61±5.296	37.34±4.649	73.43±6.045
100 µM Curcumin	14.63±7.730	0.26±0.157	34.40±7.868	50.71±7.851	85.11±7.819

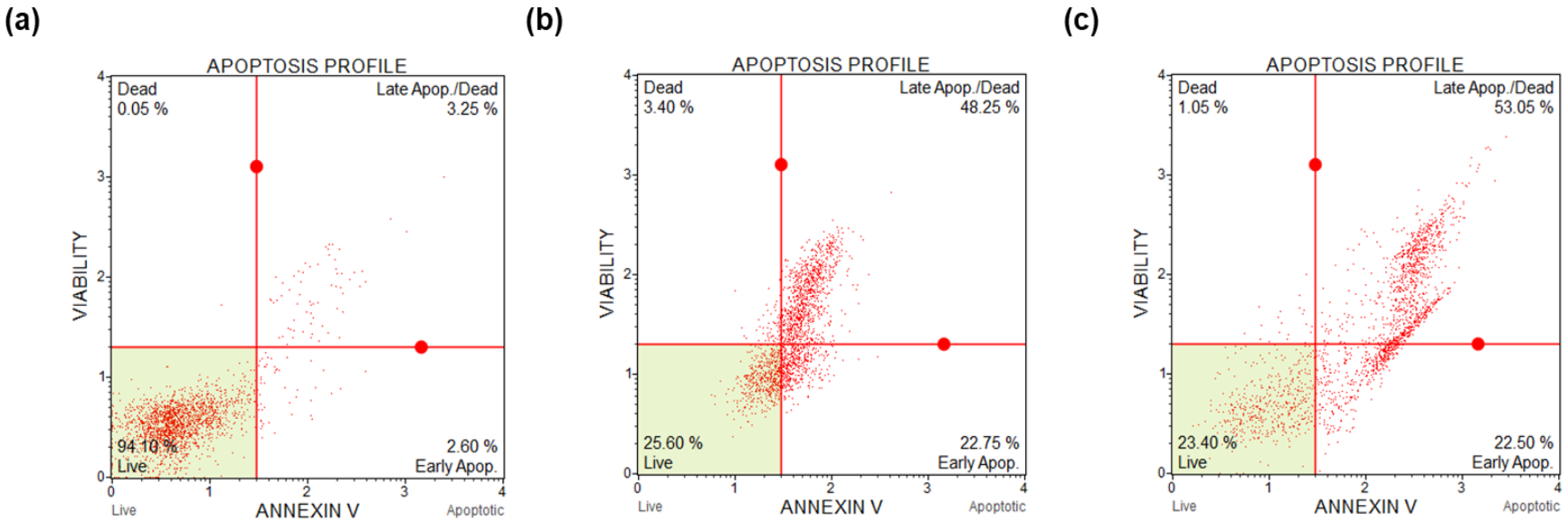

Figure 6.8 – Apoptosis profiles of MCF-7 cells after 24 h treatment: (a)-Control, (b)-32 µM arsenic trioxide, (c)-100 µM curcumin. The data was analysed using Muse® Cell Analyser.

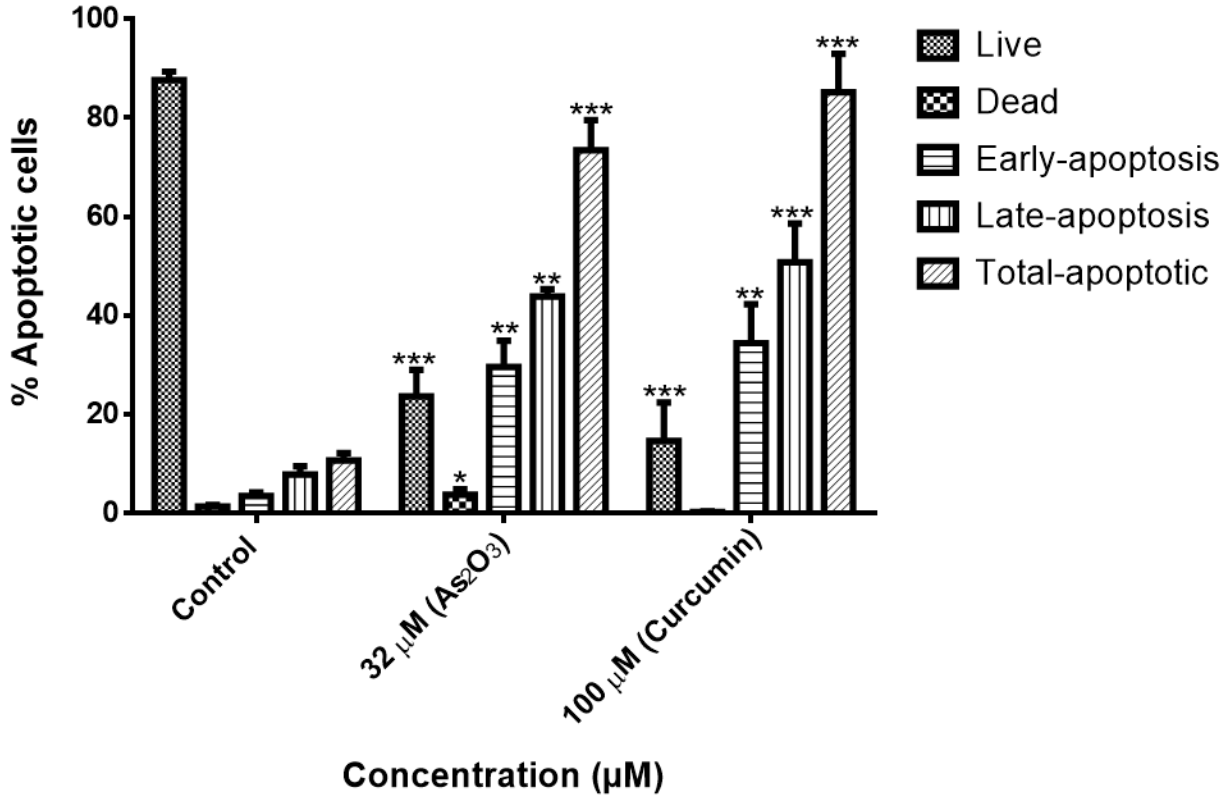

Figure 6.9 – Apoptotic cell percentages of the MCF-7 cells: Shown are representative data of three independent experiments (percentage mean ±SEM). The difference were found to be statistically significant (* $p<0.05$, ** $p<0.01$ and *** $p<0.001$).

6.7. Arsenic trioxide did not disrupt the mitochondrial membrane of MCF-7 cells

To study the disruption of mitochondrial membrane potential and the resulting mitochondrial permeability transition, MCF-7 cells were treated with Arsenic trioxide and curcumin. The results of the Muse® Cell Analyser showed there was no obvious change in the mitochondrial membrane potential when MCF-7 breast cancer cells were treated with 32 µM arsenic trioxide for 24 hours (Figure. 6.10b). Compared to untreated cells (2.84±0.438), arsenic trioxide (1.45±0.475) and curcumin (1.99±0.658) caused less damage to the mitochondrial membrane of MCF-7 cells as demonstrated in Table 6.6.

Table 6.6: The mitochondrial membrane potential mean percentages and SEM of MCF-7 cells.

Treatment	**Mean (%)±SEM**				
	Live	**Depolarized /Live**	**Depolarized /Dead**	**Dead**	**Total-Depolarized**
Control	91.89±0.550	2.66±0.413	1.19±0.074	5.27±0.298	2.84±0.438
32 µM As_2O_3	26.88±1.270	1.22±0.362	0.17±0.078	71.66±1.659	1.45±0.475
100 µM Curcumin	23.62±1.064	0.86±0.273	1.13±0.396	74.28±0.454	1.99±0.658

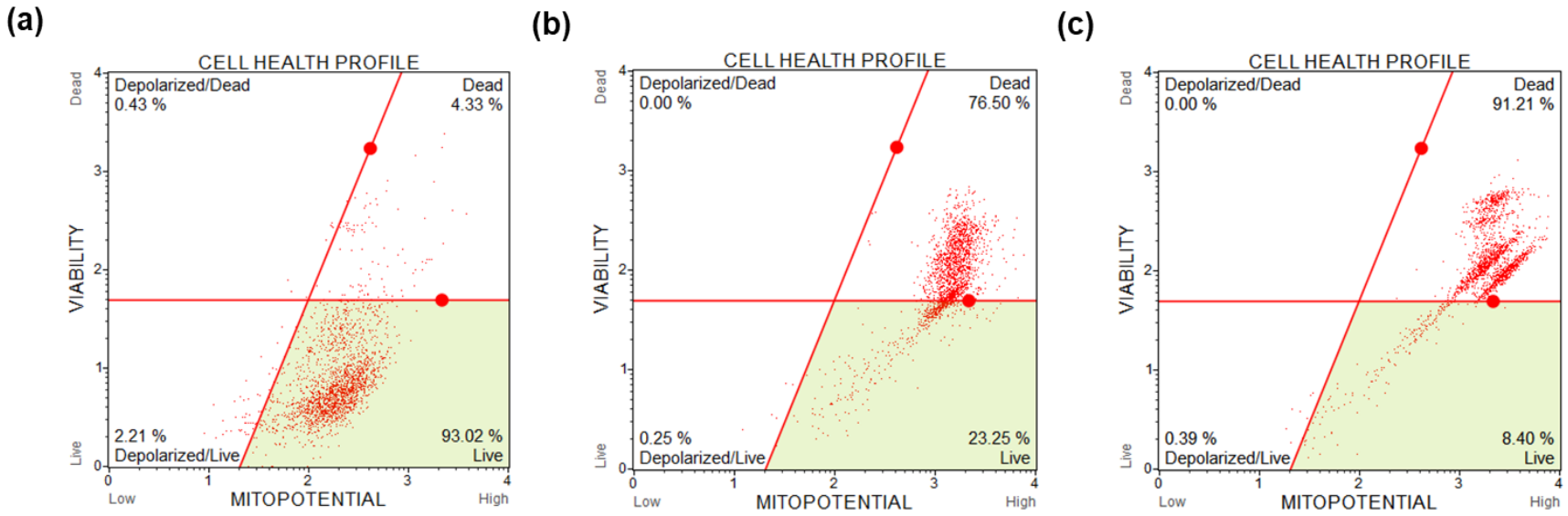

Figure 6.10 – Mitochondrial membrane integrity profiles of the MCF-7 cells after 24 h treatment: (a)-Control, (b)-32 µM arsenic trioxide, (c)-100 µM curcumin and (d)-depolarized cell percentages. The data was analysed using Muse® Cell Analyser.

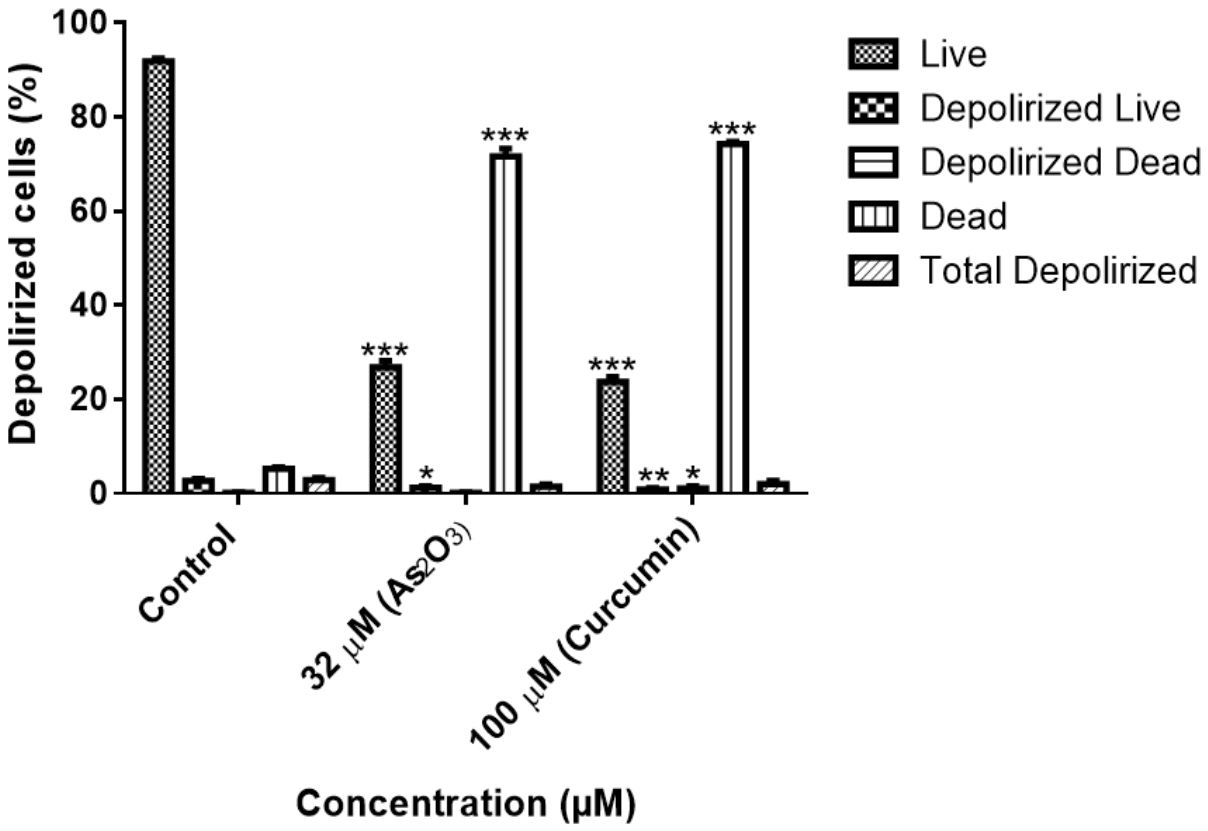

Figure 6.11 – Mitochondrial membrane depolarization percentages of the MCF-7 cells: The cells were treated with 32 µM arsenic trioxide and 100 µM curcumin. Shown are representative data of three independent experiments (percentage mean ±SEM). The difference were found to be statistically significant (* $p<0.05$, ** $p<0.01$ and *** $p<0.001$).

6.8. Multi-Caspase activation of MCF-7 cells

As shown in figures 6.6 and 6.7, arsenic trioxide- induced apoptosis in MCF-7. Multi-Caspase Assay was used to ascertain the induction of caspase-dependent apoptosis by arsenic trioxide in the MCF-7 breast cancer cells. The Muse® Multi-Caspase Kit with the aid of the Muse® cell Analyser were used after 24 hour treatment. It was observed that 32 µM of arsenic trioxide and 100 µM curcumin significantly induced the activation of several caspases including (1, 3, 4, 5, 6, 7, 8 and 9) [Figure 6.12], to 94.07±4.324 and 87.29±5.483 ($p<0.001$) comparing with the untreated cells which had 8.62±1.336 as shown in Table 6.7, respectively.

Table 6.7: The Multi-Caspase mean percentages and SEM of MCF-7 cells.

Treatment	**Mean (%)±SEM**				
	Live	**Dead**	**Caspase+**	**Caspase+ Dead**	**Total-caspase**
Control	91.07±0.933	0.73±0.292	2.18±0.619	6.44±1.076	8.62±1.336
32 µM As_2O_3	18.95±5.837	0.22±0.160	27.07±6.473	55.42±4.999	94.07±4.324
100 µM Curcumin	12.43±5.416	0.08±0.422	40.62±5.556	46.67±7.404	87.29±5.483

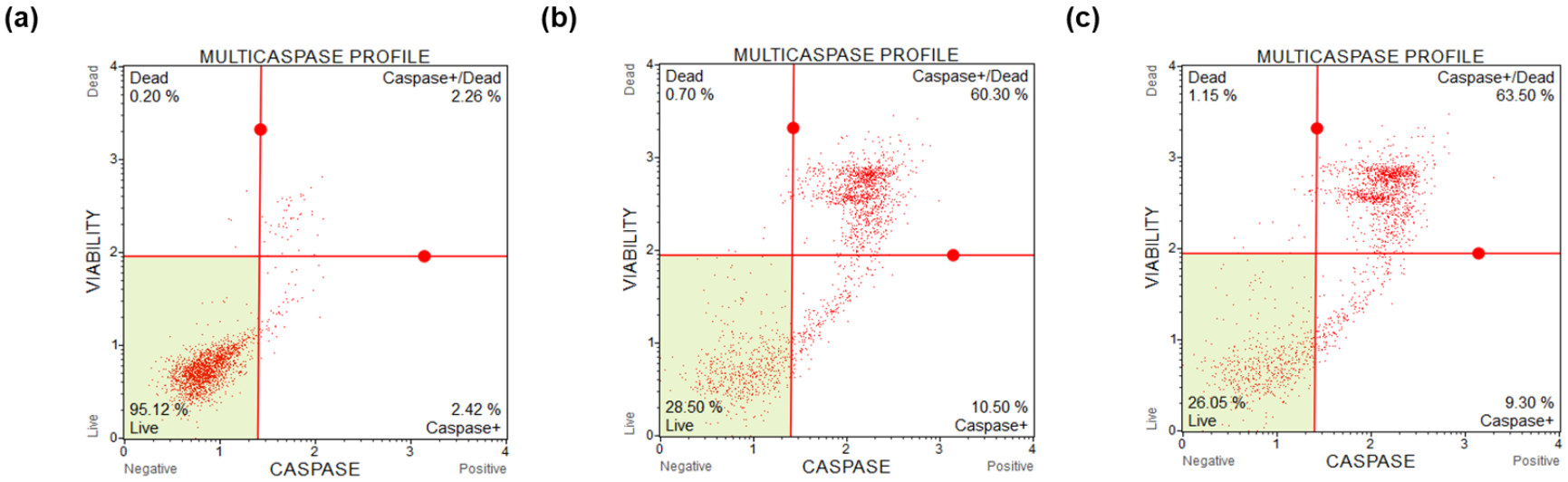

Figure 6.12 – Multi-Caspase profiles of the MCF-7 cells after 24 h treatment: (a)-Control, (b)-32 µM arsenic trioxide and (c)-100 µM curcumin. The data was analysed using Muse® Cell Analyser.

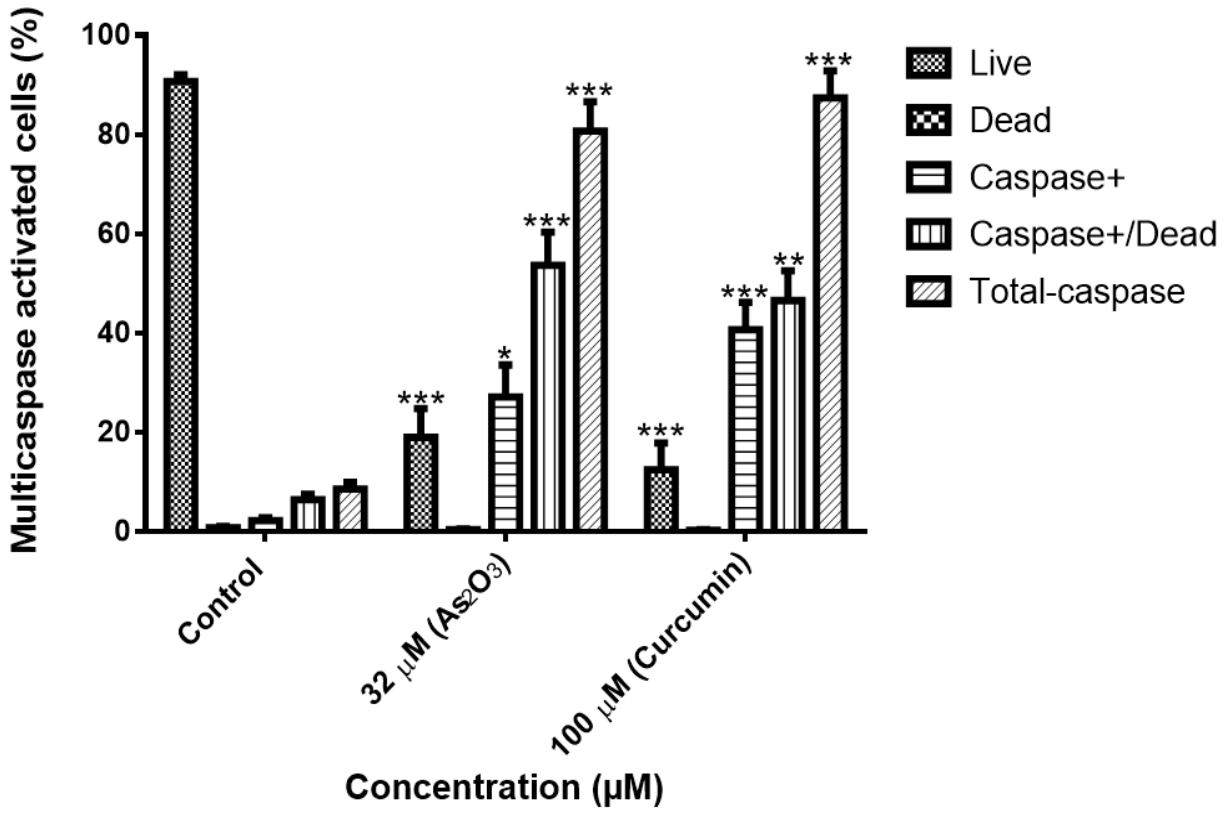

Figure 6.13 – Multi-Caspase analysis of the MCF-7 cells: Shown are representative data of three independent experiments (percentage mean ±SEM). The difference were found to be statistically significant (* $p<0.05$, ** $p<0.01$ and *** $p<0.001$).

6.9. Arsenic trioxide downregulated MAPK activation in MCF-7 cells

To analyse the mechanism in which arsenic trioxide inhibit growth, its anti-tumour activity through inactivation of MAPK and PI3K signalling pathways was investigated.

The mitogen-activated protein kinase (MAPK) pathway is a signalling cascade activated by pro-inflammatory stimuli and cellular stresses, playing a critical role in the translational regulation of pro-inflammatory cytokine synthesis. The MAPK Assay was performed to evaluate the effect of arsenic trioxide on the total expression of MAPK (Erk1/2). Muse® Cell Analyser was used to measure the amount of MAPK activated in MCF-7 cells after 24 hour treatment with 11 µM and 32 µM arsenic trioxide, 100 µM cobalt chloride and 100 µM curcumin. The results in figure 6.14 demonstrated higher levels of activated MAPK in the untreated cells (75.35±4.308) and the levels significantly decreased to 43.18±3.902 ($p<0.01$) and 40.23±8.805 ($p<0.05$) after treatment with 11 µM and 32 µM of arsenic trioxide. Cobalt chloride and curcumin severely decreased the activated MAPK to (30.47±4.707) and (27.43±12.941), respectively. The results are summarized in Table 6.8.

Table 6.8: The MAPK population mean percentages and SEM of MCF-7 cells.

Treatment	**Mean (%)±SEM**		
	Inactivated	**Activated**	**Non-expressing**
Control	10.60±4.123	75.35±4.308	18.15±4.274
11 µM As_2O_3	13.56±2.723	43.18±3.902	23.175±4.524
100 µM ($CoCl_2$)	10.73±4.332	30.47±4.707	37.63±8.777
32 µM As_2O_3	18.67±3.783	40.23±8.805	27.87±11.129
100 µM curcumin	27.37±10.133	27.43±12.941	37.47±11.795

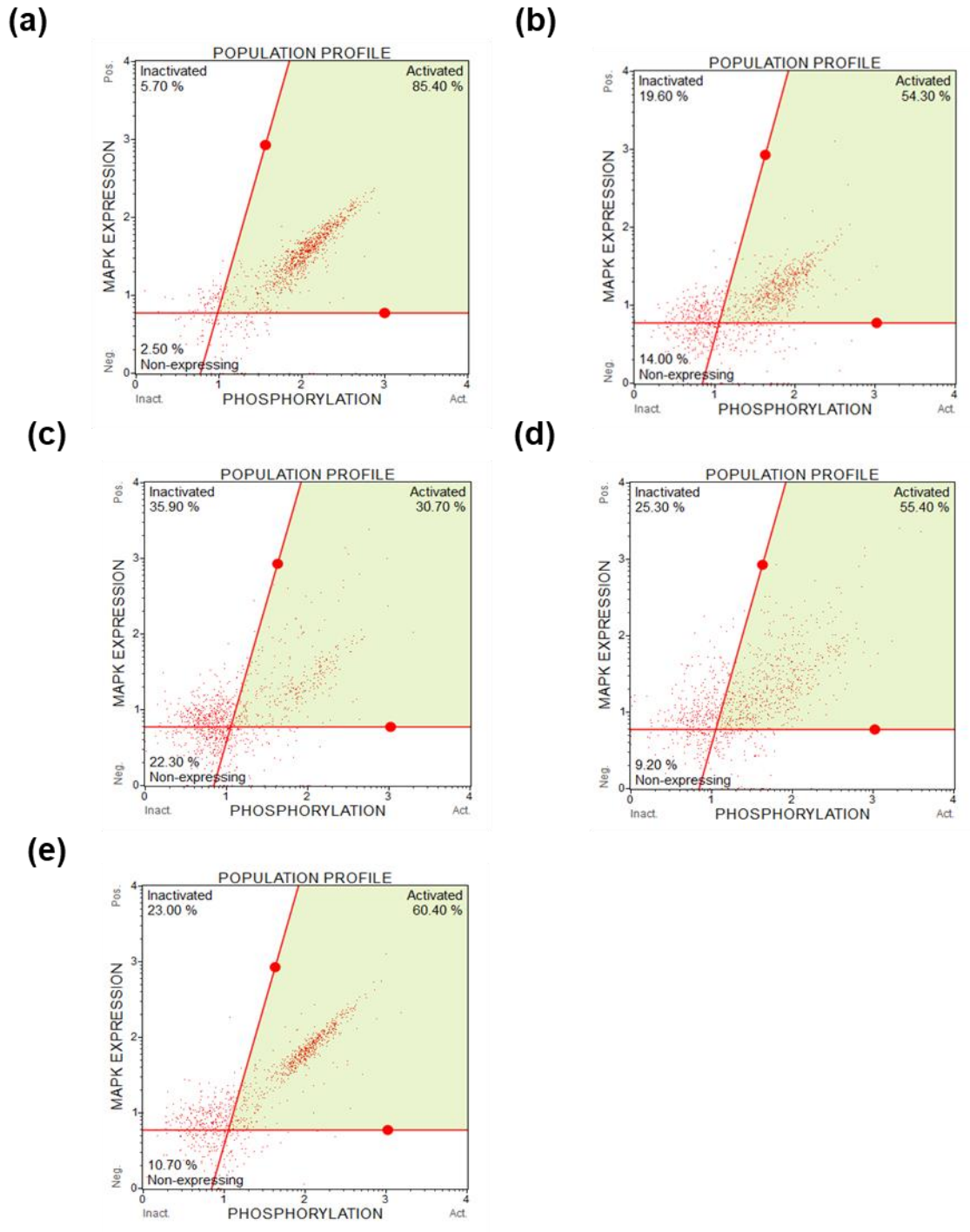

Figure 6.14 – MAPK population profiles of the MCF-7 cells after 24 h treatment: (a)-Control, (b)-11 µM arsenic trioxide, (c)-32 µM arsenic trioxide, (d)- 100 µM cobalt chloride and 100 µM curcumin. The data was analysed using Muse® Cell Analyser.

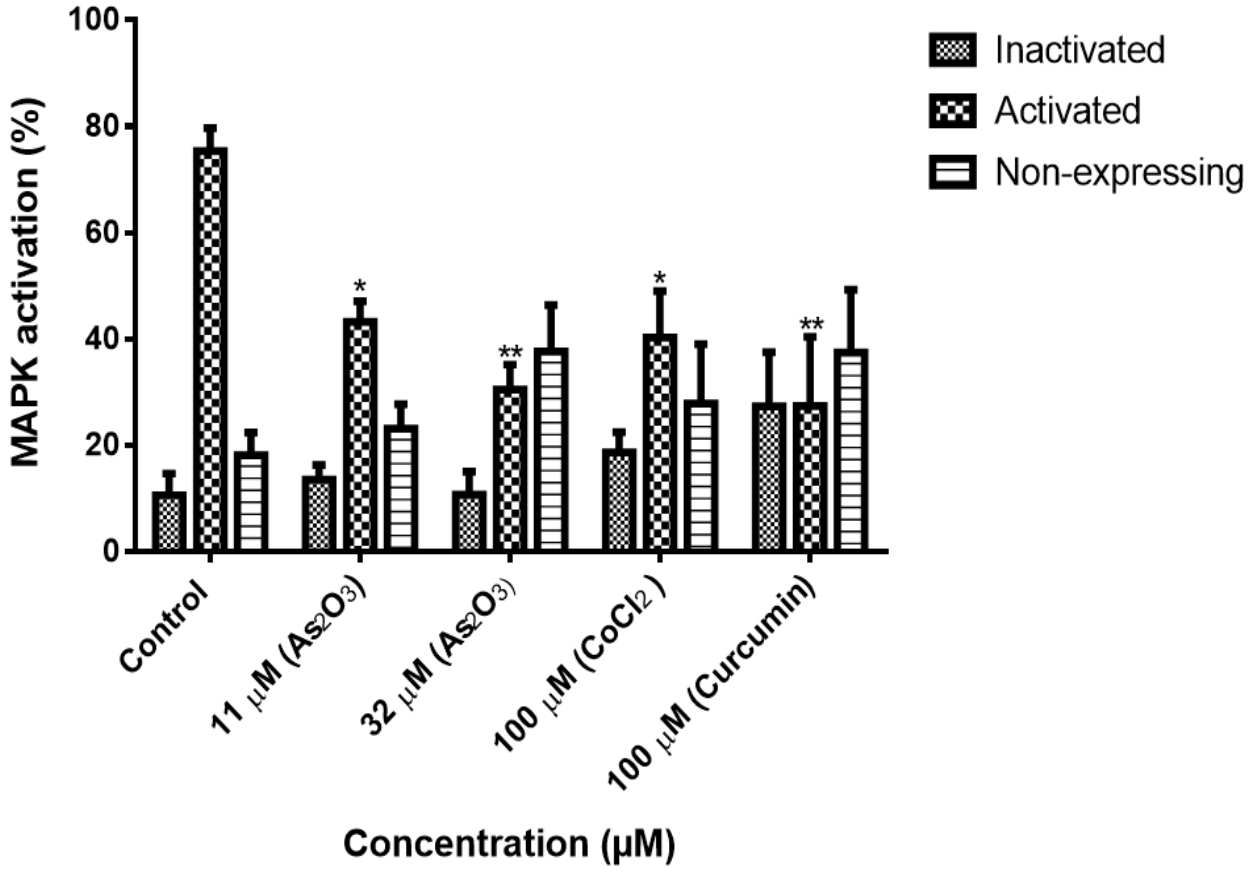

Figure 6.15 – MAPK activation percentages of the MCF-7 cells: The cells were treated with 11 μM and 32 μM arsenic trioxide, 100 μM cobalt chloride and 100 μM curcumin for 24 hours. Shown are representative data of three independent experiments (percentage mean ±SEM). The difference were found to be statistically significant (* $p<0.05$, ** $p<0.01$ and *** $p<0.001$).

6.10. Arsenic trioxide supressed PI3K activation in MCF-7 cells

To investigate the activation of PI3K, MCF-7 cells were exposed to 11 and 32 µM arsenic trioxide, 100 µM cobalt chloride and 100 µM curcumin for 24 hours and PI3K levels were evaluated. As depicted by Muse® Cell Analyzer in figure. 6.16, arsenic trioxide reduced a strong and sustained activation of PI3K in a dose-dependent manner. The level of the untreated cells after PI3K activation was 81.80±2.626. However, a decline of 53.59±8.073 was observed after treatment with 11 µM arsenic trioxide ($p<0.05$) and 46.08±3.738 after treatment with 32 µM arsenic trioxide ($p<0.01$). Cobalt chloride and curcumin decreased the level of activated PI3K to 46.08±3.738 and 0.601±601 respectively (Table 6.9).

Table 6.9: Deactivation of PI3K signalling pathway and SEM of MCF-7 cells.

Treatment	**Mean (%)±SEM**		
	Inactivated	Activated	Non-expressing
Control	4.68±1.636	81.80±2.626	3.43±0.876
11 µM As_2O_3	2.88±0.501	53.59±8.073	7.97±2.092
100 µM ($CoCl_2$)	4.93±1.129	50.12±7.450	13.99±4.886
32 µM As_2O_3	23.68±7.842	46.08±3.738	7.40±1.687
100 µM curcumin	1.63±0.328	90.53±0.601	2.27±0.187

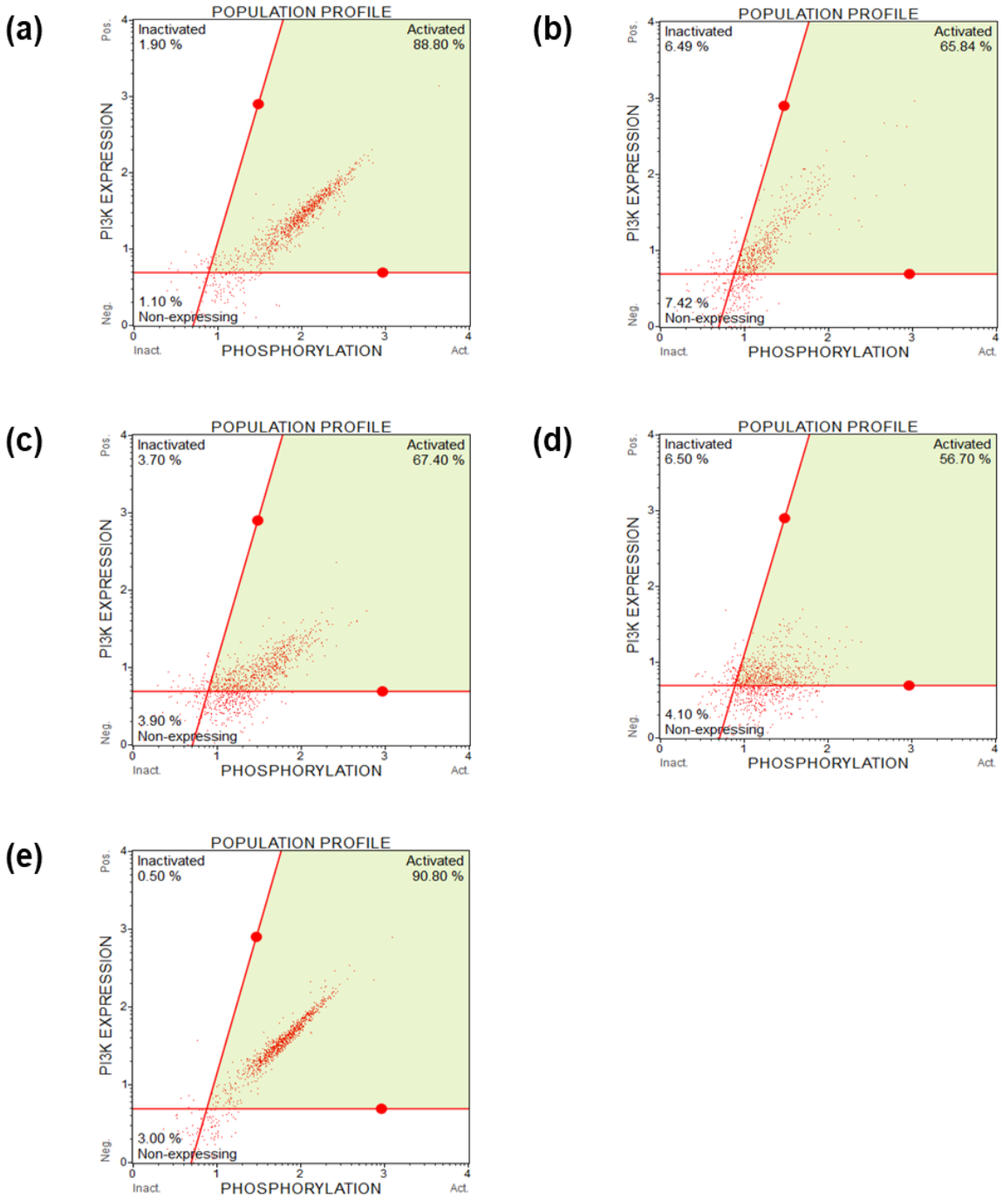

Figure 6.16 – PI3K population profiles of the MCF-7 cells after 24 h treatment: a-Control, b-11 µM arsenic trioxide, c-32 µM arsenic trioxide, d-100 µM cobalt chloride and e-100 µM curcumin. The data was analysed using Muse® Cell Analyser.

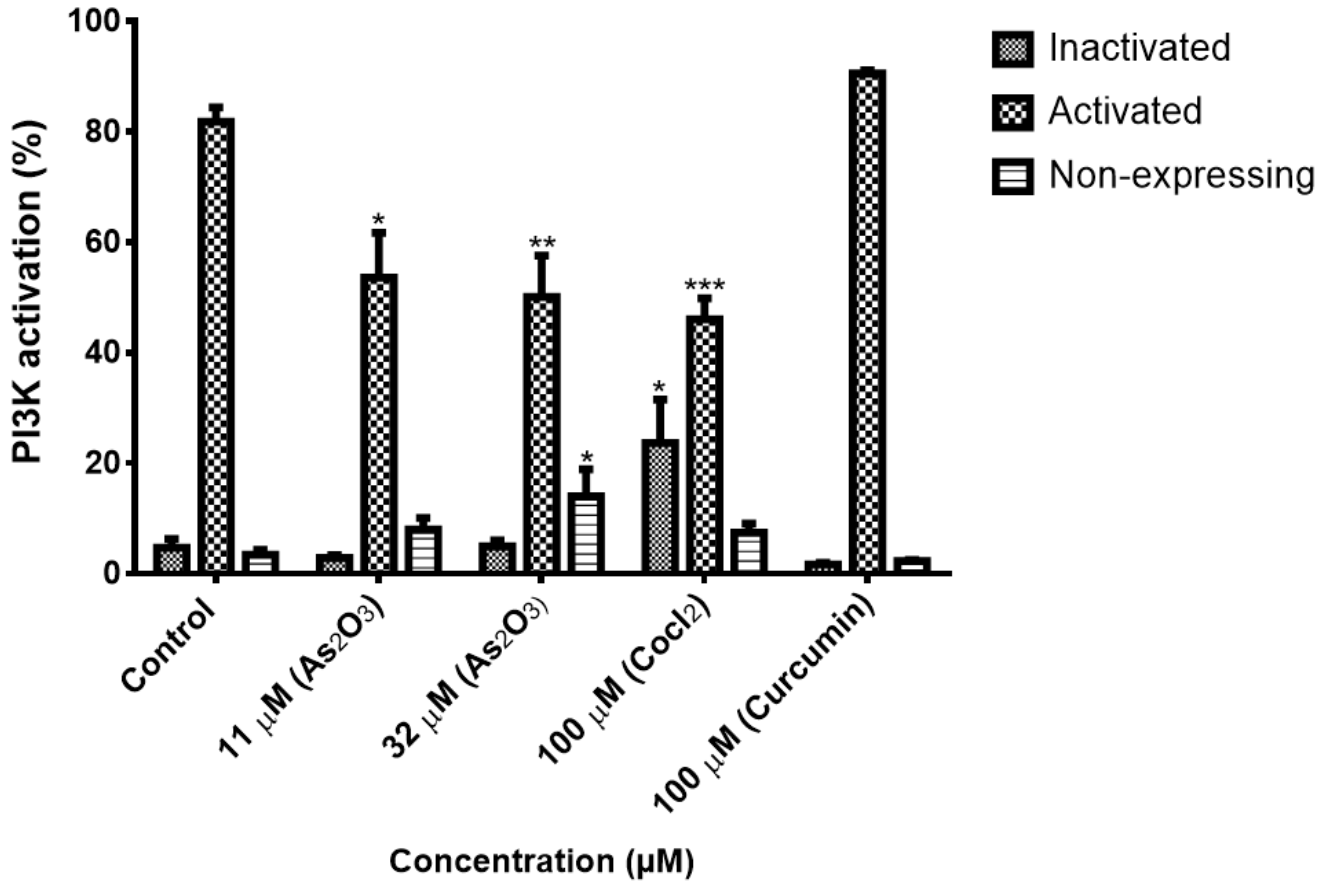

Figure 6.17 – PI3K activation signalling pathway of the MCF-7 cells: The cells were treated with 11 and 32 μM arsenic trioxide, 100 μM cobalt chloride and 100 μM curcumin for 24 hours. Shown are representative data of three independent experiments (percentage mean ±SEM). The difference were found to be statistically significant (*p<0.05, ** p<0.01 and *** p<0.001).

6.11. Deregulation of survivin splice variants in MCF-7 cells depend on various biological pathways

Due to alternative splicing, the human *survivin* (*BIR5*) gene was transcribed into six dissimilar mRNA transcripts namely: wild-type survivin, survivin-2B, survivin-ΔEx3, survivin 3B, survivin 3α and survivin 2α. Survivin variant 2B was found to be highly upregulated during arsenic trioxide-induced cell cycle arrest but not cobalt chloride-induced cell cycle arrest, arsenic trioxide-induced and curcumin-induced apoptosis (Figure. 6.18a). During arsenic trioxide- and cobalt chloride-induced G2/M cell cycle arrest and arsenic trioxide-induced apoptosis, survivin 3α was found to be upregulated compared to the untreated cells (Figure. 6.18b). Survivin wild-type was highly expressed in the untreated MCF-7 cells, the expression was upregulated during arsenic trioxide-induced G2/M cell cycle arrest, but was downregulated during cobalt chloride-induced G2/M cell cycle arrest, arsenic trioxide-induced and curcumin-induced apoptosis (Figure. 6.18c). Survivin variant ΔEx3 was undetectable in untreated and treated MCF-7 cells (Figure. 6.18d). Variant ΔEx3 was only found in colon cancer cells. Survivin 2α was upregulated during arsenic trioxide-induced and curcumin-induced apoptosis (Figure. 6.18e), whereas survivin 3B was lowly expressed only in the untreated cells (Figure. 6.18f). GAPDH was used as a loading control. The band density results are summarised in Table 6.10 and represented in figure 6.19.

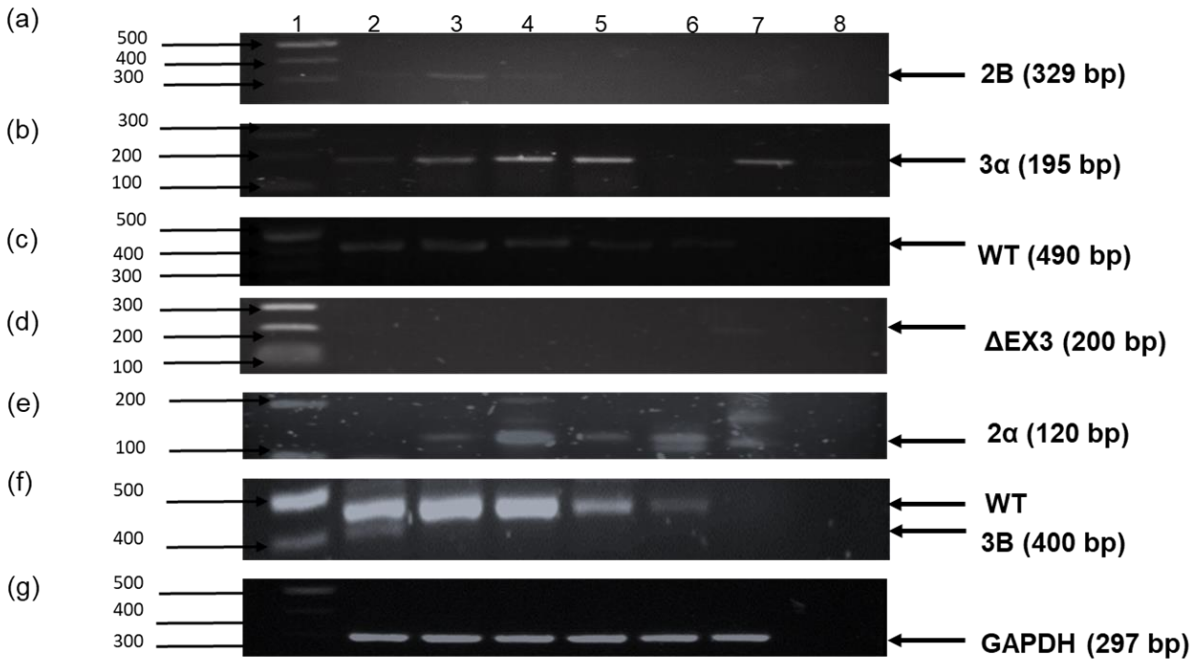

Figure 6.18 – RT-PCR analysis of survivin splice variants. (a) Survivin variants (wild-type, 2B, 3α, 3B, 2α and ΔEx3) in MCF-7 breast cancer cells after 24 h treatment with the arsenic trioxide, cobalt chloride and curcumin. Lane 1: Marker, Lane 2: untreated, Lane 3: 11 μM arsenic trioxide, Lane 4: 32 μM arsenic trioxide, Lane 5: 100 μM Cobalt chloride, Lane 6: 100 μM curcumin, Lane 7: Caco2 untreated, Lane 8: blank. GAPDH was used as a loading control. (b) Relative mRNA expression percentages of survivin splice variants measure using Quanty-One 4.6.5 software (BioRad, USA).

Table 6.10: The mean band densities and SEM of survivin splice variants.

Treatment	Mean (INT/mm^2)±SEM						
	2B	3α	WT	ΔEx3	2α	3B	GAPDH
Control	561.75±27.885	1582.00±90.145	4551.00±11.321	0.00±0.000	0.00±0.000	1662.00±42.874	3060.80±14.020
11 μM As_2O_3	1255.50±30.991	2204.80±54.928	4860.30±17.594	0.00±0.000	2171.30±10.640	0.00±0.000	3123.50±30.278
32 μM As_2O_3	956.00±10.901	2816.00±35.178	4460.50±17.400	0.00±0.000	3070.00±24.230	0.00±0.000	3080.80±15.008
100 μM $CoCl_2$	0.00±0.000	3375.00±159.500	3635.00±16.926	0.00±0.000	2300.80±84.037	0.00±0.000	3067.30±47.271
100 μM curcumin	0.00±0.000	0.00±0.000	1643.80±15.472	0.00±0.000	2352.80±12.619	0.00±0.000	3049.00±22.162
Caco2	0.00±0.000	3722.00±128.450	0.00±0.000	2057.00±21.829	1806.00±42.870	0.00±0.000	3036.80±10.633

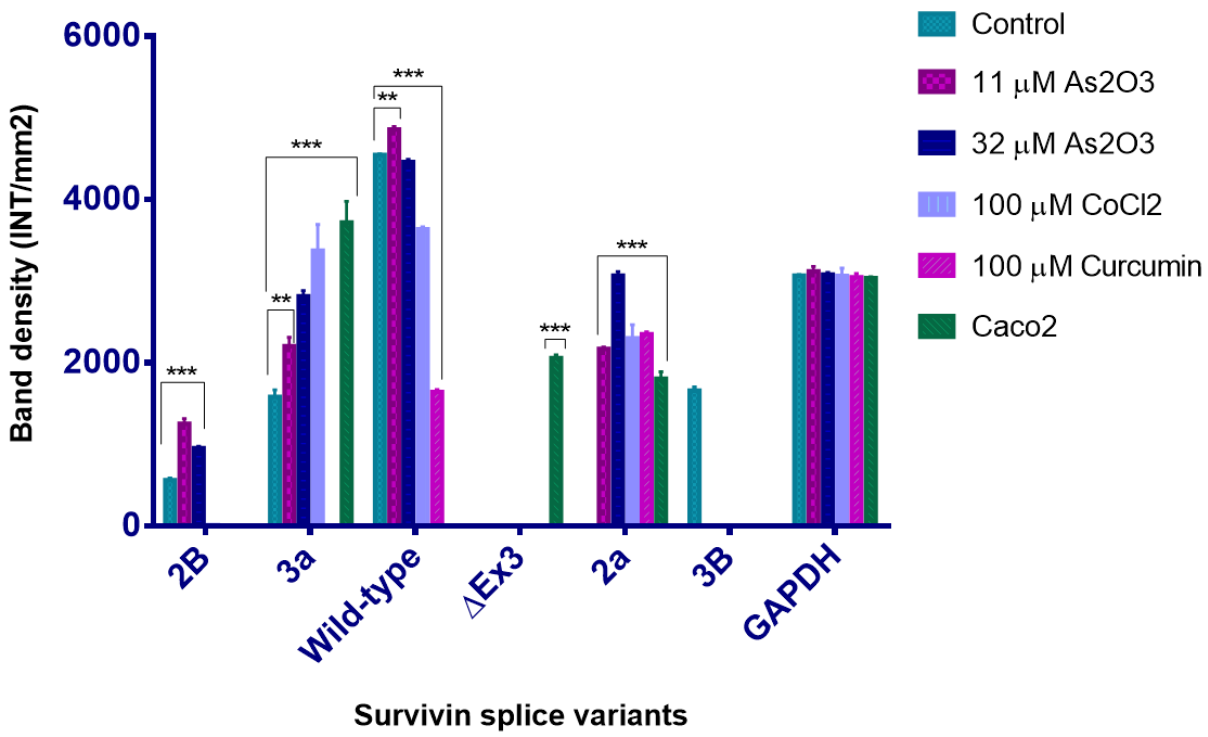

Figure 6.19 – The band density differences of survivin splice variants. Shown are representative data of three independent experiments (percentage mean ±SEM). The difference were found to be statistically significant (** $p<0.01$ and *** $p<0.001$). The density was measured using Quanty-One software (BioRad, USA).

6.12. The sub-cellullar localization of survivin protein in breast cancer cell line MCF-7

Immunohistochemistry was performed to localize and assess survivin protein expression in breast cancer MCF-7 cells. The staining of survivin protein was mainly localized in the cytoplasm and nucleus as shown in figure. 6.20. Survivin proteins are expressed more in the cells treated with 11 µM Arsenic trioxide (G2/M phase) and decreased during apoptosis (Figure 6.20f and Figure 6.21). The results correlate with the mRNA expression of survivin 2B and survivin wild-type in figure 6.18b and figure 6.20. The fluorescence intensity results are summarised in Table 6.11.

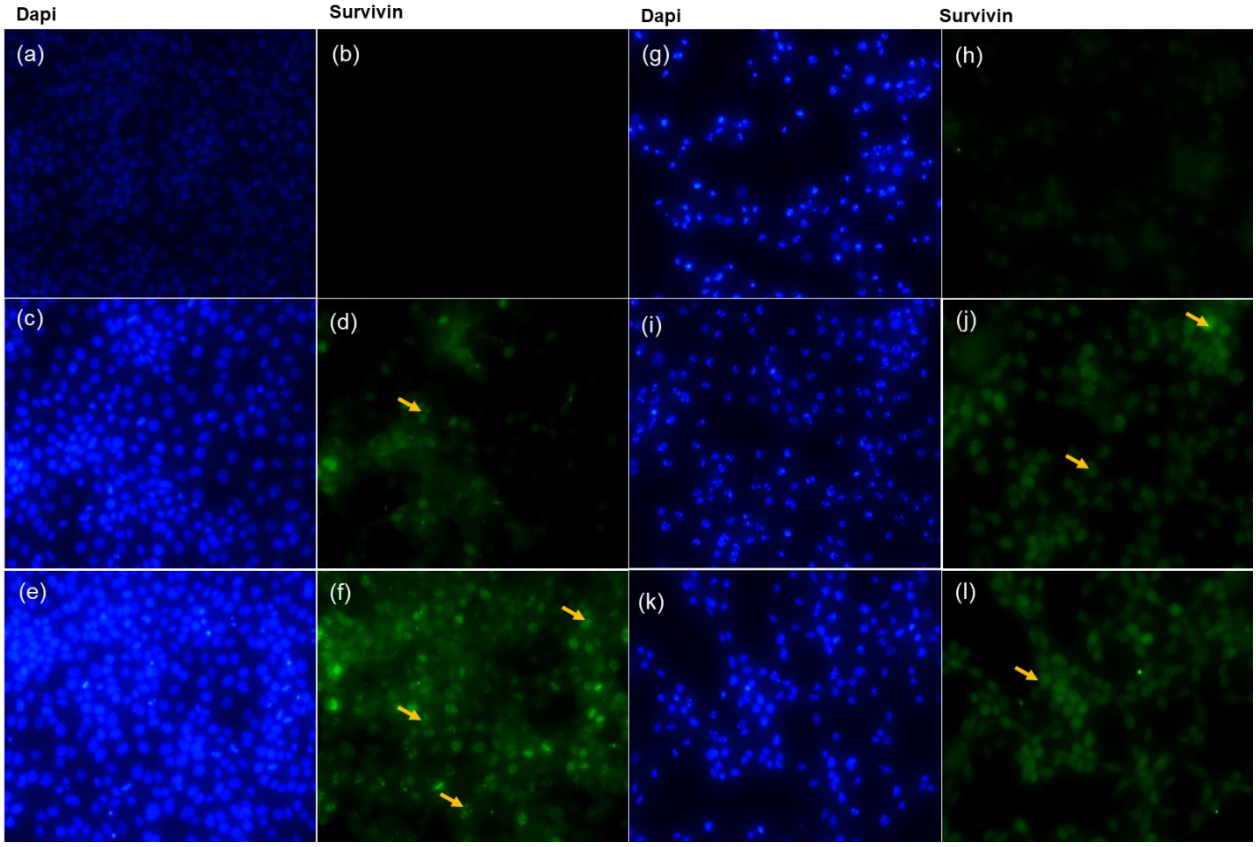

Figure 6.20 – Immunostaining of survivin protein in MCF-7cells after 24 h treatment: The untreated cells without primary antibody (a-b) and with both antibodies (c-d). The cells were treated with 11 (e-f) and 32 (g-h) µM arsenic trioxide, 100 µM cobalt chloride (i-j) and 100 µM curcumin (k-l) for 24 h. The staining of survivin was mainly located in the cytoplasm and nucleus. The arrows (yellow) indicate survivin protein.

Table 6.11: The mean fluorescence intensities and SEM of survivin proteins

Treatment	Mean Intensity (%)±SEM
Control	28.42±1.957
11 μM As_2O_3	43.00±0.212
100 μM ($CoCl_2$)	13.84±0.819
32 μM As_2O_3	34.30±0.156
100 μM curcumin	29.89±0.152

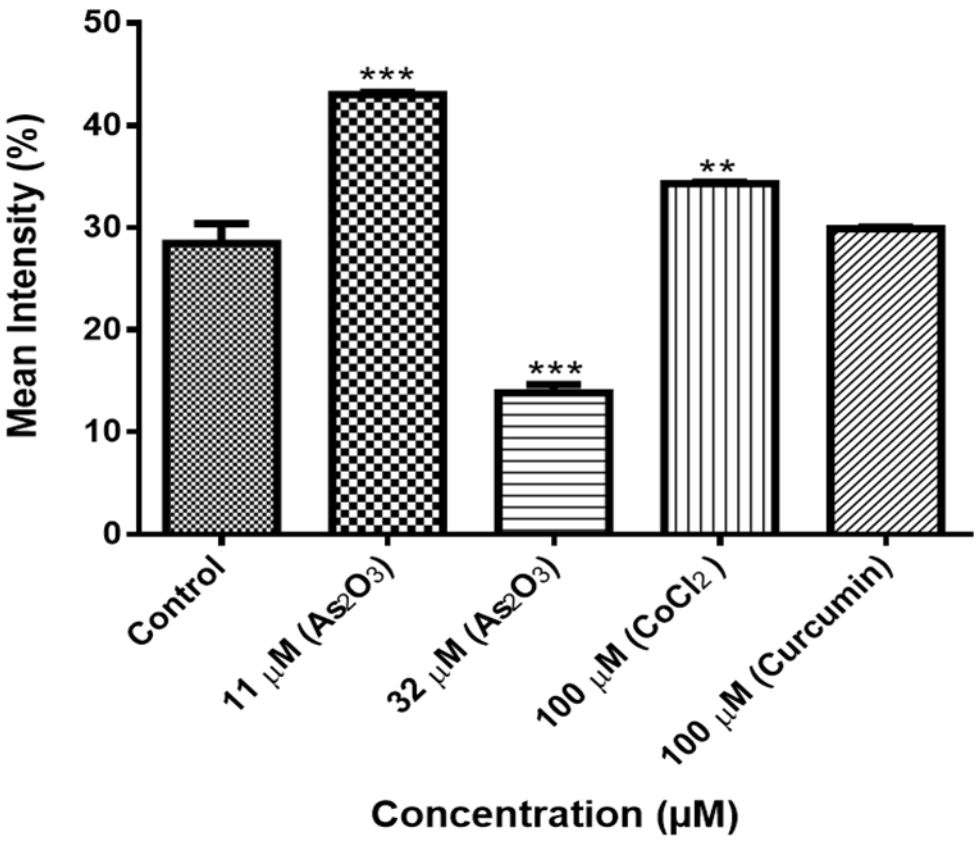

Figure 6.21 – The mean intensity percentage of the survivin proteins expression: Shown are representative data of three independent experiments (percentage mean ±SEM). The difference were found to be statistically significant (* $p<0.05$, ** $p<0.01$ and *** $p<0.001$). The mean intensity was measure using the Image J software (https://imagej.nih.gov/ij/docs/index.html).

6.13. Analysis of survivin variants-specific MiRs and their expression in breast and other cancers.

No work has been done to identify MiRNAs which are specific to all the survivin variants. Reports in literature only mentioned MiRNAs which down-regulate survivin expression and hence, it is assumed it is wild-type survivin. Unexpectedly, according to MiRNA databases (MirTarbase.mbc.nctu.edu.tw, www.TargetScan.org and www.MIRD.org) all the reported MiRNAs are specific to survivin wild-type, survivin 2B and survivin ΔEx3. All the MiRs validated and predicted in Bioinformatics databases only target survivin transcripts (survivin wild-type, survivin 2B and survivin ΔEx3) that have complete sequences in the NCBI (www.ncbi.gov) [Table 6.12]. Survivin variant 2B was found to be the most validated target of MiR-542-3p, MiR-218-5p and MiR-335-5p while, survivin wild-type and survivin ΔEx3 are the predicted splice variants (Table 6.12). Almost all the MiRs targeting survivin variants are involved in apoptosis and only a few such as MiR-203a-3p and MiR-150-5p are upregulated during both apoptosis and cell cycle arrest while, MiR-218-5p is only upregulated during cell cycle (Table 6.13).

Table 6.12: MiRs that are specific to survivin variants.

Survivin splice variants	MiRs Databases		
	MiRTarBase	MIRDB	TargetScan
Survivin wild-type	MiR-542-3p MiR-218-5p MiR-335-5p MiR-708-5p MiR-203a-3p MiR-34a-5p MiR-195-5p MiR-497-5p MiR-150-5p MiR-16-5p MiR-214-3p	0	MiR-542-3p MiR-218-5p MiR-335-5p MiR-708-5p MiR-203a-3p MiR-34a-5p MiR-195-5p MiR-497-5p MiR-150-5p MiR-16-5p MiR-214-3p
Survivin 2B	MiR-542-3p MiR-218-5p MiR-335-5p MiR-708-5p MiR-203a-3p MiR-34a-5p MiR-195-5p MiR-497-5p	MiR-542-3p MiR-218-5p MiR-335-5p	MiR-542-3p MiR-218-5p MiR-335-5p MiR-708-5p MiR-203a-3p MiR-34a-5p MiR-195-5p MiR-497-5p

	MiR-150-5p MiR-16-5p MiR-214-3p		MiR-150-5p MiR-16-5p MiR-214-3p
Survivin ΔEx3	MiR-542-3p MiR-218-5p MiR-335-5p MiR-708-5p MiR-203a-3p MiR-34a-5p MiR-195-5p MiR-497-5p MiR-150-5p MiR-16-5p MiR-214-3p	0	MiR-542-3p MiR-218-5p MiR-335-5p MiR-708-5p MiR-203a-3p MiR-34a-5p MiR-195-5p MiR-497-5p MiR-150-5p MiR-16-5p MiR-214-3p
Survivin 2α	0	0	0
Survivin 3B	0	0	0
Survivin 3α	0	0	0

Table 6.13: The expression of survivin specific MiRs in cancer cells.

MiRs	Cell cycle	Apoptosis	Cancer cell line	Reference
MiR-542-3p	Not involved	Involved	Osteoblast ↓ MCF-7 ↓ MDA-MB-231 ↓ NSCL ↓	Kureel *et al*., 2014; Wang *et al*., 2016; Liu *et al*., 2017.; Wu *et al*., 2017
MiR-218-5p	Involved	Not involved	MCF-7 ↓ MDA-MB-231-a & b ↓ NSCL ↓ BCA tissues ↓	Cheng *et al*., 2015; Taipaleenmamaki *et al*., 2016; Zhu *et al*., 2016.

MiR-335-5p	Not involved	Involved	MCF-7 ↓ Gastric cancer ↓	Heyn *et al*., 2011; Li *et al*., 2014
MiR-214-3p	Not involved	Involved	Esophageal cancer ↓	Phatak *et al*., 2016
MiR-34a-5p	Not involved	Involved	HPV-positive cervical cancer ↓ Gastric cancer ↓	Cao *et al*., 2014; Geng *et al*., 2015
MiR-203a-3p	Involved	Involved	HepG2 ↓ Pancreatic cancer cells ↓ Pancreatic cancer ↓ MCF-7 ↓	Wei *et al*., 2013; Xu *et al*., 2013
MiR-708-5p	Not involved	Involved	Renal cancer ↓	Saini *et al*., 2011
MiR-16-5p	Not involved	Involved	Colorectal cancer ↓ Lung cancer ↑	Ke *et al*., 2013; Ma *et al*., 2013

MiR-150-5p	Involved	involved	Nasopharyngeal carcinoma ↓ Human acute lymphoblastic leukemia ↓	Fang *et al*., 2016; Li *et al*., 2017
MiR-497-5p	Not involved	Involved	Angiosarcoma ↓	Chen *et al*., 2016

Key: Upregulated = ↓

Downregulated = ↓

6.14. Discussion

The aim of this study was to determine the effect of arsenic trioxide on the expression of survivin splice variants and their specific MiRs during cell cycle progression and apoptosis in breast cancer cell line, MCF-7. To date, there is a very limited number of studies directly or indirectly investigating the expression of survivin splice variants breast cancer cells. The focus has been on the wild-type only, where its expression has been shown to favour the carcinogenesis process (Garg *et al*., 2016). Additionally, arsenic trioxide has been used for ages to treat proteolytic leukaemia (Yedjou *et al*., 2009). In this study, arsenic trioxide showed cytotoxic effect against the MCF-7 breast cancer cells. In order to understand the expression of survivin splice variants during arsenic trioxide-induced cell cycle arrest and apoptosis, the viability of MCF-7 cells was investigated using MTT Assay, the Muse® Count and Viability Assay. Both confirmed that arsenic trioxide reduced the viability of the MCF-7 cells in a concentration-dependent manner (Figure. 6.1 and 6.2). This is in line with the previous report (Liu *et al*., 2015), which showed that arsenic trioxide suppressed the growth of MCF-7 cells. Eleven micro molar (11 µM) of arsenic trioxide suppressed 50% cell growth, while 32 µM of arsenic trioxide yielded the lowest cell viability of the MCF-7 cells and was then used to investigate apoptosis in this study, while 11 µM was used to investigate cell cycle arrest potential of arsenic trioxide against MCF-7 cells.

The morphology of cells can be affected by the conditions in which the cells are exposed to. To examine the effect of arsenic trioxide on the morphology of MCF-7 breast cancer cells, the cells were exposed to various concentrations of arsenic trioxide for a period of 24 hours. As demonstrated in figure. 6.4a, the untreated cells maintained their epithelial morphological shape. However, the cells treated with arsenic trioxide exhibited morphological changes typical to apoptosis (Figure. 6.4b-e). Arsenic trioxide reduced the MCF-7 cell numbers in a concentration-dependent manner, which can be attributed to characteristics observed from the treated cells. The treated cells displayed increased cellular volumes and ruptured nuclear membrane. These are characteristics of cells undergoing apoptosis. This data concurred with what was demonstrated by Liu *et al*. (2015), where it was shown that arsenic trioxide treated cells changed from polygonal to round shape, displaying partly condensed chromatin and the appearance of vacuoles.

Fluorescence microscopy further confirmed apoptotic features induced by arsenic trioxide (Figure. 6.5). When the untreated control cells were stained with DAPI, they showed normal intact nuclei, whereas the treated MCF-7 cells with 11 μM arsenic trioxide displayed mostly mitotic morphology, suggesting that the cells may be arrested at the G2/M cell cycle arrest checkpoint. As the concentration of arsenic trioxide increased to 16 μM (Figure. 6.5d), cell numbers decreased with several apoptotic features such as membrane blebbing and nuclear condensation appearing. The cells that were treated with 32 μM showed more membrane blebbing and nuclei fragmentation (Figure. 6.5e). This concurred with another study that reported that arsenic trioxide induces apoptosis in breast cancer MCF-7 cells (Zhang *et al*., 2015). As the concentration of arsenic trioxide increased, the number of apoptotic cells also increased, which confirmed that the compound induces cellular apoptosis in a concentration-dependent manner.

To further elucidate the cell cycle arrest potential of arsenic trioxide, the DNA content using the Muse® Cell Cycle Kit was examined. In this study, figures. 6.6 and 6.7 showed the G2/M percentage of cells after treatment with 11 μM arsenic trioxide (45.13±0.942) was much higher than the complement of G2/M cells in the control untreated cells (25.73±1.824) [Table 6.4]. The cell cycle results showed that arsenic trioxide- induced G2/M cell cycle arrest of MCF-7 cells. Several studies have also reported arsenic trioxide as a therapeutic agent, which can induce cell cycle arrest and expression of certain cell cycle-specific genes in malignant tumours (Chen *et al*., 2016; Park *et al*., 2003).

Additionally, Table 6.5 and Figure. 6.8 showed arsenic trioxide- induced late apoptosis rather than early apoptosis. The same trend was previously observed in the breast cancer cell line MCF-7 (Wang *et al*., 2011) and other cell lines such as T80, HEY and SKOV3 ovarian cancer cells (Smith *et al*., 2010). The data from this study suggests that arsenic trioxide induces the extrinsic pathway as it was shown to have no effect on the mitochondrial-mediated apoptotic pathway (Figures. 6.10 and 6.11). This is in line with another study that showed the same results when HepG2 cells were exposed to arsenic trioxide for a period of 7 days (Siu *et al*., 2002). The caspases (cysteine-directed aspartate-specific proteases) are important in directing the process of programmed cell death in response to apoptotic signals (Forgarty *et al*., 2017). In this study, Multi-Caspase Assay revealed that 32 μM arsenic trioxide lead to the activation of several caspases

including 1, 3, 4, 5, 6, 7, 8 and 9 suggesting that arsenic trioxide induces caspase-dependent apoptosis (Figures. 6.12 and 6.13) because all the activated caspases include the initiator caspases (caspase 8 and 9) and execution caspases (3 and 7).

To further characterize the mechanism by which arsenic trioxide suppresses cell growth of MCF-7 cells, intracellular signalling pathways known to be activated during proliferation and development of cancer were analysed. Many of these signal transduction pathways involve activation of protein serine/threonine kinase of extracellular signal-regulated kinases (ERK) family by oestrogen and are involved in cellular growth (Kim and Choi, 2010). To determine the effect of arsenic trioxide on these cell survival pathways, the MCF-7 cells were exposed to 11 and 32 μM arsenic trioxide for 24 h and the levels of MAPK and PI3K activation were determine using the Muse® Cell Analyser. The MAPK levels (Figures. 6.14 and 6.15) and PI3K levels (Figures. 6.16 and 6.17) were significantly deactivated during arsenic trioxide-induced cell cycle arrest and apoptosis. Previously, arsenic trioxide was shown to inhibit the activation of MAPK and PI3K pathways in U118-MG cells and in gastric cancer cells (Chiu *et al*., 2009; Li *et al*., 2009). Based on these results, MAPK and PI3K total expression and phosphorylation can be said to be associated with cancer cell survival and growth.

Reverse-Transcription Polymerase Chain Reaction (RT-PCR) was used to analyse the differential expression of survivin splice variants during arsenic trioxide-induced cell cycle arrest and apoptosis in the breast MCF-7 cancer cells. Although expression of survivin during cell cycle progression has been studied, little is known about the expression of splice variants, especially in arsenic trioxide-mediated cell cycle arrest. Survivin 2B is a variant that is pro-apoptotic or anti-apoptotic depending on the type and stage of the cancer. In this study, the expression of variant 2B was undetectable in the untreated MCF-7 cells but upregulated during arsenic trioxide-induced cell cycle arrest (Figure. 6.18a and Figure 19) and the expression was downregulated during arsenic trioxide-induced apoptosis. This data suggests that survivin 2B has a role in cell cycle regulation than in apoptosis. Previously, a more variable expression of survivin 2B level was found at different breast cancer stages (Khan *et al*., 2014). This study showed that survivin wild-type was highly expressed in the untreated MCF-7 cells and interestingly, the expression was upregulated at G2/M cell cycle arrest. When apoptosis was induced by arsenic

trioxide, its expression was decreased. The data revealed low expression of the anti-apoptotic survivin variant 3α in MCF-7 cells (Figure. 6.18b and Figure 19). Its expression was found to be upregulated during arsenic trioxide-induced cell cycle arrest and apoptosis.

The findings of this study concur with previous studies that have shown that apoptosis induction decreases the expression of survivin wild-type (Neophytou *et al*., 2014; Li *et al*., 2015). This study further showed that survivin ΔEx3 is undetectable in MCF-7 cells and during arsenic trioxide-induced cell cycle arrest and apoptosis but was detected in Caco2 colon cancer cells. This supports previous report that showed little or no expression of ΔEx3 in breast carcinoma (Végran *et al*, 2011). Végran *et al*. (2005) revealed that survivin wild-type, survivin-ΔEx3, and survivin 2B have no prognostic role in breast carcinoma. In this study, no trace of survivin 2α was found in the untreated MCF-7 cells. The expression was upregulated during arsenic trioxide-induced apoptosis and G2/M cell cycle arrest. The expression increased during apoptosis induced by arsenic trioxide. The results is in agreement with literature whereby the expression of variant 2α was noticed after treatment of acute promyelocytic leukaemia cell line with arsenic trioxide (Zaki Dizaji *et al*., 2017).

There is concrete evidence showing that survivin variants are highly expressed in cancer cells including MCF-7 cells (Khan *et al*., 2014; Pavlidou *et al*., 2014) and demonstrated a cell-cycle dependent expression with a noticeable increase in the G2/M phase (Li *et al*., 1998). This study, for the first time suggests that survivin splice variants are differentially expressed in MCF-7 cells during both arsenic trioxide-induced cell cycle arrest and apoptosis. These results may suggest that the mode of action of arsenic trioxide in the inhibition of cell proliferation may be dependent on the expression of different survivin splice variants. Furthermore, the role of survivin in breast cancer progression may be boundless to its role in the inhibition of apoptosis, which is a hallmark of cancer.

Human survivin is a 16.5 kDa protein encoded by the *BIRC5* gene, which is located on chromosome 17q25, approximately 3% of the distance from the telomere. *BIRC5* gene comprises three introns and four exons, thus encoding 142 amino acids, with a copy of the BIR domain, essential for the apoptosis inhibition (Li *et al*., 1999). In this study, an

immunocytochemical analysis of the expression of survivin proteins in breast cancer MCF-7 cells was performed. Survivin proteins were found to be expressed in the nuclei and cytoplasm of MCF-7 cells. The expression significantly increased during arsenic trioxide-induced G2/M cell cycle arrest (Figure. 6.20f and Figure 6.21) and low expression was observed in arsenic trioxide-induced apoptosis (Figure. 6.20h and Figure 6.21). This data is consistent with the results from conventional PCR analysis of survivin 2B mRNA expression in MCF-7 cells (Figure. 6.18a) using an antibody that was specific to all the isoforms which contains the first 1-142 amino acids. This further suggest that survivin 2B may have significant role in these processes than initially thought.

Small non-coding microRNAs (MiRs) have established functions in both cancer formation and bone remodeling (Taipaleenmäki *et al*., 2012; Sheng *et al*., 2015). A large pool of evidence proposes that MiRs are potential targets for therapeutic intervention of cancer (White *et al*., 2011; Garofalo *et al*., 2014). By shutting down the expression of hundreds of genes at the same time, MiR on its own can act as an epigenetic master regulator of important biological processes (Pal *et al*., 2015). Numerous MiRs have been confirmed as key regulator of many cellular biological processes in breast cancer such as cell proliferation and metastasis (Song *et al*., 2015; Xia *et al*., 2016). MiR-542-3p is a novel MiR, which has been characterized as a tumor suppressor in human cancers by targeting life-threatening cancer-related pathways (Cai *et al*., 2015; Shen *et al*., 2015). Previous report demonstrated that the expression of MiR-542-3p was downregulated in breast cancer cell lines (MCF-7 and MDAMB-231). Over-expression of MiR-542-3p inhibited breast cancer cell proliferation, colony formation, migration and invasion (Rang *et al*., 2016). Additionally, Taipaleenmäki *et al*. (2016) revealed that MiR-218-5p is highly expressed in bone metastasis from breast cancer patients, but is not detected in normal mammary epithelial cells. MiR-218-5p expression is significant in breast cancer cells that metastasize to bones to provide strong support for a component of biological control that goes beyond regulation by transcription factors. The results in Table 6.13 revealed MiR-218-5p show some sort of a relationship with the expression of survivin 2B as they are both involved in cell cycle arrest and not apoptosis. MiR-335-5p and MiR-542-3p are only expressed during apoptosis and have no role in the cell cycle progression (Table 6.13). Based on these findings, MiRs can function as tumour suppressors through regulation of

apoptosis and cell cycle progression of different cancers including breast cancer by targeting survivin splice variants.

6.15. Conclusion

Arsenic trioxide inhibited the growth and affected the morphology of the MCF-7 breast cancer cells in a concentration-dependent manner and this further confirms that this compound has anti-tumour activities against MCF-7 breast cancer cells through the inhibition of growth and cell proliferation. The Muse Cell Analyser showed that arsenic trioxide induces G2/M cell cycle arrest and promotes caspase-dependent apoptosis of MCF-7 cells without causing any damage to the mitochondrial membrane. Deactivation of MAPK and PI3K was accompanied by upregulation of survivin 2B and 3α variants in breast cancer cell line, MCF-7. Wild-type survivin has been reported as a therapeutic target, involvement of survivin 2B in anticancer activities and inhibition of cell survival pathways is a promising finding for future drug development.

Chapter Seven: General conclusion

7.1. General Conclusion

From this study, novel *β*-cyclodextrin CNSs from a waste material were successfully used to deliver arsenic trioxides. TEM studies showed coal fly ash-derived *β*-cyclodextrin CNSs were spherical in shape and had a monodispersed particle size distribution. Thermal stability studies showed that the material would be suitable for *in vitro* studies in medical applications. Cell viability studies showed the coal fly ash-derived *β*-cyclodextrin CNSs are safe and could be used as potential drug delivery vehicles. Arsenic trioxide alone also showed to be safe against the normal KMST-6 cells, hence the compound can be a good candidate for cancer therapeutics. The study also that showed that the fly-ash derived arsenic trioxide-*β*-cyclodextrin nanospheres reduced the viability of MCF-7 breast cancer cells. The *β*-cyclodextrin decreased the viability of MCF-7 cells, which was enhanced by deposition of arsenic trioxide, cell viability further decreased, showing the inhibition of cell growth in a dose-dependent manner. MTT Assay, morphological analysis, and apoptosis analysis results showed that of arsenic trioxide-*β*-cyclodextrin fly ash-derived nanospheres extraordinarily reduced cell viability of MCF-7 cells and induced apoptosis. Arsenic trioxide-*β*-cyclodextrin fly-ash-derived nanospheres showed activity against breast cancer. Therefore, for the first time, this study showed that it is promising that delivering arsenic trioxide using nanotechnology can be employed as an anti-cancer drug option in treating a variety of solid cancers with better efficacy and less toxicity.

Arsenic trioxide inhibited the proliferation and affected the morphology of the MCF-7 breast cancer cells in a concentration-dependent manner, and this shows that this compound has anti-tumour activities against MCF-7 breast cancer cells through the inhibition of growth and cell proliferation. The compound, arsenic trioxide induced G2/M cell cycle arrest and promoted caspase-dependent cell death of MCF-7 cells without any damage to the mitochondrial membrane. This suggest that arsenic trioxide induces the death receptor-mediated apoptosis in MFC-7 cells.

Consequently, arsenic trioxide deactivated the expression of MAPK and PI3K. As a result, deactivation of the two pathways was accompanied by differential expression of survivin

splice variants in breast cancer MCF-7 cells. All these findings suggest that survivin expression has the potential for use as a predictive biomarker to identify cancer. The high expression of survivin in cancer cells, with little expression in most normal tissues, marks survivin as an attractive anticancer molecular therapeutic target. Survivin variants specific MiRs can be used to regulate apoptosis and cell cycle regulation; this can be useful in facilitating the development of effective cancer therapies against breast cancer.

The results in this study showed the enhanced cytotoxicity and the potential of arsenic trioxide-*β*-cyclodextrin CNSs as a potential therapeutic strategy against breast cancer. The future for coal fly ash derived-*β*-cyclodextrin CNSs in drug delivery is bright, although how CNSs behave *in vivo* and many more improvements are needed before they can be considered for clinical applications. Further studies concerning the controlling mechanisms of survivin splice variants expression and function in normal and cancerous cells will help to clarify the biology of survivin and consequently help to develop innovative strategies for selective survivin inhibition.

7.2. Limitations of the study

Cell lines- In this study, there were no normal equivalent mammary gland cells and the different breast cancer subtypes.

Chapter Eight: References

Adamkov, M., Halasova, E., Rajcani, J., Bencat, M., Vybohova, D., Rybarova, S. and Galbavy, S., 2011. Relation between expression pattern of p53 and survivin in cutaneous basal cell carcinomas. Medical Science Monitor: *International Medical Journal of Experimental and Clinical Research*, 17 (3), 74-80.

Adamkov, M., Kajo, K., Vybohova, D., Krajcovic, J., Stuller, F. and Rajcani, J., 2012. Correlations of survivin expression with clinicomorphological parameters and hormonal receptor status in breast ductal carcinoma. *Neoplasma*, 59 (1), 30-37.

Al Faraj, A., Shaik, A.P. and Shaik, A.S., 2015. Magnetic single-walled carbon nanotubes as efficient drug delivery nanocarriers in breast cancer murine model: noninvasive monitoring using diffusion-weighted magnetic resonance imaging as sensitive imaging biomarker. *International Journal of Nanomedicine*, 10, 157-168.

Allen, T.M. and Cullis, P.R., 2004. Drug delivery systems: entering the mainstream. Science, 303 (5665), 1818-1822.

Altieri, D.C., 2003. Survivin, versatile modulation of cell division and apoptosis in cancer. Oncogene, 22 (53), 8581-8589.

Alyafee, Y.A., Alaamery, M., Bawazeer, S., Almutairi, M.S., Alghamdi, B., Alomran, N., Sheereen, A., Daghestani, M. and Massadeh, S., 2018. Preparation of anastrozole loaded Peg-Pla nanoparticles: evaluation of apoptotic response of breast cancer cell lines. *International Journal of Nanomedicine*, 13, 199-208.

Anderson, J.M. and Shive, M.S., 1997. Biodegradation and biocompatibility of PLA and PLGA microspheres. *Advanced Drug Delivery Reviews*, 28 (1), 5-24.

Antman, K.H., 2001. Introduction: the history of arsenic trioxide in cancer therapy. *The Oncologist*, 6 (2), 1-2.

Ashhab, Y., Alian, A., Polliack, A., Panet, A. and Yehuda, D.B., 2001. Two splicing variants of a new inhibitor of apoptosis gene with different biological properties and tissue distribution pattern. *FEBS Letters*, 495 (1-2), 56-60.

Ashkenazi, A., 2008. Targeting the extrinsic apoptosis pathway in cancer. *Cytokine and Growth Factor Reviews*, 19 (3), 325-331.

Athanasoula, K.C., Gogas, H., Polonifi, K., Vaiopoulos, A.G., Polyzos, A. and Mantzourani, M., 2014. Survivin beyond physiology: orchestration of multistep carcinogenesis and therapeutic potentials. *Cancer Letters*, 347 (2), 175-182.

Atlasi, Y., Mowla, S.J. and Ziaee, S.A.M., 2009. Differential expression of survivin and its splice variants, survivin-ΔEx3 and survivin-2B, in bladder cancer. *Cancer Detection and Prevention*, 32 (4), 308-313.

Badran, A., Yoshida, A., Ishikawa, K., Goi, T., Yamaguchi, A., Ueda, T. and Inuzuka, M., 2004. Identification of a novel splice variant of the human anti-apoptopsis gene survivin. *Biochemical and Biophysical Research Communications*, 314 (3), 902-907.

Baj, G., Arnulfo, A., Deaglio, S., Mallone, R., Vigone, A., De Cesaris, M.G., Surico, N., Malavasi, F. and Ferrero, E., 2002. Arsenic trioxide and breast cancer: analysis of the apoptotic, differentiative and immunomodulatory effects. *Breast cancer research and treatment*, 73 (1), 61-73.

Balakier, H., Xiao, R., Zhao, J., Zaver, S., Dziak, E., Szczepanska, K., Opas, M., Yie, S. and Librach, C., 2013. Expression of survivin in human oocytes and preimplantation embryos. *Fertility and Sterility*, 99 (2), 518-525.

Barnes, N., Haywood, P., Flint, P., Knox, W.F. and Bundred, N.J., 2006. Survivin expression in in situ and invasive breast cancer relates to COX-2 expression and DCIS recurrence. *British Journal of Cancer*, 94 (2), 253-258.

Bartling, B., Lewensohn, R. and Zhivotovsky, B., 2004. Endogenously released Smac is insufficient to mediate cell death of human lung carcinoma in response to etoposide. *Experimental Cell Research*, 298 (1), 83-95.

Bauer, K.R., Brown, M., Cress, R.D., Parise, C.A. and Caggiano, V., 2007. Descriptive analysis of estrogen receptor (ER)-negative, progesterone receptor (PR)-negative, and HER2-negative invasive breast cancer, the so-called triple-negative phenotype. *Cancer*, 109 (9), 1721-1728.

Bian, K., Fan, J., Zhang, X., Yang, X.W., Zhu, H.Y., Wang, L., Sun, J.Y., Meng, Y.L., Cui, P.C., Cheng, S.Y. and Zhang, J., 2012. MicroRNA-203 leads to G1 phase cell cycle arrest in laryngeal carcinoma cells by directly targeting survivin. *FEBS Letters*, 586 (6), 804-809.

Brownell, I., Guevara, E., Bai, C.B., Loomis, C.A. and Joyner, A.L., 2011. Nerve-derived sonic hedgehog defines a niche for hair follicle stem cells capable of becoming epidermal stem cells. *Cell Stem Cell*, 8 (5), 552-565.

Cai, J., Zhao, J., Zhang, N., Xu, X., Li, R., Yi, Y., Fang, L., Zhang, L., Li, M., Wu, J. and Zhang, H., 2015. MicroRNA-542-3p suppresses tumour cell invasion via targeting AKT pathway in human astrocytoma. *Journal of Biological Chemistry*, jbc-M115, 24678-24688.

Cai, X., Wang, C., Chen, B., Hua, W., Shen, F., Yu, L., He, Z., Shi, Y., Chen, Y., Xia, G. and Cheng, J., 2014. Antitumor efficacy of DMSA modified Fe3O4 magnetic nanoparticles combined with arsenic trioxide and adriamycin in Raji cells. *Journal of Biomedical Nanotechnology*, 10 (2), 251-261.

Caldas, H., Honsey, L.E. and Altura, R.A., 2005. Survivin 2α: a novel survivin splice variant expressed in human malignancies. *Molecular Cancer*, 4 (1), 11. DOI: 10.1186/1476-4598-4-11

Caldas, H., Jiang, Y., Holloway, M.P., Fangusaro, J., Mahotka, C., Conway, E.M. and Altura, R.A., 2005. Survivin splice variants regulate the balance between proliferation and cell death. *Oncogene*, 24 (12), 1994-2007.

Calon, A., Lonardo, E., Berenguer-Llergo, A., Espinet, E., Hernando-Momblona, X., Iglesias, M., Sevillano, M., Palomo-Ponce, S., Tauriello, D.V., Byrom, D. and Cortina, C., 2015. Stromal gene expression defines poor-prognosis subtypes in colorectal cancer. *Nature Genetics*, 47 (4), 320-329.

Cao, W., Fan, R., Wang, L., Cheng, S., Li, H., Jiang, J., Geng, M., Jin, Y. and Wu, Y., 2013. Expression and regulatory function of MiRNA-34a in targeting survivin in gastric cancer cells. *Tumor Biology*, 34 (2), 963-971.

Cao, W., Yang, W., Fan, R., Li, H., Jiang, J., Geng, M., Jin, Y. and Wu, Y., 2014. miR-34a regulates cisplatin-induce gastric cancer cell death by modulating PI3K/AKT/survivin pathway. *Tumor Biology*, 35 (2), 1287-1295.

Carmena, M., Wheelock, M., Funabiki, H. and Earnshaw, W.C., 2012. The chromosomal passenger complex (CPC): from easy rider to the godfather of mitosis. *Nature Reviews Molecular Cell Biology*, 13 (12), 789-803.

Carruthers, K.H., Metzger, G., Choi, E., During, M.J. and Kocak, E., 2016. A therapeutic role for survivin in mitigating the harmful effects of ionizing radiation. *Sarcoma*, 2016 (2016) 2-8.

Carter, B.Z., Qiu, Y., Huang, X., Diao, L., Zhang, N., Coombes, K.R., Mak, D.H., Konopleva, M., Cortes, J., Kantarjian, H.M. and Mills, G.B., 2012. Survivin is highly expressed in CD34+ 38− leukemic stem/progenitor cells and predicts poor clinical outcomes in AML. *Blood*, 120 (1), 173-180.

Challa, R., Ahuja, A., Ali, J. and Khar, R.K., 2005. Cyclodextrins in drug delivery: an updated review. *Aaps Pharmscitech*, 6 (2), E329-E357.

Chen, D.Q., Pan, B.Z., Huang, J.Y., Zhang, K., Cui, S.Y., De, W., Wang, R. and Chen, L.B., 2014. HDAC 1/4-mediated silencing of microRNA-200b promotes chemoresistance in human lung adenocarcinoma cells. *Oncotarget*, 5 (10), 3333-3349.

Chen, S., Xiao, X., Feng, X., Li, W., Zhou, N., Zheng, L., Sun, Y., Zhang, Z. and Zhu, W., 2012. Resveratrol induces Sirt1-dependent apoptosis in 3T3-L1 preadipocytes by activating AMPK and suppressing AKT activity and survivin expression. *The Journal of Nutritional Biochemistry*, 23 (9), 1100-1112.

Chen, X., Duan, N., Zhang, C. and Zhang, W., 2016. Survivin and tumorigenesis: molecular mechanisms and therapeutic strategies. *Journal of Cancer*, 7 (3), 314-323.

Chen, Y., Kuang, D., Zhao, X., Chen, D., Wang, X., Yang, Q., Wan, J., Zhu, Y., Wang, Y., Zhang, S. and Wang, Y., 2016. miR-497-5p inhibits cell proliferation and invasion by targeting KCa3. 1 in angiosarcoma. *Oncotarget*, 7 (36), 58148–58161.

Cheng, S.M., Chang, Y.C., Liu, C.Y., Lee, J.Y.C., Chan, H.H., Kuo, C.W., Lin, K.Y., Tsai, S.L., Chen, S.H., Li, C.F. and Leung, E., 2015. YM155 down-regulates survivin and XIAP, modulates autophagy and induces autophagy-dependent DNA damage in breast cancer cells. *British Journal of Pharmacology*, 172 (1), 214-234.

Cheng, Y., Chang, L.W. and Tsou, T.C., 2006. Mitogen-activated protein kinases mediate arsenic- induced down-regulation of survivin in human lung adenocarcinoma cells. *Archives of Toxicology*, 80 (6), 310-318.

Cheung, C.H.A., Huang, C.C., Tsai, F.Y., Lee, J.Y.C., Cheng, S.M., Chang, Y.C., Huang, Y.C., Chen, S.H. and Chang, J.Y., 2013. Survivin–biology and potential as a therapeutic target in oncology. *Oncotargets and Therapy*, 2013 (6), 1453-1462.

Chieffi, P., 2011. New prognostic markers and potential therapeutic targets in human testicular germ cell tumors. *Current Medicinal Chemistry*, 18 (33), 5033-5040.

Chiu, H.W., Ho, S.Y., Guo, H.R. and Wang, Y.J., 2009. Combination treatment with arsenic trioxide and irradiation enhances autophagic effects in U118-MG cells through increased mitotic arrest and regulation of PI3K/Akt and ERK1/2 signaling pathways. *Autophagy*, 5 (4), 472-483.

Chiu, H.W., Ho, Y.S. and Wang, Y.J., 2011. Arsenic trioxide induces autophagy and apoptosis in human glioma cells in vitro and in vivo through downregulation of survivin. *Journal of Molecular Medicine*, 89 (9), 927-941.

Cho, G.S., Ahn, T.S., Jeong, D., Kim, J.J., Kim, C.J., Cho, H.D., Park, D.K. and Baek, M.J., 2011. Expression of the survivin-2B splice variant related to the progression of colorectal carcinoma. *Journal of the Korean Surgical Society*, 80 (6), 404-411.

Chow, S.K., Chan, J.Y. and Fung, K.P., 2004. Inhibition of cell proliferation and the action mechanisms of arsenic trioxide (As2O3) on human breast cancer cells. *Journal of Cellular Biochemistry*, 93 (1), 173-187.

Cooper, G.M., 2000. The Cell: A Molecular Approach, 2nd edn. The Cell: A Molecular Approach. Sunderland, MA.

Coumar, M.S., Tsai, F.Y., Kanwar, J.R., Sarvagalla, S. and Cheung, C.H.A., 2013. Treat cancers by targeting survivin: just a dream or future reality? *Cancer Treatment Reviews*, 39 (7), 802-811.

Dalla Via, L., N Garcia-Argaez, A., Martinez-Vazquez, M., Grancara, S., Martinis, P. and Toninello, A., 2014. Mitochondrial permeability transition as target of anticancer drugs. *Current Pharmaceutical Design*, 20 (2), 223-244.

Dawson, S.J., Tsui, D.W., Murtaza, M., Biggs, H., Rueda, O.M., Chin, S.F., Dunning, M.J., Gale, D., Forshew, T., Mahler-Araujo, B. and Rajan, S., 2013. Analysis of circulating tumor DNA to monitor metastatic breast cancer. *New England Journal of Medicine*, 368 (13), 1199-1209.

De Laurentiis, M., Cianniello, D., Caputo, R., Stanzione, B., Arpino, G., Cinieri, S., Lorusso, V. and De Placido, S., 2010. Treatment of triple negative breast cancer (TNBC): current options and future perspectives. *Cancer Treatment Reviews*, 36, 80-86.

de Necochea-Campion, R., Chen, C.S., MiRshahidi, S., Howard, F.D. and Wall, N.R., 2013. Clinico-pathologic relevance of Survivin splice variant expression in cancer. *Cancer Letters*, 339 (2), 167-174.

Dean, E.J., Ranson, M., Blackhall, F., Holt, S.V. and Dive, C., 2007. Novel therapeutic targets in lung cancer: Inhibitor of apoptosis proteins from laborarsenic trioxidery to clinic. *Cancer Treatment Reviews*, 33 (2), 203-212.

Deng, J., You, Y., Sahajwalla, V. and Joshi, R.K., 2016. Transforming waste into carbon-based nanomaterials. *Carbon*, 96, 105-115.

Dohi, T., Beltrami, E., Wall, N.R., Plescia, J. and Altieri, D.C., 2004. Mitochondrial survivin inhibits apoptosis and promotes tumorigenesis. *The Journal of Clinical Investigation*, 114 (8), 1117-1127.

Duffy, M.J., O'Donovan, N., Brennan, D.J., Gallagher, W.M. and Ryan, B.M., 2007. Survivin: a promising tumor biomarker. *Cancer Letters*, 249 (1), 49-60.

Duiker, E.W., van der Zee, A.G., de Graeff, P., Boersma-van Ek, W., Hollema, H., de Bock, G.H., de Jong, S. and de Vries, E.G., 2010. The extrinsic apoptosis pathway and its prognostic impact in ovarian cancer. *Gynecologic Oncology*, 116 (3), 549-555.

Dumitrescu, R.G. and Cotarla, I., 2005. Understanding breast cancer risk-where do we stand in 2005? *Journal of Cellular and Molecular Medicine*, 9 (1), 208-221.

Early Breast Cancer Trialists' Collaborative Group, 2005. Effects of radiotherapy and of differences in the extent of surgery for early breast cancer on local recurrence and 15-year survival: an overview of the randomised trials. *The Lancet*, 366 (9503), 2087-2106.

Easton, D.F., 1999. How many more breast cancer predisposition genes are there? *Breast Cancer Research*, 1 (1), 14-17.

Eckelman, B.P., Salvesen, G.S. and Scott, F.L., 2006. Human inhibitor of apoptosis proteins: why XIAP is the black sheep of the family. *EMBO Reports*, 7 (10), 988-994.

Eguchi, R., Fujimori, Y., Takeda, H., Tabata, C., Ohta, T., Kuribayashi, K., Fukuoka, K. and Nakano, T., 2011. Arsenic trioxide induces apoptosis through JNK and ERK in human mesothelioma cells. *Journal of Cellular Physiology*, 226 (3), 762-768.

Elledge, S.J., 1996. Cell cycle checkpoints: preventing an identity crisis. *Science*, 274 (5293), 1664-1672.

Emadi, A. and Gore, S.D., 2010. Arsenic trioxide—an old drug rediscovered. *Blood Reviews*, 24 (4), 191-199.

Evens, A.M., Tallman, M.S. and Gartenhaus, R.B., 2004. The potential of arsenic trioxide in the treatment of malignant disease: past, present, and future. *Leukemia Research*, 28 (9), 891-900.

Fang, Z.H., Wang, S.L., Zhao, J.T., Lin, Z.J., Chen, L.Y., Su, R., Xie, S.T., Carter, B.Z. and Xu, B., 2016. MiR-150 exerts antileukemia activity in vitro and in vivo through regulating genes in multiple pathways. *Cell Death and Disease*, 7 (9), 2371.

Farazi, T.A., Hoell, J.I., Morozov, P. and Tuschl, T., 2013. MicroRNAs in human cancer. *MicroRNA Cancer Regulation*. 1-20.

Faversani, A., Vaira, V., Moro, G.P., Tosi, D., Lopergolo, A., Schultz, D.C., Rivadeneira, D., Altieri, D.C. and Bosari, S., 2014. Survivin family proteins as novel molecular determinants of doxorubicin resistance in organotypic human breast tumors. *Breast Cancer Research*, 16 (3), 3409.

Feng, W., Yoshida, A. and Ueda, T., 2013. YM155 induces caspase-8 dependent apoptosis through downregulation of survivin and Mcl-1 in human leukemia cells. *Biochemical and Biophysical Research Communications*, 435 (1), 52-57.

Fernandez, J.G., Rodríguez, D.A., Valenzuela, M., Calderon, C., Urzúa, U., Munroe, D., Rosas, C., Lemus, D., Díaz, N., Wright, M.C. and Leyton, L., 2014. Survivin expression

promotes VEGF- induced tumor angiogenesis via PI3K/Akt enhanced β-catenin/Tcf-Lef dependent transcription. *Molecular Cancer*, 13 (1), 209.

Ferreira, M.J.U., Duarte, N., Reis, M., Madureira, A.M. and Molnár, J., 2014. Euphorbia and Momordica metabolites for overcoming multidrug resistance. *Phytochemistry Reviews*, 13 (4), 915-935.

Fields, A.C., Cotsonis, G., Sexton, D., Santoianni, R. and Cohen, C., 2004. Survivin expression in heparsenic trioxidecellular carcinoma: correlation with proliferation, prognostic parameters, and outcome. *Modern Pathology*, 17 (11), 1378-1385.

Fiore, D., Quintavalle, C., Donnarumma, E., Roscigno, G., Iaboni, M., Russo, V., Adamo, A., De Martino, F., Greco, A., Romano, G. and Ylermi, S., 2015. Survival in glioblastoma cancer patients is predicted by MiR-340, which regulates key cancer hallmarks by inhibiting NRAS. *Cancer Research*, 75 (15), 11-15.

Fogarty, C.E. and Bergmann, A., 2017. Killers creating new life: caspases drive apoptosis- induced proliferation in tissue repair and disease. *Cell Death and Differentiation*, 24 (8), 1390-1400.

Foulkes, W.D., Smith, I.E. and Reis-Filho, J.S., 2010. Triple-negative breast cancer. *New England Journal of Medicine*, 363 (20), 1938-1948.

Fukuda, S., Hoggatt, J., Singh, P., Abe, M., Speth, J.M., Hu, P., Conway, E.M., Nucifora, G., Yamaguchi, S. and Pelus, L.M., 2015. Survivin modulates genes with divergent molecular functions and regulates proliferation of hematopoietic stem cells through Evi-1. *Leukemia*, 29 (2), 433-440.

Futakuchi, H., Ueda, M., Kanda, K., Fujino, K., Yamaguchi, H. and Noda, S., 2007. Transcriptional expression of survivin and its splice variants in cervical carcinomas. *International Journal of Gynecological Cancer*, 17 (5), 1092-1098.

Garg, H., Suri, P., Gupta, J.C., Talwar, G.P. and Dubey, S., 2016. Survivin: a unique target for tumor therapy. *Cancer Cell International*, 16 (1), 49.

Garofalo, M., Di Leva, G. and M Croce, C., 2014. MicroRNAs as anti-cancer therapy. *Current Pharmaceutical Design*, 20 (33), 5328-5335.

Gavamukulya, Y., Abou-Elella, F., Wamunyokoli, F. and AEl-Shemy, H., 2014. Phytochemical screening, anti-oxidant activity and in vitro anticancer potential of ethanolic and water leaves extracts of Annona muricata (Graviola). *Asian Pacific Journal of Tropical Medicine*, 7, 355-363.

Gayathri, C. and Rao, G.V., 2017. Immunohistochemical expression of Survivin in oral leukoplakia and oral squamous cell carcinoma. *Journal of Dr. NTR University of Health Sciences*, 6 (1), 39-44.

Gaytan-Cervantes, J., Gonzalez-Torres, C., Maldonado, V., Zampedri, C., Ceballos-Cancino, G. and Melendez-Zajgla, J., 2017. Protein Sam68 regulates the alternative splicing of survivin ΔEx3. *Journal of Biological Chemistry*, 292 (33), 13745-13757.

Geng, D., Song, X., Ning, F., Song, Q. and Yin, H., 2015. MiR-34a inhibits viability and invasion of human papillomavirus–positive cervical cancer cells by targeting E2F3 and regulating survivin. *International Journal of Gynecological Cancer*, 25 (4), 707-713.

Ghobrial, I.M., Witzig, T.E. and Adjei, A.A., 2005. Targeting apoptosis pathways in cancer therapy. CA: *Cancer Journal for Clinicians*, 55 (3), 178-194.

Giaccone, G., Zatloukal, P., Roubec, J., Floor, K., Musil, J., Kuta, M., van Klaveren, R.J., Chaudhary, S., Gunther, A. and Shamsili, S., 2009. Multicenter phase II trial of YM155, a small-molecule suppressor of survivin, in patients with advanced, refractory, non–small-cell lung cancer. *Journal of Clinical Oncology*, 27 (27), 4481-4486.

Gu, J., Fang, X., Hao, J. and Sha, X., 2015. Reversal of P-glycoprotein-mediated multidrug resistance by CD44 antibody-targeted nanocomplexes for short hairpin RNA-encoding plasmid DNA delivery. *Biomaterials*, 45 (2015), 99-114.

Gurtan, A.M. and Sharp, P.A., 2013. The role of MiRNAs in regulating gene expression networks. *Journal of Molecular Biology*, 425 (19), 3582-3600.

Hai, J.J., Gill, H., Tse, H.F., Kumana, C.R., Kwong, Y.L. and Siu, C.W., 2015. Torsade de Pointes during oral arsenic trioxide therapy for acute promyelocytic leukemia in a patient with heart failure. *Annals of Hematology*, 94 (3), 501-503.

Hengartner, M.O., 2000. The biochemistry of apoptosis. *Nature*, 407 (6805), 770-776.

Hintsho, N., Shaikjee, A., Masenda, H., Naidoo, D., Billing, D., Franklyn, P. and Durbach, S., 2014. Direct synthesis of carbon nanofibers from South African coal fly ash. *Nanoscale Research Letters*, 9 (1), 387.

Hintsho, N., Shaikjee, A., Triphati, P.K., Masenda, H., Naidoo, D., Franklyn, P. and Durbach, S., 2016. Effect of nitrogen and hydrogen gases on the synthesis of carbon nanomaterials from coal waste fly ash as a catalyst. *Journal of Nanoscience and Nanotechnology*, 16 (5), 4672-4683.

Hoffman, E.A., Gizelska, K., MiRowski, M. and Mielicki, W., 2015. Arsenic trioxide downregulates cancer procoagulant activity in MCF-7 and WM-115 cell lines in vitro. *Contemporary oncology* (Pozn), 19 (2), 108-112.

Hou, Y.C.C., Chittaranjan, S., Barbosa, S.G., McCall, K. and Gorski, S.M., 2008. Effector caspase Dcp-1 and IAP protein Bruce regulate starvation- induced autophagy during Drosophila melanogaster oogenesis. *The Journal of Cell Biology*, 182 (6), 1127-1139.

http://www.nioh.ac.za/assets/files/NCR%202012%20results.pdf.

Huang, J., Lyu, H., Wang, J. and Liu, B., 2015. MicroRNA regulation and therapeutic targeting of survivin in cancer. *American Journal of Cancer Research*, 5 (1), 20.

Iijima, S., 1991. Helical microtubules of graphitic carbon. Nature, 354 (6348), 56.

Jemal, A., Bray, F., Center, M.M., Ferlay, J., Ward, E. and Forman, D., 2011. Global cancer statistics. CA: *Cancer Journal for Clinicians*, 61 (2), 69-90.

Jha, K., Shukla, M. and Pandey, M., 2012. Survivin expression and targeting in breast cancer. *Surgical Oncology*, 21 (2), 125-131.

Jin, H.O., Yoon, S.I., Seo, S.K., Lee, H.C., Woo, S.H., Yoo, D.H., Lee, S.J., Choe, T.B., An, S., Kwon, T.J. and Kim, J.I., 2006. Synergistic induction of apoptosis by sulindac and arsenic trioxide in human lung cancer A549 cells via reactive oxygen species-dependent down-regulation of survivin. *Biochemical Pharmacology*, 72 (10), 1228-1236.

Jutooru, I., Chadalapaka, G., Sreevalsan, S., Lei, P., Barhoumi, R., Burghardt, R. and Safe, S., 2010. Arsenic trioxide downregulates specificity protein (Sp) transcription factors

and inhibits bladder cancer cell and tumor growth. *Experimental Cell Research*, 316 (13), 2174-2188.

Kang, Y.H. and Lee, S.J., 2008. Role of p38 MAPK and JNK in enhanced cervical cancer cell killing by the combination of arsenic trioxide and ionizing radiation. *Oncology Reports*, 20 (3), 637-643.

Kawasaki, H., Toyoda, M., Shinohara, H., Okuda, J., Watanabe, I., Yamamoto, T., Tanaka, K., Tenjo, T. and Tanigawa, N., 2001. Expression of survivin correlates with apoptosis, proliferation, and angiogenesis during human colorectal tumorigenesis. *Cancer*, 91 (11), 2026-2032.

Ke, Y., Zhao, W., Xiong, J. and Cao, R., 2013. Downregulation of miR-16 promotes growth and motility by targeting HDGF in non-small cell lung cancer cells. *FEBS Letters*, 587 (18), 3153-3157.

Kerlikowske, K., 2010. Epidemiology of ductal carcinoma in situ. *Journal of the National Cancer Institute Monographs*, 2010 (41), 139-141.

Key, T.J., Verkasalo, P.K. and Banks, E., 2001. Epidemiology of breast cancer. *The Lancet Oncology*, 2 (3), 133-140.

Khan, S., Bennit, H.F., Turay, D., Perez, M., MiRshahidi, S., Yuan, Y. and Wall, N.R., 2014. Early diagnostic value of survivin and its alternative splice variants in breast cancer. *BMC Cancer*, 14 (1), 176.

Khan, Z., Khan, N., Tiwari, R.P., Patro, I.K., Prasad, G.B.K.S. and Bisen, P.S., 2010. Down-regulation of survivin by oxaliplatin diminishes radioresistance of head and neck squamous carcinoma cells. *Radiotherapy and Oncology*, 96 (2), 267-273.

Kim, E.K. and Choi, E.J., 2010. Pathological roles of MAPK signaling pathways in human diseases. *Biochimica et Biophysica Acta (BBA)-Molecular Basis of Disease*, 1802 (4), 396-405.

King, M.C., Marks, J.H. and Mandell, J.B., 2003. Breast and ovarian cancer risks due to inherited mutations in BRCA1 and BRCA2. *Science*, 302 (5645), 643-646.

Knauer, S.K., Bier, C., Schlag, P., Fritzmann, J., Dietmaier, W., Rödel, F., Klein-Hitpass, L., Kovács, A.F., Döring, C., Hansmann, M.L. and Hofmann, W.K., 2007. The survivin isoform survivin-3B is cytoprotective and can function as a chromosomal passenger complex protein. *Cell Cycle*, 6 (12), 1501-1508.

Kossatz, S., Grandke, J., Couleaud, P., Larsenic trioxiderre, A., Aires, A., Crosbie-Staunton, K., Ludwig, R., Dähring, H., Ettelt, V., Lazaro-Carrillo, A. and Calero, M., 2015. Efficient treatment of breast cancer xenografts with multifunctionalized iron oxide nanoparticles combining magnetic hyperthermia and anti-cancer drug delivery. *Breast Cancer Research*, 17 (1), 66.

Krieg, A., Mahotka, C., Krieg, T., Grabsch, H., Müller, W., Takeno, S., Suschek, C.V., Heydthausen, M., Gabbert, H.E. and Gerharz, C.D., 2002. Expression of different survivin variants in gastric carcinomas: first clues to a role of survivin-2B in tumour progression. *British Journal of Cancer*, 86 (5), 737-743.

Kumar, A. and Chauhan, S., 2016. How much successful are the medicinal chemists in modulation of SIRT1: a critical review. *European Journal of Medicinal Chemistry*, 119, 45-69.

Kumar, R., Singh, R.K. and Singh, D.P., 2016. Natural and waste hydrocarbon precursors for the synthesis of carbon based nanomaterials: graphene and CNTs. *Renewable and Sustainable Energy Reviews*, 58, 976-1006.

Kyani, K., Babaei, E., Feizi, M.A.H., Vandghanooni, S., Montazeri, V. and Halimi, M., 2014. Detection of survivin 2α gene expression in thyroid nodules. *Journal of Cancer Research and Therapeutics*, 10 (2), 312-316.

Lam, S.K., Mak, J.C.W., Zheng, C.Y., Li, Y.Y., Kwong, Y.L. and Ho, J.C.M., 2014. Downregulation of thymidylate synthase with arsenic trioxide in lung adenocarcinoma. *International Journal of Oncology*, 44 (6), 2093-2102.

Lee, J.Y.C., Kuo, C.W., Tsai, S.L., Cheng, S.M., Chen, S.H., Chan, H.H., Lin, C.H., Lin, K.Y., Li, C.F., Kanwar, J.R. and Leung, E.Y., 2016. Inhibition of HDAC3-and HDAC6-promoted survivin expression plays an important role in SAHA- induced autophagy and viability reduction in breast cancer cells. *Frontiers in Pharmacology*, 7, 81.

Lee, M.O., Moon, S.H., Jeong, H.C., Yi, J.Y., Lee, T.H., Shim, S.H., Rhee, Y.H., Lee, S.H., Oh, S.J., Lee, M.Y. and Han, M.J., 2013. Inhibition of pluripotent stem cell-derived teratoma formation by small molecules. *Proceedings of the National Academy of Sciences*, 110 (35), 3281-3290.

Lei, Y., Geng, Z., Guo-Jun, W., He, W. and Jian-Lin, Y., 2010. Prognostic significance of survivin expression in renal cell cancer and its correlation with radioresistance. *Molecular and Cellular Biochemistry*, 344 (1-2), 23-31.

Li, F., Ackermann, E.J., Bennett, C.F., Rothermel, A.L., Plescia, J., Tognin, S., Villa, A., Marchisio, P.C. and Altieri, D.C., 1999. Pleiotropic cell-division defects and apoptosis induced by interference with survivin function. *Nature Cell Biology*, 1(8), 461-466.

Li, F., Ambrosini, G., Chu, E.Y., Plescia, J., Tognin, S., Marchisio, P.C. and Altieri, D.C., 1998. Control of apoptosis and mitotic spindle checkpoint by survivin. *Nature*, 396 (6711), 580-584.

Li, F., Yang, J., Ramnath, N., Javle, M.M. and Tan, D., 2005. Nuclear or cytoplasmic expression of survivin: what is the significance? *International Journal of Cancer*, 114 (4), 509-512.

Li, T., Li, Y., Wang, C., Gao, Z.D. and Song, Y.Y., 2015. Nitrogen-doped carbon nanospheres derived from cocoon silk as metal-free electrocatalyst for glucose sensing. *Talanta*, 144, 1245-1251.

Li, W., Chen, Y.Q., Shen, Y.B., Shu, H.M., Wang, X.J., Zhao, C.L. and Chen, C.J., 2013. HIF-1α knockdown by MiRNA decreases survivin expression and inhibits A549 cell growth in vitro and in vivo. *International Journal of Molecular Medicine*, 32 (2), 271-280.

Li, X., Ding, X. and Adrian, T.E., 2004. Arsenic trioxide causes redistribution of cell cycle, caspase activation, and GADD expression in human colonic, breast, and pancreatic cancer cells. *Cancer Investigation*, 22 (3), 389-400.

Li, X., Liu, F., Lin, B., Luo, H., Liu, M., Wu, J., Li, C., Li, R., Zhang, X., Zhou, K. and Ren, D., 2017. miR 150 inhibits proliferation and tumorigenicity via retarding G1/S phase transition in nasopharyngeal carcinoma. *International Journal of Oncology*, 50 (4), 1097-1108.

Li, Y., Liu, D., Zhou, Y., Li, Y., Xie, J., Lee, R.J., Cai, Y. and Teng, L., 2015. Silencing of survivin expression leads to reduced proliferation and cell cycle arrest in cancer cells. *Journal of Cancer*, 6 (11), 1187-1194.

Liao, M.H., Lin, W.C., Wen, H.C. and Pu, H.F., 2011. Tithonia diversifolia and its main active component tagitinin C induce survivin inhibition and G2/M arrest in human malignant glioblastoma cells. *Fitoterapia*, 82 (3), 331-341.

Ling, X., Cao, S., Cheng, Q., Keefe, J.T., Rustum, Y.M. and Li, F., 2012. A novel small molecule FL118 that selectively inhibits survivin, Mcl-1, XIAP and cIAP2 in a p53-independent manner, shows superior antitumor activity. *PloS one*, 7 (9), 45571.

Ling, X., Cheng, Q., Black, J.D. and Li, F., 2007. Forced expression of survivin-2B abrogates mitotic cells and induces mitochondria-dependent apoptosis by blockade of tubulin polymerization and modulation of Bcl-2, Bax, and survivin. *Journal of Biological Chemistry*, 282 (37), 27204-27214.

Liston, P., Fong, W.G. and Korneluk, R.G., 2003. The inhibitors of apoptosis: there is more to life than Bcl2. *Oncogene*, 22 (53), 8568–8580.

Liu, J., Bu, J., Bu, W., Zhang, S., Pan, L., Fan, W., Chen, F., Zhou, L., Peng, W., Zhao, K. and Du, J., 2014. Real-Time In Vivo Quantitative Monitoring of Drug Release by Dual-Mode Magnetic Resonance and Upconverted Luminescence Imaging. *Angewandte Chemie International Edition*, 53 (18), 4551-4555.

Liu, W., Gong, Y., Li, H., Jiang, G., Zhan, S., Liu, H. and Wu, Y., 2012. Arsenic trioxide-induced growth arrest of breast cancer MCF-7 cells involving FOXO3a and IκB kinase β expression and localization. *Cancer Biotherapy and Radiopharmaceuticals*, 27 (8), 504-512.

Liu, Z.M., Tseng, H.Y., Cheng, Y.L., Yeh, B.W., Wu, W.J. and Huang, H.S., 2015. TG-interacting factor transcriptionally induced by AKT/FOXO3A is a negative regulatory that antagonizes arsenic trioxide-induced cancer cell apoptosis. *Toxicology and Applied Pharmacology*, 285 (1), 41-50.

Lopergolo, A., Tavecchio, M., Lisanti, S., Ghosh, J.C., Dohi, T., Faversani, A., Vaira, V., Bosari, S., Tanigawa, N., Delia, D. and Kossenkov, A.V., 2012. Chk2 phosphorylation of

survivin-ΔEx3 contributes to a DNA damage–sensing checkpoint in cancer. *Cancer Research*, 72 (13), 3251-3259.

Lyu, H., Wang, S., Huang, J., Wang, B., He, Z. and Liu, B., 2018. Survivin-targeting miR-542-3p overcomes HER3 signaling-induced chemoresistance and enhances the antitumor activity of paclitaxel against HER2-overexpressing breast cancer. *Cancer Letters*, 420, 97-108.

Ma, Q., Wang, X., Li, Z., Li, B., Ma, F., Peng, L., Zhang, Y., Xu, A. and Jiang, B., 2013. microRNA-16 represses colorectal cancer cell growth in vitro by regulating the p53/survivin signaling pathway. *Oncology Reports*, 29 (4), 1652-1658.

Ma, Y., Wang, J., Liu, L., Zhu, H., Chen, X., Pan, S., Sun, X. and Jiang, H., 2011. Genistein potentiates the effect of arsenic trioxide against human hepatocellular carcinoma: role of Akt and nuclear factor-κB. *Cancer Letters*, 301 (1), 75-84.

Maeda, H., Hori, S., Ohizumi, H., Segawa, T., Kakehi, Y., Ogawa, O. and Kakizuka, A., 2004. Effective treatment of advanced solid tumors by the combination of arsenic trioxide and L-buthionine-sulfoximine. *Cell Death and Differentiation*, 11 (7), 737-746.

Mahotka, C., Krieg, T., Krieg, A., Wenzel, M., Suschek, C.V., Heydthausen, M., Gabbert, H.E. and Gerharz, C.D., 2002. Distinct in vivo expression patterns of survivin splice variants in renal cell carcinomas. *International Journal of Cancer*, 100 (1), 30-36.

Mahotka, C., Liebmann, J., Wenzel, M., Suschek, C.V., Schmitt, M., Gabbert, H.E. and Gerharz, C.D., 2002. Differential subcellular localization of functionally divergent survivin splice variants. *Cell Death and Differentiation*, 9 (12), 1334-1342.

Malam, Y., Loizidou, M. and Seifalian, A.M., 2009. Liposomes and nanoparticles: nanosized vehicles for drug delivery in cancer. *Trends in Pharmacological Sciences*, 30 (11), 592-599.

Malcles, M.H., Wang, H.W., Koumi, A., Tsai, Y.H., Yu, M., Godfrey, A. and Boshoff, C., 2007. Characterisation of the anti-apoptotic function of survivin-ΔEx3 during TNFα−mediated cell death. *British Journal of Cancer*, 96 (11), 1659-1666.

Markou, A., Sourvinou, I., Vorkas, P.A., Yousef, G.M. and Lianidou, E., 2013. Clinical evaluation of microRNA expression profiling in non small cell lung cancer. *Lung Cancer*, 81 (3), 388-396.

Martini, E., Schneider, E., Neufert, C., Neurath, M.F. and Becker, C., 2016. Survivin is a guardian of the intestinal stem cell niche and its expression is regulated by TGF-β. *Cell Cycle*, 15 (21), 2875-2881.

McKay, T.R., Bell, S., Tenev, T., Stoll, V., Lopes, R., Lemoine, N.R. and McNeish, I.A., 2003. Procaspase 3 expression in ovarian carcinoma cells increases survivin transcription which can be countered with a dominant-negative mutant, survivin T34A; a combination gene therapy strategy. *Oncogene*, 22 (23), 3539-3547.

McPherson, K., Steel, C. and Dixon, J.M., 2000. ABC of breast diseases: breast cancer—epidemiology, risk factors, and genetics. BMJ: *British Medical Journal*, 321 (7261), 624-628.

Mishra, R., Palve, V., Kannan, S., Pawar, S. and Teni, T., 2015. High expression of survivin and its splice variants survivin ΔEx3 and survivin 2 B in oral cancers. *Oral Surgery, Oral Medicine, Oral Pathology and Oral Radiology*, 120 (4), 497-507.

Mola, G., Vela, E., Fernández-Figureueras, M.T., Isamat, M. and Muñoz-Mármol, A.M., 2007. Exonization of Alu-generated splice variants in the survivin gene of human and non-human primates. *Journal of Molecular Biology*, 366 (4), 1055-1063.

Moniri J.S., Gharechahi, J., Hosseinpour F.M.A., Montazeri, V. and Halimi, M., 2013. Transcriptional expression analysis of survivin splice variants reveals differential expression of survivin-3α in breast cancer. *Genetic Testing and Molecular Biomarkers*, 17 (4), 314-320.

Moore, A.S., Alonzo, T.A., Gerbing, R.B., Lange, B.J., Heerema, N.A., Franklin, J., Raimondi, S.C., Hirsch, B.A., Gamis, A.S. and Meshinchi, S., 2014. BIRC5 (survivin) splice variant expression correlates with refractory disease and poor outcome in pediatric acute myeloid leukemia: a report from the Children's Oncology Group. *Pediatric Blood and Cancer*, 61 (4), 647-652.

Morrish, F., Noonan, J., Perez-Olsen, C., Gafken, P.R., Fitzgibbon, M., Kelleher, J., VanGilst, M. and Hockenbery, D., 2010. Myc-dependent mitochondrial generation of acetyl-CoA contributes to fatty acid biosynthesis and histone acetylation during cell cycle entry. *Journal of Biological Chemistry*, 285 (47), 36267-36274.

Mudduluru, G., Ilm, K., Fuchs, S. and Stein, U., 2016. S100A4 is post-transcriptionally inhibited by MiR-505-5p and MiR-520c-3p in colorectal cancer. *Cancer Research*, 10 (1158), 1538-7445.

Mull, A.N., Klar, A. and Navara, C.S., 2014. Differential localization and high expression of survivin splice variants in human embryonic stem cells but not in differentiated cells implicate a role for survivin in pluripotency. *Stem Cell Research*, 12 (2), 539-549.

Munari, C.C., de Oliveira, P.F., Campos, J.C.L., Martins, S.D.P.L., Da Costa, J.C., Bastos, J.K. and Tavares, D.C., 2014. Antiproliferative activity of Solanum lycocarpum alkaloidic extract and their constituents, solamargine and solasonine, in tumor cell lines. *Journal of Natural Medicines*, 68 (1), 236-241.

Na, Y.S., Yang, S.J., Kim, S.M., Jung, K.A., Moon, J.H., Shin, J.S., Yoon, D.H., Hong, Y.S., Ryu, M.H., Lee, J.L. and Lee, J.S., 2012. YM155 induces EGFR suppression in pancreatic cancer cells. *PLoS One*, 7 (6), 38625.

Nakagawa, Y., Yamaguchi, S., Hasegawa, M., Nemoto, T., Inoue, M., Suzuki, K., Hirokawa, K. and Kitagawa, M., 2004. Differential expression of survivin in bone marrow cells from patients with acute lymphocytic leukemia and chronic lymphocytic leukemia. *Leukemia Research*, 28 (5), 487-494.

Nakahara, T., Takeuchi, M., Kinoyama, I., Minematsu, T., Shirasuna, K., Matsuhisa, A., Kita, A., Tominaga, F., Yamanaka, K., Kudoh, M. and Sasamata, M., 2007. YM155, a novel small-molecule survivin suppressant, induces regression of established human hormone-refractory prostate tumor xenografts. *Cancer Research*, 67 (17), 8014-8021.

Nalwa, H.S., 2004. Encyclopedia of Nanoscience and Nanotechnology; Volume 7. American Scientific Publishers.

Navratil, J., Fabian, P., Palacova, M., Petrakova, K., Vyzula, R. and Svoboda, M., 2015. Triple negative breast cancer. Klinicka Onkologie: *Casopis Ceske a Slovenske Onkologicke Spolecnosti*, 28 (6), 405-415.

Neophytou, C.M., Constantinou, C., Papageorgis, P. and Constantinou, A.I., 2014. D-alpha-tocopheryl polyethylene glycol succinate (TPGS) induces cell cycle arrest and apoptosis selectively in Survivin-overexpressing breast cancer cells. *Biochemical Pharmacology*, 89 (1), 31-42.

Obexer, P. and Ausserlechner, M.J., 2014. X-linked inhibitor of apoptosis protein–a critical death resistance regulator and therapeutic target for personalized cancer therapy. *Frontiers in Oncology*, 4.

Okada, E., Murai, Y., Matsui, K., Isizawa, S., Cheng, C., Masuda, M. and Takano, Y., 2001. Survivin expression in tumor cell nuclei is predictive of a favorable prognosis in gastric cancer patients. *Cancer Letters*, 163 (1), 109-116.

Okada, H. and Mak, T.W., 2004. Pathways of apoptotic and non-apoptotic death in tumour cells. *Nature Reviews Cancer*, 4 (8), 592-603.

Osterman, C.J.D., Gonda, A., Stiff, T., Sigaran, U., Valenzuela, M.M.A., Bennit, H.R.F., Moyron, R.B., Khan, S. and Wall, N.R., 2016. Curcumin induces pancreatic adenocarcinoma cell death via reduction of the inhibitors of apoptosis. *Pancreas*, 45 (1), 101-109.

Pal, B., Chen, Y., Bert, A., Hu, Y., Sheridan, J.M., Beck, T., Shi, W., Satterley, K., Jamieson, P., Goodall, G.J. and Lindeman, G.J., 2015. Integration of microRNA signatures of distinct mammary epithelial cell types with their gene expression and epigenetic portraits. *Breast Cancer Research*, 17 (1), 85.

Pan, L. and Chen, P., 2018. In vitro and in vivo suppression of hepatocellular carcinoma by amorphophallus konjac tuber through regulation of survivin and bax. *Translational Cancer Research*, 7 (2), 240-247.

Pantel, K. and Alix-Panabières, C., 2010. Circulating tumour cells in cancer patients: challenges and perspectives. *Trends in Molecular Medicine*, 16 (9), 398-406.

Park, W.H., Cho, Y.H., Jung, C.W., Park, J.O., Kim, K., Im, Y.H., Lee, M.H., Kang, W.K. and Park, K., 2003. Arsenic trioxide inhibits the growth of A498 renal cell carcinoma cells via cell cycle arrest or apoptosis. *Biochemical and Biophysical Research Communications*, 300 (1), 230-235.

Parvani, J.G., Davuluri, G., Wendt, M.K., Espinosa, C., Tian, M., Danielpour, D., Sossey-Alaoui, K. and Schiemann, W.P., 2015. Deptor enhances triple-negative breast cancer metastasis and chemoresistance through coupling to survivin expression. *Neoplasia*, 17 (3), 317-328.

Pavlidou, A., Dalamaga, M., Kroupis, C., Konstantoudakis, G., Belimezi, M., Athanasas, G. and Dimas, K., 2011. Survivin isoforms and clinicopathological characteristics in colorectal adenocarcinomas using real-time qPCR. *World Journal of Gastroenterology*, 17 (12), 1614-1621.

Pavlidou, A., Kroupis, C., Goutas, N., Dalamaga, M. and Dimas, K., 2014. Validation of a real-time quantitative polymerase chain reaction method for the quantification of 3 survivin transcripts and evaluation in breast cancer tissues. *Clinical Breast Cancer*, 14 (2), 122-131.

Peer, D., Karp, J.M., Hong, S., Farokhzad, O.C., Margalit, R. and Langer, R., 2007. Nanocarriers as an emerging platform for cancer therapy. *Nature Nanotechnology*, 2 (12), 751-760.

Pennati, M., Folini, M. and Zaffaroni, N., 2007. Targeting survivin in cancer therapy: fulfilled promises and open questions. *Carcinogenesis*, 28 (6), 1133-1139.

Pennati, M., Millo, E., Gandellini, P., Folini, M. and Zaffaroni, N., 2012. RNA interference-mediated validation of survivin and Apollon/BRUCE as new therapeutic targets for cancer therapy. *Current Topics in Medicinal Chemistry*, 12 (2), 69-78.

Phatak, P., Byrnes, K.A., Mansour, D., Liu, L., Cao, S., Li, R., Rao, J.N., Turner, D.J., Wang, J.Y. and Donahue, J.M., 2016. Overexpression of miR-214-3p in esophageal squamous cancer cells enhances sensitivity to cisplatin by targeting survivin directly and indirectly through CUG-BP1. *Oncogene*, 35 (16), 2087–2097

Pisarev, V., Yu, B., Salup, R., Sherman, S., Altieri, D.C. and Gabrilovich, D.I., 2003. Full-length dominant-negative survivin for cancer immunotherapy. *Clinical Cancer Research*, 9 (17), 6523-6533.

Praetorius, N.P. and Mandal, T.K., 2007. Engineered nanoparticles in cancer therapy. *Recent Patents on Drug Delivery and Formulation*, 1 (1), 37-51.

Rakha, E.A., Reis-Filho, J.S., Baehner, F., Dabbs, D.J., Decker, T., Eusebi, V., Fox, S.B., Ichihara, S., Jacquemier, J., Lakhani, S.R. and Palacios, J., 2010. Breast cancer prognostic classification in the molecular era: the role of histological grade. *Breast Cancer Research*, 12 (4), 207.

Rang, Z., Yang, G., Wang, Y.W. and Cui, F., 2016. MiR-542-3p suppresses invasion and metastasis by targeting the proto-oncogene serine/threonine protein kinase, PIM1, in melanoma. *Biochemical and Biophysical Research Communications*, 474 (2), 315-320.

Rauch, A., Hennig, D., Schaefer, C., Wirth, M., Marx, C., Heinzel, T., Schneider, G. and Krämer, O.H., 2014. Survivin and YM155: how faithful is the liaison? *Biochimica et Biophysica Acta (BBA)-Reviews on Cancer*, 1845 (2), 202-220.

Ravi K.M., Hellermann, G., Lockey, R.F. and Mohapatra, S.S., 2004. Nanoparticle-mediated gene delivery: state of the art. *Expert Opinion on Biological Therapy*, 4 (8), 1213-1224.

Reitz, E., Jia, W., Gentile, M., Wang, Y. and Lei, Y., 2008. CuO nanospheres based nonenzymatic glucose sensor. *Electroanalysis*, 20 (22), 2482-2486.

Rich, I.N., Worthington-White, D., Garden, O.A. and Musk, P., 2000. Apoptosis of leukemic cells accompanies reduction in intracellular pH after targeted inhibition of the Na+/H+ exchanger. *Blood*, 95 (4), 1427-1434.

Robertson, F.M., Bondy, M., Yang, W., Yamauchi, H., Wiggins, S., Kamrudin, S., Krishnamurthy, S., Le-Petross, H., Bidaut, L., Player, A.N. and Barsky, S.H., 2010. Inflammatory breast cancer: the disease, the biology, the treatment. CA: *Cancer Journal for Clinicians*, 60 (6), 351-375.

Ruan, S., Zhu, B., Zhang, H., Chen, J., Shen, S., Qian, J., He, Q. and Gao, H., 2014. A simple one-step method for preparation of fluorescent carbon nanospheres and the

potential application in cell organelles imaging. *Journal of Colloid and Interface Science*, 422, 25-29.

Ruchaud, S., Carmena, M. and Earnshaw, W.C., 2007. The chromosomal passenger complex: one for all and all for one. *Cell*, 131 (2), 230-231.

Ryan, B., O'donovan, N., Browne, B., O'shea, C., Crown, J., Hill, A.D.K., McDermott, E., O'Higgins, N. and Duffy, M.J., 2005. Expression of survivin and its splice variants survivin-2B and survivin-ΔEx3 in breast cancer. *British Journal of Cancer*, 92 (1), 120-124.

Ryan, B.M., O'Donovan, N. and Duffy, M.J., 2009. Survivin: a new target for anti-cancer therapy. *Cancer Treatment Reviews*, 35 (7), 553-562.

Sadaf, N., Kumar, N., Ali, M., Ali, V., Bimal, S. and Haque, R., 2018. Arsenic trioxide induces apoptosis and inhibits the growth of human liver cancer cells. *Life Sciences*, 205, 9-17.

Sah, N.K. and Seniya, C., 2015. Survivin splice variants and their diagnostic significance. *Tumor Biology*, 36 (9), 6623-6631.

Sah, N.K., Khan, Z., Khan, G.J. and Bisen, P.S., 2006. Structural, functional and therapeutic biology of survivin. *Cancer Letters*, 244 (2), 164-171.

Saini, S., Yamamura, S., Majid, S., Shahryari, V., Hirata, H., Tanaka, Y. and Dahiya, R., 2011. MicroRNA-708 induces apoptosis and suppresses tumorigenicity in renal cancer cells. *Cancer Research*, 71 (8) 6208-6219.

Sakaue-Sawano, A., Kurokawa, H., Morimura, T., Hanyu, A., Hama, H., Osawa, H., Kashiwagi, S., Fukami, K., Miyata, T., Miyoshi, H. and Imamura, T., 2008. Visualizing spatiotemporal dynamics of multicellular cell-cycle progression. *Cell*, 132 (3), 487-498.

Saleem, M., Qadir, M.I., Perveen, N., Ahmad, B., Saleem, U. and Irshad, T., 2013. Inhibitors of apoptotic proteins: new targets for anticancer therapy. *Chemical Biology and Drug Design*, 82 (3), 243-251.

Salvesen, G.S. and Duckett, C.S., 2002. Apoptosis: IAP proteins: blocking the road to death's door. *Nature Reviews Molecular Cell Biology*, 3 (6), 401-410.

Schwab, G., Chavany, C., Duroux, I., Goubin, G., Lebeau, J., Helene, C. and Saison-Behmoaras, T., 1994. Antisense oligonucleotides adsorbed to polyalkylcyanoacrylate nanoparticles specifically inhibit mutated Ha-ras-mediated cell proliferation and tumorigenicity in nude mice. *Proceedings of the National Academy of Sciences*, 91 (22), 10460-10464.

Selvi, B.R., Jagadeesan, D., Suma, B.S., Nagashankar, G., Arif, M., Balasubramanyam, K., Eswaramoorthy, M. and Kundu, T.K., 2008. Intrinsically fluorescent carbon nanospheres as a nuclear targeting vector: delivery of membrane-impermeable molecule to modulate gene expression in vivo. *Nano Letters*, 8 (10), 3182-3188.

Serp, P., Feurer, R., Kalck, P., Kihn, Y., Faria, J.L. and Figureueiredo, J.L., 2001. A chemical vapour deposition process for the production of carbon nanospheres. *Carbon*, 39 (4), 621-626.

Serrano, M., Hannon, G.J. and Beach, D., 1993. A new regulatory motif in cell-cycle control causing specific inhibition of cyclin D/CDK4. *Nature*, 366 (6456), 704-707.

Serrano-López, J., Serrano, J., Figureueroa, V., Torres-Gomez, A., Tabares, S., Casaño, J., Fernandez-Escalada, N. and Sánchez-Garcia, J., 2013. Cytoplasmic localization of wild-type survivin is associated with constitutive activation of the PI3K/Akt signaling pathway and represents a favorable prognostic factor in patients with acute myeloid leukemia. *Haematologica*, 98 (12), 1877-1885.

Shen, L., Zhang, G., Lou, Z., Xu, G. and Zhang, G., 2017. Cryptotanshinone enhances the effect of Arsenic trioxide in treating liver cancer cell by inducing apoptosis through downregulating phosphorylated-STAT3 in vitro and in vivo. *BMC Complementary and Alternative Medicine*, 17 (1), 106.

Shen, X., Si, Y., Yang, Z., Wang, Q., Yuan, J. and Zhang, X., 2015. MicroRNA-542-3p suppresses cell growth of gastric cancer cells via targeting oncogene astrocyte-elevated gene-1. *Medical Oncology*, 32 (1), 361.

Shen, Z.X., Chen, G.Q., Ni, J.H., Li, X.S., Xiong, S.M., Qiu, Q.Y., Zhu, J., Tang, W., Sun, G.L., Yang, K.Q. and Chen, Y., 1997. Use of arsenic trioxide (As2O3) in the treatment of

acute promyelocytic leukemia (APL): II. Clinical efficacy and pharmacokinetics in relapsed patients. *Blood*, 89 (9), 3354-3360.

Sheng, W.H., Sheng, K.T., Zhao, Y.X., Li, H., Zhou, J.L., Yao, H.Y. and Li, X.H., 2015. Identifying the biomarkers of multiple sclerosis based on non-coding RNA signature. *European Review for Medical Pharmacological Sciences*, 19 (19), 3635-42.

Shi, X., Wang, D., Ding, K., Lu, Z., Jin, Y., Zhang, J. and Pan, J., 2010. GDP366, a novel small molecule dual inhibitor of survivin and Op18, induces cell growth inhibition, cellular senescence and mitotic catastrophe in human cancer cells. *Cancer Biology and Therapy*, 9 (8), 640-650.

Shinohara, E.T., Gonzalez, A., Massion, P.P., Chen, H., Li, M., Freyer, A.S., Olson, S.J., Andersen, J.J., Shyr, Y., Carbone, D.P. and Johnson, D.H., 2005. Nuclear survivin predicts recurrence and poor survival in patients with resected nonsmall cell lung carcinoma. *Cancer*, 103 (8), 1685-1692.

Siegel, R.L., Miller, K.D. and Jemal, A., 2015. Cancer statistics, 2015. CA: *Cancer Journal for Clinicians*, 65 (1), 5-29.

Singh, A., Garg, G. and Sharma, P.K., 2010. Nanospheres: a novel approach for targeted drug delivery system. *International Journal of Pharmaceutical Sciences Review and Research*, 5 (3), 84-88.

Siu, K.P., Chan, J.Y. and Fung, K.P., 2002. Effect of arsenic trioxide on human hepatocellular carcinoma HepG2 cells: inhibition of proliferation and induction of apoptosis. *Life Sciences*, 71 (3), 275-285.

Smith, D., Patel, S., Raffoul, F., Haller, E., Mills, G.B. and Nanjundan, M., 2010. Arsenic trioxide induces a beclin-1 independent autophagic pathway via modulation of snon/skil expression in ovarian carcinoma cells. *Cell Death and Differentiation*, 17 (12), 1867-1881.

Soliman, M., Al-Najjar, S., El-Husseini, S., Mushtak, A., Al-Marri, K., Majeed, Y., Samuel, S.M., Triggle, C.R., Ding, H. and Liberska, A.M., 2016, March. Inhibition of the Akt Kinase Down-regulates ERK, Bcl-2 and Survivin and Suppresses Proliferation and Survival of Murine VEGF-dependent Angiosarcoma Cells. *In Qatar Foundation Annual Research Conference Proceedings*, 2016 (1), 2235.

Song, C., Liu, L.Z., Pei, X.Q., Liu, X., Yang, L., Ye, F., Xie, X., Chen, J., Tang, H. and Xie, X., 2015. MiR-200c inhibits breast cancer proliferation by targeting KRAS. *Oncotarget*, 6 (33), 34968–34978.

Span, P.N., Tjan-Heijnen, V.C., Heuvel, J.J., de Kok, J.B., Foekens, J.A. and Sweep, F.C., 2006. Do the survivin (BIRC5) splice variants modulate or add to the prognostic value of total survivin in breast cancer? *Clinical Chemistry*, 52 (9), 1693-1700.

Srinivasula, S.M. and Ashwell, J.D., 2008. IAPs: what's in a name?. *Molecular Cell*, 30 (2), 123-135.

Stevens, J.J., Graham, B., Dugo, E., Berhaneselassie-Sumner, B., Ndebele, K. and Tchounwou, P.B., 2017. Arsenic trioxide induces apoptosis via specific signaling pathways in HT-29 colon cancer cells. *Journal of Cancer Science and Therapy*, 9 (1), 298.

Sui, L., Dong, Y., Ohno, M., Watanabe, Y., Sugimoto, K. and Tokuda, M., 2002. Survivin expression and its correlation with cell proliferation and prognosis in epithelial ovarian tumors. *International Journal of Oncology*, 21 (2), 315-320.

Sun, X.P., Dong, X., Lin, L., Jiang, X., Wei, Z., Zhai, B., Sun, B., Zhang, Q., Wang, X., Jiang, H. and Krissansen, G.W., 2014. Up-regulation of survivin by AKT and hypoxia-inducible factor 1α contributes to cisplatin resistance in gastric cancer. *The FEBS Journal*, 281 (1), 115-128.

Sutradhar, K.B. and Amin, M.L., 2013. Nanoemulsions: increasing possibilities in drug delivery. *European Journal of Nanomedicine*, 5 (2), 97-110.

Swana, H.S., Grossman, D., Anthony, J.N., Weiss, R.M. and Altieri, D.C., 1999. Tumor content of the antiapoptosis molecule survivin and recurrence of bladder cancer. *New England Journal of Medicine*, 341 (6), 452-453.

Swindell, E.P., Hankins, P.L., Chen, H., Miodragović, Đ.U. and O'Halloran, T.V., 2013. Anticancer activity of small-molecule and nanoparticulate arsenic (III) complexes. *Inorganic Chemistry*, 52 (21), 12292-12304.

Tabaries, S., Ouellet, V., Hsu, B.E., Annis, M.G., Rose, A.A., Meunier, L., Carmona, E., Tam, C.E., Mes-Masson, A.M. and Siegel, P.M., 2015. Granulocytic immune infiltrates

are essential for the efficient formation of breast cancer liver metastases. *Breast Cancer Research*, 17 (1), 45.

Taipaleenmäki, H., Hokland, L.B., Chen, L., Kauppinen, S. and Kassem, M., 2012. Mechanisms in endocrinology: micro-RNAs: targets for enhancing osteoblast differentiation and bone formation. *European Journal of Endocrinology*, 166 (3), 359-371.

Takai, N., Miyazaki, T., Nishida, M., Nasu, K. and Miyakawa, I., 2002. RETRACTED: Survivin expression correlates with clinical stage, histological grade, invasive behavior and survival rate in endometrial carcinoma. *Cancer Letters*, 184 (1), 105-116.

Takai, Y., Miyoshi, J., Ikeda, W. and Ogita, H., 2008. Nectins and nectin-like molecules: roles in contact inhibition of cell movement and proliferation. *Nature reviews Molecular Cell Biology*, 9 (8), 603-615.

Tan, C.P., Lu, Y.Y., Ji, L.N. and Mao, Z.W., 2014. Metallomics insights into the programmed cell death induced by metal-based anticancer compounds. *Metallomics*, 6 (5), 978-995.

Tanaka, K., Iwamoto, S., Gon, G., Nohara, T., Iwamoto, M. and Tanigawa, N., 2000. Expression of survivin and its relationship to loss of apoptosis in breast carcinomas. *Clinical Cancer Research*, 6 (1), 127-134.

Tang, K., Fu, L., White, R.J., Yu, L., Titirici, M.M., Antonietti, M. and Maier, J., 2012. Hollow carbon nanospheres with superior rate capability for sodium-based batteries. *Advanced Energy Materials*, 2 (7), 873-877.

Tiwari, G., Tiwari, R., Sriwastawa, B., Bhati, L., Pandey, S., Pandey, P. and Bannerjee, S.K., 2012. Drug delivery systems: An updated review. *International Journal of Pharmaceutical Investigation*, 2 (1), 2-11.

Torre, L.A., Bray, F., Siegel, R.L., Ferlay, J., Lortet-Tieulent, J. and Jemal, A., 2015. Global cancer statistics, 2012. CA: *Cancer Journal for Clinicians*, 65 (2), 87-108.

Tran, J., Master, Z., Joanne, L.Y., Rak, J., Dumont, D.J. and Kerbel, R.S., 2002. A role for survivin in chemoresistance of endothelial cells mediated by VEGF. *Proceedings of the National Academy of Sciences*, 99 (7), 4349-4354.

Tripathi, P.K., Gan, L., Liu, M. and Rao, N.N., 2014. Mesoporous carbon nanomaterials as environmental adsorbents. *Journal of Nanoscience and Nanotechnology*, 14 (2), 1823-1837.

Valeri, N., Braconi, C., Gasparini, P., Hart, J., Grivennikov, S., Lovat, F., Lanza, G., Gafa, R., Nuovo, G., Frankel, W. and Groden, J., 2013. microRNA-135b promotes cancer progression acting as a downstream effector of oncogenic pathways in colon cancer. *The Lancet*, 381, 17.

Van Vuuren, R.J., Visagie, M.H., Theron, A.E. and Joubert, A.M., 2015. Antimitotic drugs in the treatment of cancer. *Cancer Chemotherapy and Pharmacology*, 76 (6), 1101-1112.

Végran, F., Boidot, R., Bonnetain, F., Cadouot, M., Chevrier, S. and Lizard-Nacol, S., 2011. Apoptosis gene signature of Survivin and its splice variant expression in breast carcinoma. *Endocrine-Related Cancer*, 18 (6), 783-792.

Végran, F., Boidot, R., Oudin, C., Defrain, C., Rebucci, M. and Lizard-Nacol, S., 2011. Association of p53 gene alterations with the expression of antiapoptotic survivin splice variants in breast cancer. *Oncogene*, 26 (2), 290-297.

Végran, F., Boidot, R., Oudin, C., Riedinger, J.M. and Lizard-Nacol, S., 2005. Distinct expression of Survivin splice variants in breast carcinomas. *International Journal of Oncology*, 27 (4), 1151-1157.

Végran, F., Mary, R., Gibeaud, A., MiRjolet, C., Collin, B., Oudot, A., Charon-Barra, C., Arnould, L., Lizard-Nacol, S. and Boidot, R., 2013. Survivin-3B potentiates immune escape in cancer but also inhibits the toxicity of cancer chemotherapy. *Cancer Research*, 73 (17), 5391-5401.

Vischioni, B., Van der Valk, P., Span, S.W., Kruyt, F.A.E., Rodriguez, J.A. and Giaccone, G., 2004. Nuclear localization of survivin is a positive prognostic factor for survival in advanced non-small-cell lung cancer. *Annals of Oncology*, 15 (11), 1654-1660.

Vorobiof, D.A., Sitas, F. and Vorobiof, G., 2001. Breast cancer incidence in South Africa. *Journal of Clinical Oncology*, 19 (18), 125-125.

Waligórska-Stachura, J., Andrusiewicz, M., Sawicka-Gutaj, N., Biczysko, M., Jankowska, A., Kubiczak, M., Czarnywojtek, A., Wrotkowska, E. and Ruchała, M., 2014. Survivin delta Ex3 overexpression in thyroid malignancies. *PLoS One*, 9 (6), 100534.

Walker, A.R., Adam, F.I. and Walker, B.F., 2004. Breast cancer in black African women: a changing situation. *The Journal of the Royal Society for the Promotion of Health*, 124 (2), 81-85.

Wang, F.L., Pang, L.L., Jiang, Y.Y., Chen, B., Lin, D., Lun, N., Zhu, H.L., Liu, R., Meng, X.L., Wang, Y. and Bai, Y.J., 2009. Simple synthesis of hollow carbon spheres from glucose. *Materials Letters*, 63 (29), 2564-2566.

Wang, H. and Ye, Y.F., 2015. Effect of survivin siRNA on biological behaviour of breast cancer MCF7 cells. *Asian Pacific Journal of Tropical Medicine*, 8 (3), 225-228.

Wang, J.D. and Levin, P.A., 2009. Metabolism, cell growth and the bacterial cell cycle. *Nature Reviews Microbiology*, 7 (11), 822-827.

Wang, S., Wang, L., Chen, M. and Wang, Y., 2015. Gambogic acid sensitizes resistant breast cancer cells to doxorubicin through inhibiting P-glycoprotein and suppressing survivin expression. *Chemico-Biological Interactions*, 235, .76-84.

Wang, S., Wu, X., Tan, M., Gong, J., Tan, W., Bian, B., Chen, M. and Wang, Y., 2012. Fighting fire with fire: poisonous Chinese herbal medicine for cancer therapy. *Journal of Ethnopharmacology*, 140 (1), 33-45.

Wang, T.A., Zhang, X.D., Guo, X.Y., Xian, S.L. and Lu, Y.F., 2016. 3-Bromopyruvate and sodium citrate target glycolysis, suppress survivin, and induce mitochondrial-mediated apoptosis in gastric cancer cells and inhibit gastric orthotopic transplantation tumor growth. *Oncology Reports*, 35 (3), 1287-1296.

Wang, W., Luo, H. and Wang, A., 2006. Expression of survivin and correlation with PCNA in osteosarcoma. *Journal of Surgical Oncology*, 93 (7), 578-584.

Wang, X., Jiang, F., Mu, J., Ye, X., Si, L., Ning, S., Li, Z. and Li, Y., 2014. Arsenic trioxide attenuates the invasion potential of human liver cancer cells through the demethylation-activated microRNA-491. *Toxicology Letters*, 227 (2), 75-83.

Wang, X., Ren, J.H., Lin, F., Wei, J.X., Long, M., Yan, L. and Zhang, H.Z., 2010. Stathmin is involved in arsenic trioxide-induced apoptosis in human cervical cancer cell lines via PI3K linked signal pathway. *Cancer Biology and Therapy*, 10 (6), 632-643.

Wang, Y., Zhang, Y., Yang, L., Cai, B., Li, J., Zhou, Y., Yin, L., Yang, L., Yang, B. and Lu, Y., 2011. Arsenic trioxide induces the apoptosis of human breast cancer MCF-7 cells through activation of caspase-3 and inhibition of HERG channels. *Experimental and Therapeutic Medicine*, 2 (3), 481-486.

Wang, Y.F., Zhang, W., He, K.F., Liu, B., Zhang, L., Zhang, W.F., Kulkarni, A.B., Zhao, Y.F. and Sun, Z.J., 2014. Induction of autophagy-dependent cell death by the survivin suppressant YM155 in salivary adenoid cystic carcinoma. *Apoptosis*, 19 (4), 748-758.

Waxman, S. and Anderson, K.C., 2001. History of the development of arsenic derivatives in cancer therapy. *The Oncologist*, 6 (Supplement 2), 3-10.

Wei, W., Wanjun, L., Hui, S., Dongyue, C., Xinjun, Y. and Jisheng, Z., 2013. miR-203 inhibits proliferation of HCC cells by targeting survivin. *Cell Biochemistry and Function*, 31 (1), 82-85.

Wei, Y., Xu, Y., Han, X., Qi, Y., Xu, L., Xu, Y., Yin, L., Sun, H., Liu, K. and Peng, J., 2013. Anti-cancer effects of dioscin on three kinds of human lung cancer cell lines through inducing DNA damage and activating mitochondrial signal pathway. *Food and Chemical Toxicology*, 59, 118-128.

Wen, K., Fu, Z., Wu, X., Feng, J., Chen, W. and Qian, J., 2013. Oct-4 is required for an antiapoptotic behavior of chemoresistant colorectal cancer cells enriched for cancer stem cells: effects associated with STAT3/Survivin. *Cancer Letters*, 333 (1), 56-65.

Werner, T.A., Tamkan-Ölcek, Y., Dizdar, L., Riemer, J.C., Wolf, A., Cupisti, K., Verde, P.E., Knoefel, W.T. and Krieg, A., 2016. Survivin and XIAP: two valuable biomarkers in medullary thyroid carcinoma. *British Journal of Cancer*, 114 (4), 427-434.

White, N.M., Fatoohi, E., Metias, M., Jung, K., Stephan, C. and Yousef, G.M., 2011. MetastaMiRs: a stepping stone towards improved cancer management. *Nature Reviews Clinical Oncology*, 8 (2), 75.

World Health Organization, 2017. *Depression and Other Common Mental Disorders: Global Health Estimates* (No. WHO/MSD/MER/2017.2). World Health Organization.

Xia, M., Li, H., Wang, J.J., Zeng, H.J. and Wang, S.H., 2016. MiR-99a suppress proliferation, migration and invasion through regulating insulin-like growth factor 1 receptor in breast cancer. *European Review for Medical Pharmacological Sciences*, 20 (9), 1755-1763.

Xu, C., Yamamoto-Ibusuki, M., Yamamoto, Y., Yamamoto, S., Fujiwara, S., Murakami, K., Okumura, Y., Yamaguchi, L., Fujiki, Y. and Iwase, H., 2014. High survivin mRNA expression is a predictor of poor prognosis in breast cancer: a comparative study at the mRNA and protein level. *Breast Cancer*, 21 (4), 482-490.

Xu, D., Wang, Q., An, Y. and Xu, L., 2013. MiR 203 regulates the proliferation, apoptosis and cell cycle progression of pancreatic cancer cells by targeting Survivin. *Molecular Medicine Reports*, 8 (2), 379-384.

Yamamoto, N., Kinoshita, T., Nohata, N., Itesako, T., Yoshino, H., Enokida, H., Nakagawa, M., Shozu, M. and Seki, N., 2013. Tumor suppressive microRNA-218 inhibits cancer cell migration and invasion by targeting focal adhesion pathways in cervical squamous cell carcinoma. *International Journal of Oncology*, 4 (5), 1523-1532.

Yamanaka, K., Nakata, M., Kaneko, N., Fushiki, H., Kita, A., Nakahara, T., Koutoku, H. and Sasamata, M., 2011. YM155, a selective survivin suppressant, inhibits tumor spread and prolongs survival in a spontaneous metastatic model of human triple negative breast cancer. *International Journal of Oncology*, 39 (3), 569-575.

Yang, J.H., Hsia, T.C., Kuo, H.M., Chao, P.D.L., Chou, C.C., Wei, Y.H. and Chung, J.G., 2006. Inhibition of lung cancer cell growth by quercetin glucuronides via G2/M arrest and induction of apoptosis. *Drug Metabolism and Disposition*, 34 (2), 296-304.

Yang, Q.H., Church-Hajduk, R., Ren, J., Newton, M.L. and Du, C., 2003. Omi/HtrA2 catalytic cleavage of inhibitor of apoptosis (IAP) irreversibly inactivates IAPs and facilitates caspase activity in apoptosis. *Genes and Development*, 17 (12), 1487-1496.

Ye, Q., Cai, W., Zheng, Y., Evers, B.M. and She, Q.B., 2014. ERK and AKT signaling cooperate to translationally regulate survivin expression for metastatic progression of colorectal cancer. *Oncogene*, 33 (14), 1828-1839.

Yedjou, C., Thuisseu, L., Tchounwou, C., Gomes, M., Howard, C. and Tchounwou, P., 2009. Ascorbic acid potentiation of arsenic trioxide anticancer activity against acute promyelocytic leukemia. *Archives of Drug Information*, 2 (4), 59-65.

Yun, S.M., Woo, S.H., Oh, S.T., Hong, S.E., Choe, T.B., Ye, S.K., Kim, E.K., Seong, M.K., Kim, H.A., Noh, W.C. and Lee, J.K., 2016. Melatonin enhances arsenic trioxide-induced cell death via sustained upregulation of Redd1 expression in breast cancer cells. *Molecular and Cellular Endocrinology*, 422, 64-73.

Zaffaroni, N., Pennati, M., Colella, G., Perego, P., Supino, R., Gatti, L., Pilotti, S., Zunino, F. and Daidone, M.G., 2002. Expression of the anti-apoptotic gene survivin correlates with taxol resistance in human ovarian cancer. *Cellular and Molecular Life Sciences*, 59 (8), 1406-1412.

Zaki Dizaji, M., Ghaffari, S.H., Hosseini, E., Alizadeh, N., Rostami, S., Momeny, M., Alimoghaddam, K. and Ghavamzadeh, A., 2017. Survivin isoform expression in arsenic trioxide-treated acute promyelocytic leukemia cell line and patients: The odd expression pattern of survivin-2α. *Asia-Pacific Journal of Clinical Oncology*, 13 (2), 21-30.

Zarogoulidis, P., Chatzaki, E., Hohenforst-Schmidt, W., Goldberg, E.P., Galaktidou, G., Kontakiotis, T., Karamanos, N. and Zarogoulidis, K., 2012. Management of malignant pleural effusion by suicide gene therapy in advanced stage lung cancer: a case series and literature review. *Cancer Gene Therapy*, 19 (9), 593-600.

Zekri, A., Ghaffari, S.H., Yousefi, M., Ghanizadeh-Vesali, S., Mojarrad, M., Alimoghaddam, K. and Ghavamzadeh, A., 2013. Autocrine human growth hormone increases sensitivity of mammary carcinoma cell to arsenic trioxide-induced apoptosis. *Molecular and Cellular Endocrinology*, 377 (1-2), 84-92.

Zhang, J., Wang, S., Han, F., Li, J., Yu, L., Zhou, P., Chen, Z., Xue, S., Dai, C. and Li, Q., 2016. MicroRNA-542-3p suppresses cellular proliferation of bladder cancer cells through post-transcriptionally regulating survivin. *Gene*, 579 (2), 146-152.

Zhang, P., 1996. Arsenic trioxide treated 72 cases of acute promyelocytic leukemia. *International Journal of Hemarsenic trioxidelogy*, 17, 58-62.

Zhang, X.W., Yan, X.J., Zhou, Z.R., Yang, F.F., Wu, Z.Y., Sun, H.B., Liang, W.X., Song, A.X., Lallemand-Breitenbach, V., Jeanne, M. and Zhang, Q.Y., 2010. Arsenic trioxide controls the fate of the PML-RARα oncoprotein by directly binding PML. *Science*, 328 (5975), 240-243.

Zhang, Y.F., Zhang, M., Huang, X.L., Fu, Y.J., Jiang, Y.H., Bao, L.L., Maimaitiyiming, Y., Zhang, G.J., Wang, Q.Q. and Naranmandura, H., 2015. The combination of arsenic and cryptotanshinone induces apoptosis through induction of endoplasmic reticulum stress-reactive oxygen species in breast cancer cells. *Metallomics*, 7 (1), 165-173.

Zhao, S., Zhang, X., Zhang, J., Zhang, J., Zou, H., Liu, Y., Dong, X. and Sun, X., 2008. Intravenous administration of arsenic trioxide encapsulated in liposomes inhibits the growth of C6 gliomas in rat brains. *Journal of Chemotherapy*, 20 (2), 253-262.

Zhao, Z., Wang, X., Zhang, Z., Zhang, H., Liu, H., Zhu, X., Li, H., Chi, X., Yin, Z. and Gao, J., 2015. Real-time monitoring of arsenic trioxide release and delivery by activatable T1 imaging. *ACS Nano*, 9 (3), 2749-2759.

Zhao, Z., Zhang, H., Chi, X., Li, H., Yin, Z., Huang, D., Wang, X. and Gao, J., 2014. Silica nanovehicles endow arsenic trioxide with an ability to effectively treat cancer cells and solid tumors. *Journal of Materials Chemistry B*, 2 (37), 6313-6323.

Zhou, W., Cheng, L., Shi, Y., Ke, S.Q., Huang, Z., Fang, X., Chu, C.W., Xie, Q., Bian, X.W., Rich, J.N. and Bao, S., 2015. Arsenic trioxide disrupts glioma stem cells via promoting PML degradation to inhibit tumour growth. *Oncotarget*, 6 (35), 37300.

Zhu, N., Gu, L., Findley, H.W., Li, F. and Zhou, M., 2004. An alternatively spliced survivin variant is positively regulated by p53 and sensitizes leukemia cells to chemotherapy. *Oncogene*, 23 (45), 7545-7551.

Appendices

Appendix-A: General primer design rules

Primer length: 18-22

Primer melting temperature (T_M): 55-72°C

$$(T_M)= 2 (A+T) + 4 (G+C)$$

GC content: 45-55%

GC clamp: G or C bases within the last 5 bases of the 3’ end. More than 3 G’s or C’s should be avaoided.

Appendix-B: Survivin rabbit monoclonal antibody

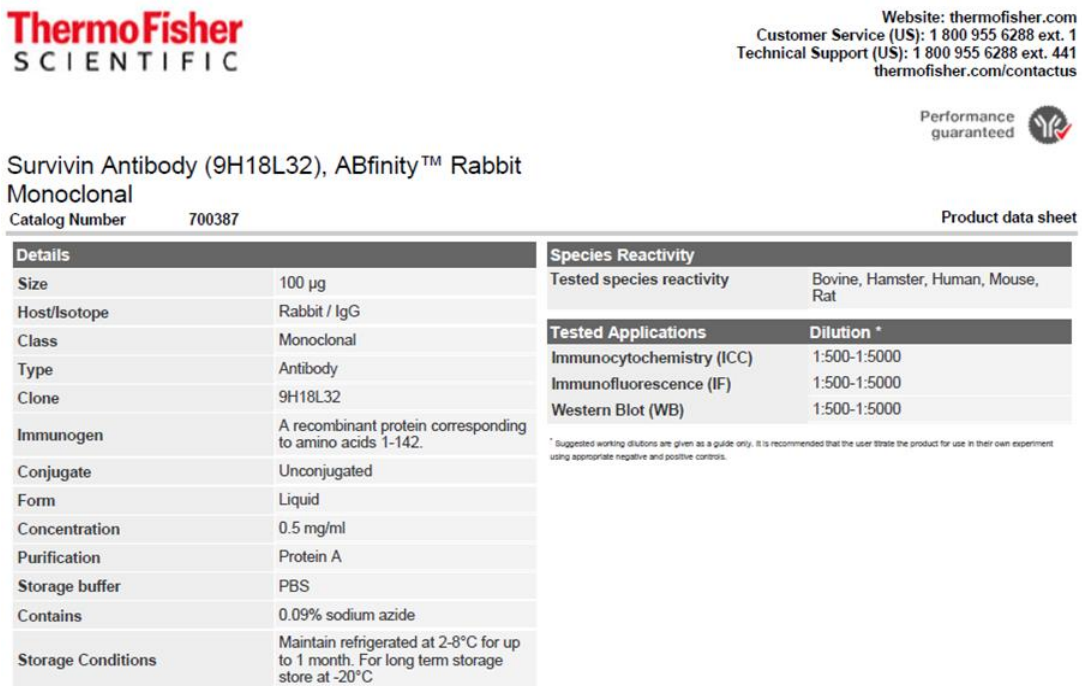

ThermoFisher SCIENTIFIC

Website: thermofisher.com
Customer Service (US): 1 800 955 6288 ext. 1
Technical Support (US): 1 800 955 6288 ext. 441
thermofisher.com/contactus

Performance guaranteed

Survivin Antibody (9H18L32), ABfinity™ Rabbit Monoclonal

Catalog Number 700387

Product data sheet

Details	
Size	100 µg
Host/Isotope	Rabbit / IgG
Class	Monoclonal
Type	Antibody
Clone	9H18L32
Immunogen	A recombinant protein corresponding to amino acids 1-142.
Conjugate	Unconjugated
Form	Liquid
Concentration	0.5 mg/ml
Purification	Protein A
Storage buffer	PBS
Contains	0.09% sodium azide
Storage Conditions	Maintain refrigerated at 2-8°C for up to 1 month. For long term storage store at -20°C

Species Reactivity	
Tested species reactivity	Bovine, Hamster, Human, Mouse, Rat

Tested Applications	Dilution *
Immunocytochemistry (ICC)	1:500-1:5000
Immunofluorescence (IF)	1:500-1:5000
Western Blot (WB)	1:500-1:5000

* Suggested working dilutions are given as a guide only. It is recommended that the user titrate the product for use in their own experiment using appropriate negative and positive controls.

The survivin rabbit monoclonal antibody information: The antibody was purchased ThermoFisher Scientific, in USA.

Appendix-C: Laser Raman spectra

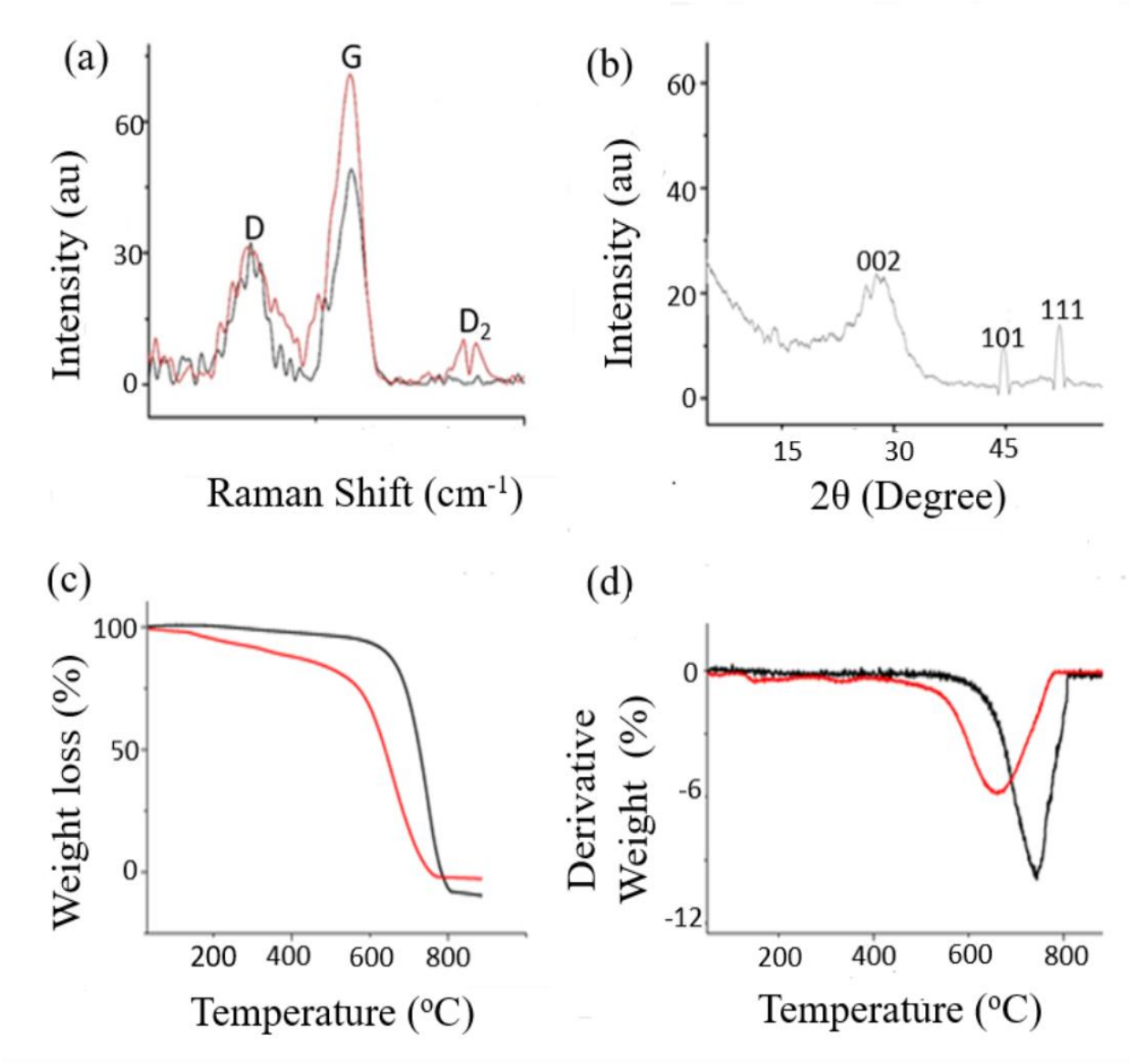

Laser Raman spectra of *β*-cyclodextrin CNSs and CNSs. (a), XRD pattern of *β*-cyclodextrin CNSs (b), TGA plot (c) and derivative plot of CNSs and *β*-cyclodextrin CNSs (d). In (a), (c) and (d), the red line represents *β*-cyclodextrin CNSs while the black line represents CNSs.

Appendix-D: Laser Raman spectra

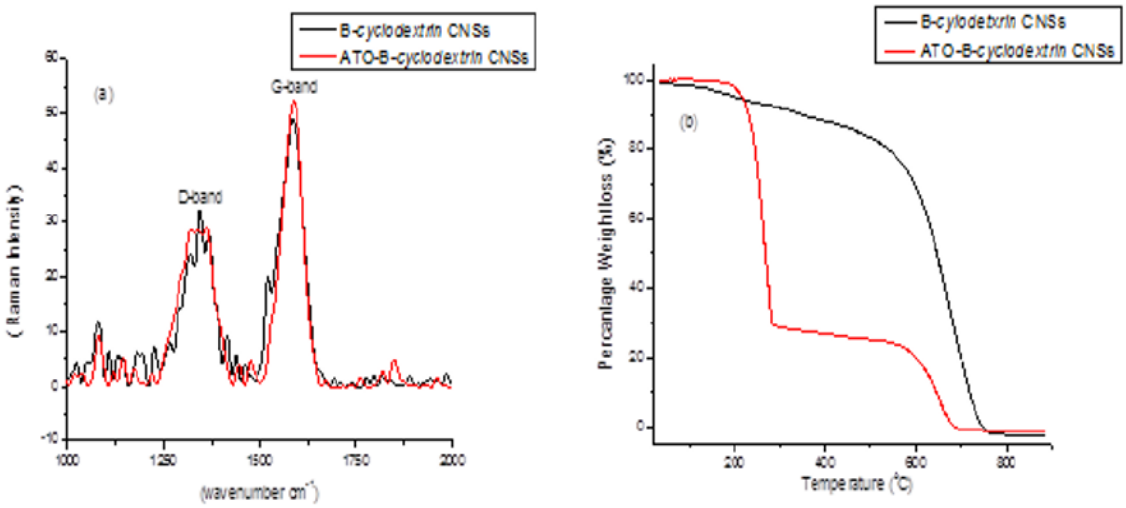

Laser Raman spectra. (a) Laser Raman of the *β*-cyclodextrin CNSs and arsenic trioxide-β-cyclodextrin CNSs and (b) TGA of the *β*-cyclodextrin CNSs and arsenic trioxide-β cyclodextrin CNSs.